

# **DYNAMIC RESPONSE AND STABILITY OF A COMPOSITE PROP-FAN MODEL**

(NASA-CR-179528) DYNAMIC RESPONSE AND  
STABILITY OF A COMPOSITE PROP-FAN MODEL

N87-21956

Final Report (Hamilton Standard) 92 p

Avail: NTIS HC A05/MF A01

CSCD 21E

G3/07

Unclass

0072745

By

**Arthur F. Smith  
and  
Bennett M. Brooks**

**HAMILTON STANDARD DIVISION  
UNITED TECHNOLOGIES CORPORATION  
WINDSOR LOCKS, CONNECTICUT 06096**

**October, 1986**

**NASA**

**National Aeronautics and Space Administration  
Lewis Research Center  
Cleveland, Ohio 44135**

**Contract NAS3-24088**

# **DYNAMIC RESPONSE AND STABILITY OF A COMPOSITE PROP-FAN MODEL**

**By  
Arthur F. Smith  
and  
Bennett M. Brooks**

**HAMILTON STANDARD DIVISION  
UNITED TECHNOLOGIES CORPORATION  
WINDSOR LOCKS, CONNECTICUT 06096**

**October, 1986**



**National Aeronautics and Space Administration  
Lewis Research Center  
Cleveland, Ohio 44135**

**Contract NAS3-24088**

1. Report No. CR-179528		2. Government Accession No.		3. Recipient's Catalog No.	
4. Title and Subtitle  Dynamic Response and Stability of a Composite Prop-Fan Model				5. Report Date October, 1986	
				6. Performing Organization Code	
7. Author(s)  A. F. Smith* and B. M. Brooks+				8. Performing Organization Report No. HSER 11057	
				10. Work Unit No.	
9. Performing Organization Name and Address  Hamilton Standard Division United Technologies Corporation Windsor Locks, CT 06096				11. Contract or Grant No. NAS3-24088	
				13. Type of Report and Period Covered Contractor	
12. Sponsoring Agency Name and Address  National Aeronautics and Space Administration Washington, D. C. 20546				14. Sponsoring Agency Code	
15. Supplementary Notes  Final Report. Project Technical Monitor, Mr. O. Mehmed, NASA-Lewis Research Center, Cleveland OH 44135.  * Now with: Hicrock Corporation, 1 Main Road, Granville, MA 01034 + Now with: Kollmorgen Corporation, 347 King Street, Northampton, MA 01060					
16. Abstract  Results are presented for blade response and stability during wind tunnel tests of a 62.2 cm (24.5 in) diameter model of a Prop-Fan, advanced turboprop, with swept graphite/epoxy composite blades. Measurements of dynamic response were made with the rotor mounted on an isolated nacelle, with varying tilt for non-uniform inflow, at flow speeds from 0.36 to 0.9 Mach number.  The blade displayed no instabilities over the operating range tested, up to 0.9 Mach number and 10000 RPM.  Measurements are compared with those for other Prop-Fan models of both solid metal and graphite composite construction. The swept composite blade had less response than an unswept (straight) composite blade. Composite blades had more response than metal blades.  Measurements are compared with theoretically based predictions. The 1-P blade response was significantly overpredicted using unimproved methods and somewhat overpredicted using improved methods.  Unexpectedly high 2-P strain levels were measured and suggest the presence of non-linear effects on blade response.					
17. Key Words (Suggested by Author(s))  Advanced Turboprop      Propeller Aeroelastic Test      Prop-Fan Composite      Structural Response Energy Efficient      Wind Tunnel Test				18. Distribution Statement  Unlimited.	
19. Security Classif. (of this report) Unclassified		20. Security Classif. (of this page) Unclassified		21. No. of pages 94	
				22. Price*	

## FOREWORD

All of the testing reported herein was performed by NASA-Lewis personnel in the 8 x 6 wind tunnel at NASA-Lewis. The data were reduced, analyzed and reported by personnel from Hamilton Standard, a division of United Technologies Corporation.

Mr. Oral Mehmed was the NASA Technical Monitor for this project. At Hamilton Standard, Mr. Donald Marshall performed the data reduction, Mr. Prem Bansal performed the theoretical predictions with assistance from Mr. Peter Arseneaux, and Mr. Arthur F. Smith conducted the data analysis and correlation with predictions. Mr. Bennett M. Brooks was the Hamilton Standard Project Manager.

This work was accomplished under contract NASA-24088 for the NASA Lewis Research Center in Cleveland, Ohio.

## TABLE OF CONTENTS

	<u>Page</u>
ABSTRACT .....	i
FOREWORD .....	iii
TABLE OF CONTENTS .....	v
SUMMARY .....	vii
SYMBOLS AND ABBREVIATIONS .....	ix
 1.0 INTRODUCTION .....	 1
2.0 DESCRIPTION OF THE EXPERIMENTAL PROGRAM .....	3
2.1 Test Model .....	3
2.2 Wind Tunnel Facility .....	3
2.3 Model Instrumentation .....	3
2.4 Test Procedures .....	4
2.5 Test Conditions .....	4
2.6 Data Reduction .....	4
3.0 ANALYTICAL TECHNIQUES .....	7
3.1 Approach .....	7
3.2 Calculated Modes and Frequencies .....	7
3.3 Calculated Vibratory Strains .....	8
4.0 TEST DATA EVALUATION AND COMPARISON WITH CALCULATIONS .....	11
4.1 Flutter Clearance .....	11
4.2 Total Strain Measurements .....	11
4.3 Spectral Analysis .....	12
4.4 Modal Frequencies and Comparison to Predictions .....	12
4.5 P-Order Vibratory Strains .....	13
4.6 Shaft Tilt and the Excitation Factor .....	14
4.7 Power Coefficient .....	15
4.8 Strain Sensitivity vs. Power Coefficient .....	16
4.9 Comparison of 1-P Measurements to Predictions .....	16
4.10 Comparison to other Prop-Fan Models .....	17
5.0 CONCLUSIONS .....	19
6.0 RECOMMENDATIONS .....	21
7.0 REFERENCES .....	23
TABLES .....	25
FIGURES .....	35
APPENDIX I - Peak Total Strain Tabulation .....	67
APPENDIX II - P-order Strain Tabulation .....	75

## SUMMARY

High speed dynamic response and stability tests were conducted on a model Prop-Fan, with swept composite blades, which was found to be structurally adequate over the entire operating range.

## TEST

The tests were conducted, in the NASA-Lewis Research Center 8 x 6 foot wind tunnel, on the SR-3C-3 model Prop-Fan, advanced turboprop, operating in an isolated nacelle installation. The SR-3C-3 model is nominally 62.2 cm (24.5 in) in diameter, and has eight swept blades constructed of graphite/epoxy composite material. It was operated at conditions of up to 0.9 Mach number flight speed and 10000 RPM. Also, it was tested in non-uniform inflow, with the rotor shaft yawed up to 15 degrees from the freestream flow direction.

## DATA ANALYSIS and CORRELATION to CALCULATIONS

Blade vibratory strain gage test data were reduced and analyzed to determine response and stability trends for variations of operating parameters. Non-dimensionalized blade strain sensitivities are presented as a function of rotor power coefficient.

Calculations of blade response were made using lifting line aerodynamic and finite element structural methodologies. The calculations are compared to test data. Also, data for the SR-3C-3 model are compared to data for other, previously tested, Prop-Fan models of both solid titanium and graphite composite construction.

## CONCLUSIONS

- 1) The SR-3C-3 model was structurally adequate over the range of operation, demonstrating the success of composite structural tailoring in preventing instability.
- 2) The swept composite blade had less response than the straight composite blade.
- 3) The trends of 1-P blade response were well defined using non-dimensional parameters.
- 4) The composite blades were more strain sensitive than the metal blades.
- 5) The SR-3C-3 1-P response was significantly overpredicted using unimproved methods. Improved finite element calculation methods reduced the amount of 1-P overprediction.

### SUMMARY (continued)

- 6) High measured 2-P strain levels suggest the presence of undetermined non-linear effects on blade response.

### RECOMMENDATIONS

- 1) The improved finite element prediction method should be confirmed by additional 1-P calculations.
- 2) Existing test data for other Prop-Fan models should be reviewed to determine the extent of non-linear effects on blade response.
- 3) Non-linear effects should be included in future improvements to the blade response calculation method.

## SYMBOLS AND ABBREVIATIONS

AF	Blade Activity Factor = $\frac{100,000}{16} \int_{0.2}^{1.0} \frac{b}{D} x^3 dx$
b	Blade Section Chord Width, m
Cl	Blade Section Design Lift Coefficient
CP	Power coefficient = $2\pi Q/\rho n^2 D^5 = \pi^3 Q/_{1/2} \rho V_{TIP}^2 D^3$
D	Rotor Diameter, m
EF	Excitation Factor = $\Psi (V_{eq}/348)^2$
N	Rotor Speed, RPM
n	Rotor Speed, revolutions/sec
Q	Rotor Torque, N-m
SHP	Shaft Horsepower
$V_{eq}$	Equivalent air speed = $V_T \sqrt{\rho/\rho_o}$ , knots
$V_T$	True airspeed, knots
$V_{TIP}$	Blade Tip rotational speed, m/s = $n\pi D$
X	Non-Dimensional Blade Radius
$\beta_{REF.}$	Reference Blade Angle deg
$\beta_{.75}$	Blade Angle at 3/4 Radius = $\beta_{REF} - 0.9$ , deg
$\epsilon$	Micro-Strain
$\rho$	Air Density, kg/m <sup>3</sup>
$\rho_o$	Air Density, Standard Sea Level = 1.2250 kg/m <sup>3</sup>
$\Psi$	Prop-Fan shaft tilt, degrees
1P	Frequency = one per propeller revolution, Hz
nP	Frequency = n per propeller revolution, Hz

SI units of measurement used throughout unless specified otherwise.



## 1.0 INTRODUCTION

The efficiency advantage offered by the Prop-Fan has been demonstrated by extensive testing, see Reference 1. It is well established that the Prop-Fan can achieve up to a 30 percent improvement in efficiency, over conventional means of propulsion. Since 1976, many experimental test programs have been conducted with model Prop-Fans. During the course of these test programs, the various model Prop-Fans were subjected to a complete range of operating conditions, including extremes in loading, such that the structural integrity of the blades as well as the advantages for rotor performance were demonstrated. The structural testing has included investigations of blade vibratory response due to angular inflow, unstalled flutter, buffeting, stall flutter, and vibratory response to a non-uniform flow field due to installation on an aircraft (wing/nacelle/fuselage) model.

The Prop-Fan models tested previously (see References 2, 3, and 4) were made of solid steel or titanium, and performed very well in view of the rigorous structural testing to which they were subjected. It is recognized that for full scale Prop-Fan applications, solid metal blades would be too heavy. Therefore, testing of Prop-Fan models constructed of lighter weight composite materials has begun. The objective of these tests is to demonstrate the efficiency advantage expected for Prop-Fans, while maintaining structural integrity in a design free of instabilities.

As part of the continuing studies of Prop-Fan structural stability and blade dynamic response, an 8-bladed model, designated the SR-3C-3, was designed by NASA-Lewis, with Hamilton Standard support, and fabricated by NASA-Ames. The SR-3C-3 blade is a solid composite design of carbon fiber in an epoxy matrix. Angular inflow and unstalled stability tests, with the Prop-Fan model mounted on an isolated nacelle, were conducted in the NASA-Lewis 8 x 6 foot wind tunnel, at free stream Mach numbers of 0.36 to 0.90. These tests were conducted during the period of July 11 through 19, 1983 with Hamilton Standard providing test support under its own funding. Then, under contract NAS3-24088, Hamilton Standard analyzed the data acquired during these tests.

This report summarizes the results of the SR-3C-3 Prop-Fan model dynamic response and stability investigation. Included are trends of measured blade strain data with operating conditions. Total vibratory strain, modal vibratory strain, P-order strain and frequency spectra were analyzed. In addition, 1-P dynamic responses were predicted, using theoretically based calculation procedures for comparison to test results. The predicted structural mode shapes and frequencies were provided by NASA-Lewis, while the airloads and structural responses were calculated by Hamilton Standard, using a NASA-Lewis supplied MSC/NASTRAN finite element model of the composite Prop-Fan. The comparisons were used to evaluate the ability of the theoretical method to predict blade loading and response, in order to verify the method's usefulness as a Prop-Fan design tool.

## 2.0 DESCRIPTION OF THE EXPERIMENTAL PROGRAM

The tests described in this report were conducted using the SR-3C-3 8-way Prop-Fan model, mounted on an isolated nacelle, in the NASA-Lewis Research Center 2.44 x 1.83 m (8 x 6 ft) wind tunnel. The primary purpose of these tests was to determine the effects of yawed flow, at Mach numbers from 0.36 to 0.84, on the blade's vibratory response. In addition, the aeroelastic stability of this configuration was investigated up to 0.9 Mach number.

### 2.1 Test Model

The SR-3C-3 Prop-Fan model is nominally 62.2 cm (24.5 in.) in diameter. The Prop-Fan concept incorporates thin airfoils (2 percent thick at the tip) and swept blades to achieve high aerodynamic efficiency with low noise generation. The SR-3C-3 geometric shape is identical to that of the SR-3 model, which is an earlier Hamilton Standard design. A description of the geometric characteristics of this blade can be found in Reference 3. Table I is a summary of the overall design parameters for the SR-3C-3 model.

The SR-3C-3 model blades were built by NASA-Ames and the hub was built by Hamilton Standard. The blades are made of carbon fiber cloth layers in an epoxy matrix. This model is one of a series of SR-3C blades of similar construction. A more complete description of the blade series is given in Reference 5. In the SR-3C-3 model, the carbon fibers are oriented at  $\pm 45$  degrees. The fiber ply orientation was chosen to provide the blade with similar structural vibratory response frequencies to those for the metal (titanium) SR-3 model, and to allow the model to be free of instabilities.

### 2.2 Wind Tunnel Facility

Figure 1 shows the SR-3C-3 model Prop-Fan rotor installed in the wind tunnel. The SR-3C-3 model was mounted on an isolated axisymmetric nacelle test rig in the NASA-Lewis 2.44 x 1.83 m (8 x 6 ft) wind tunnel. This rig was capable of orienting the rotor drive through a range of tilt angles relative to the tunnel axis, to provide non-uniform inflow excitation to the rotor. The rotor drive is the same rig that has been used to test all the model Prop-Fans at NASA-Lewis and contains a 746kW (1000 shp) air turbine. Reference 6 discusses the wind tunnel and Reference 3 discusses the nacelle test rig in greater detail.

### 2.3 Model Instrumentation

Foil strain gages mounted on the camber (suction) surfaces of selected blades were used to measure strain due to blade flexure. The strain gages were mounted by NASA-Lewis personnel, based on guidance provided by finite element analyses.

The strain gages were located at points along the blade mid-chord where the stresses associated with the first four modes were calculated to be high. Figure 2 shows the locations of the strain gages as they were applied to the blade. The gages were used to measure inboard bending, mid-blade bending, and mid-blade torsion (shear strain). Two opposing blades (numbers 1 and 5) had a full complement of the three gages. In addition, selected gages were installed on blades 2, 3 and 6, as described in Table II.

The strain gage signals were transmitted from the rotor to the fixed frame system using a rotary transformer device. The output was ultimately directed to magnetic tape recording equipment.

## 2.4 Test Procedures

Initially, the tunnel was brought up to speed with the Prop-Fan windmilling (zero power). Prop-Fan windmilling rotational speed is dependent on the blade pitch angle setting and tunnel free stream velocity. The model rotational speed, at this fixed blade angle and fixed tunnel Mach number, was incrementally increased by increasing the power to the rotor. This was done until an operating limit, such as a blade stress limit, rotational speed limit, or rig power limit was reached. This was repeated for various shaft tilt angles, with the tilt angle being varied from the control room. The whole process was repeated for different Mach numbers, also varied from the control room.

The tunnel was shut down in order to change blade pitch angle (ground adjustable). An inclinometer was used to set the blade pitch angle at a reference location on the blade (reference blade angle) prior to tunnel start up. The reference location for the SR-3C-3 is at the 0.78 radial station. The blade/hub collective pitch mechanical arrangement allowed for the adjustment of all blades simultaneously. The blade angle was defined as the average of the measurements for all of the blades.

## 2.5 Test Conditions

The conditions for these wind tunnel tests, after the tunnel has reached steady state operation at between 0.7 and 0.9 Mach number, include an air density equivalent to a standard day altitude of between 1524 to 2134 meters (5000 to 7000 feet). This is close to sea level conditions, as compared with the Prop-Fan design cruise operating condition at 10668 meters (35000 feet) altitude.

The parameters that were variable for the test were Mach number, Prop-Fan shaft tilt angle, blade angle and rotor RPM. All of these parameters were remotely controllable from the control room, except blade angle. A schedule of the Mach numbers, blade angles, and rotor shaft tilt angles which were tested is found in Table III. The RPM's tested are also found in the table and they range from 3730 RPM to 10000 RPM. The RPM was tested in 500 RPM increments, from the windmilling RPM to the upper RPM limit. Figure 3 shows the operating envelopes for this test. These boundaries include the RPM limits encountered, determined by windmilling, the maximum drive power available or blade steady loading safety limits (9000 RPM). An exception to the 9000 RPM limit was made in order to probe for flutter at 0.9 Mach number, where 10000 RPM was allowed. The upper bounds on rig tilt angle and blade angle were generally limited by high strains. One set of boundaries is shown for each Mach number tested.

## 2.6 Data Reduction

Two types of magnetic data tapes were provided to Hamilton Standard by NASA-Lewis. One contained the operating condition data found in Table III in digital form, and the other contained the strain data, in analog form, for all of the gages. The first type (condition data) was used during the data

reduction process to formulate the operating condition tables and data trend summary curves.

The second type (strain data) was also processed at Hamilton Standard using a computer based instrumentation data tape playback system. The strain gage signals were passed through a scaling amplifier and then through peak detectors. Positive and negative peak strain amplitudes were averaged over specific time intervals, and the averaged half-amplitude was determined. The peak detector output was sampled by an analog-to-digital converter, calibrated in engineering units and stored in computer memory. The data were then processed by a computer based analysis system.

Once the sampled data resided in memory, a statistical treatment of the data was used to define the "total strain". For the present work, a level defined by the half-amplitude mean plus 2 times the standard deviation was used. That is;

$$\epsilon_{\text{total}} = \bar{x} + 2 * \sigma.$$

The instantaneous strain will be below this level 97.72 percent of the time during the data sampling period. That is, only 2.28 percent of the vibratory strains are above this value.

The core of the data analysis system is a high speed mini-computer. This computer was used to store the total strain data on a dual rigid disk drive. These data were later used to create trend summary plots of total strain vs. RPM and other test operating variables.

The data analysis system has the capability to perform spectral analyses of the analog signals. The spectral data (in digital form) were stored on the disk for every steady state run analyzed. An algorithm for the computer, developed at Hamilton Standard, identified the peaks, above a specified noise level, from the spectral data. Tables of P-order strain values (strains at integer multiples of the rotational speed) and trend summary plots were made from these data, and will be discussed later in the report.

### 3.0 ANALYTICAL TECHNIQUES

#### 3.1 Approach

Extensive use was made of the MSC/NASTRAN finite element analysis computer program, described in reference 7, for the 1-P structural dynamic analysis of the model blade. Careful modeling techniques are required in order to create the finite element grids necessary to describe the Prop-Fan blade.

For most of the calculations, a finite element model for the SR-3C-3 blade, provided by NASA-Lewis, was used. This model is composed of CTRIA3 elements, and a schematic representation of the model is shown in Figure 4. Later in the project, an improved finite element model was generated by Hamilton Standard using CQUAD4 elements. It is also shown in Figure 4. A limited number of calculations were performed using this model. The study on which the improved model was based is described in Reference 8.

The theoretically based methods used for this study, to predict the 1-P response of the blade to angular inflow, have been used in previous Prop-Fan structural dynamic studies, as described in references 2 and 3. A short discussion of these methods is given here.

Figure 5 shows a block diagram of the prediction methods used in this analysis. The computer codes used in this analysis are listed in Table IV, where they are matched to their numerical designation.

Starting at the top of Figure 5, the model description, steady airloads (as computed by the HS/H039 and HS/H045 codes), and centrifugal load effects were input into MSC/NASTRAN to determine a steady displaced blade position. The 1-P airloads were computed for the angular inflow conditions, using the HS/H039 flow field analysis and the HS/H337 skewed wake analysis. These airloads were distributed over the finite element model using HS/F194, and input into the MSC/NASTRAN structural dynamics analysis. A post-processor code was used to determine the blade strain at the gage locations.

#### 3.2 Calculated Modes and Frequencies

Blade mode shapes and frequencies were determined by NASA-Lewis personnel using their NASTRAN CTRIA3 model for the SR-3C-3. Schematic diagrams of the calculated modes, in order of their respective frequencies are shown in Figure 6a, for the non-rotating (zero RPM), and the 8600 RPM conditions. The modal frequency is shown beneath each modal pattern. The first six modes are shown for the non-rotating condition, and the first four modes are shown for the 8600 RPM condition. It is seen that there is little difference in the calculated mode shapes between the zero and 8600 RPM conditions, for the first four modes. The differences in the calculated frequencies are significant, however, showing the effects of centrifugal stiffening. Centrifugal stiffening raises the modal frequencies. This effect is greatest for the lower modes.

Also shown in Figure 6a are tracings of holographic patterns from photographs taken during a vibration test. This test was conducted at NASA/Lewis, on a non-rotating SR-3C-3 model blade vibrating at its natural frequencies. The measured frequencies are shown beneath each figure. Although the measured and

calculated mode shapes are generally similar, differences are seen for all six modes. In particular, the fifth calculated mode shows a much different displacement pattern compared to the holographic data. The fifth measured mode is similar to the sixth calculated mode, which appears to be a second torsional mode. The correlation between the calculated and measured non-rotating frequencies is good for all of the modes, except the third and fifth modes. Here, the frequencies differ by almost 15 percent. It is not known how these differences affect the values of calculated blade strain.

Calculations of blade mode shapes and frequencies for the zero RPM condition, made by Hamilton Standard using the CQUAD4 model, are shown in Figure 6b. The shapes derived using the CQUAD4 model are similar to those for the NASA CTRIA3 model. However, the CQUAD4 model frequencies generally match the holographic test data more closely.

The critical speeds are seen in Figure 7, which is a Campbell diagram showing the calculated frequency data, discussed above. Generally, these frequencies are typical of Prop-Fan models. They will be compared to the rotating results, observed during the wind tunnel tests, later in the report.

### 3.3 Calculated Vibratory Strains

The results of vibratory response calculations for six cases are given in Table V. These cases were selected from the test points given in Table III. The analytical predictions were performed at the measured wind tunnel conditions. These test cases were selected so as to provide a range of operating conditions, such as RPM, Mach number and rotor power, so that important trends could be identified. The test runs are listed by a reading number, and therefore the calculated cases are designated in the same manner. The operating condition parameters of air density and temperature are shown for each case.

Blade strains were calculated using the NASA-supplied CTRIA3 NASTRAN model for all six selected conditions. The improved CQUAD4 model was used to calculate strains for case number 6 only. This case is most closely associated with the design operating condition.

The measured strains for each case which was selected for prediction are also listed in Table V. A detailed comparison of measured and predicted strains is given in Section 4.8. The calculated strains represent the vibratory blade response caused by the periodic aerodynamic loading excitation due to angular inflow. The strains are calculated at the strain gage locations, as previously discussed. These locations represent the following strain measurement positions, inboard bending, mid-blade bending and mid-blade shear (torsion). The blade responses are given as values of strain divided by excitation factor (EF), a quantity which is sometimes known as "strain sensitivity". The use of EF for normalizing strain data is intended to account for the dependence of strain on inflow angle and flight velocity (dynamic pressure). This was shown to be good practice in previous studies (References 2 and 3), and will also be discussed later in this report.

Review of the calculated blade strain sensitivities, shown in Table V, reveals them to be only weakly dependent on changes in operating condition. Strain sensitivity varies little over the range of RPM and Mach number studied. This is partially a result of normalizing the strain by EF. The only significant

change is the increase in strain sensitivity seen in cases 1 and 6 at conditions of large shaft power. The reason for this is not clear, but it is probably related to a change in the spanwise distribution, as well as the magnitude, of the aerodynamic loading on the blade. The trends of strain with operating condition will be examined further in the discussion of the measured test data, to follow.

#### 4.0 TEST DATA EVALUATION AND COMPARISON WITH CALCULATIONS

The objectives of this SR-3C-3 Prop-Fan model test were:

- 1) To demonstrate the effectiveness of structural tailoring, using composites, in preventing blade instability (flutter clearance).
- 2) To determine the effect of pure angular inflow on the vibratory response of composite material Prop-Fan model blades.
- 3) To verify and evaluate theoretical calculations by comparison to test results.
- 4) To compare the SR-3C-3 test results to the results of other Prop-Fan model tests.

#### 4.1 Flutter Clearance

The SR-3C-3 Prop-Fan was tested, at zero tilt angle, at flight speeds up to 0.9 Mach number and rotational speeds up to 10000 RPM. It was demonstrated to be free of unstalled flutter instabilities over this entire operating range. This model was intended to be stable over a large portion of its operating range, by virtue of the structural tailoring of its composite ply layups. Further discussion of the stability analysis of this model is given in Reference 5.

#### 4.2 Total Strain Measurements

Blade strain measurements were made as described above, during wind tunnel testing on the Prop-Fan operating with its drive shaft tilted relative to the tunnel centerline, to provide angular inflow to the rotor. As discussed previously (Section 2.6), the measured total strain amplitude was extracted from the data using a statistical approach. It represents the vibratory strain half amplitude mean plus twice the standard deviation ( $\bar{x} + 2 * \sigma$ ).

Total vibratory strain measurements were obtained at steady state operating conditions. Appendix I contains a table of the total strain values for all of the gages, which are listed by reading number. A reading number identifies a data sample taken at a single operating condition. The operating conditions these runs represent are found in the performance table, Table III, as discussed in Section 2.5.

For this study, plots of total vibratory strain were made, from data at all the steady state conditions. Total strain was plotted as a function of rotational speed (RPM) for various tilt angles, and combinations of blade angles and Mach number. Samples of these plots are shown in Figure 8, which contains plots of total vibratory strain as a function of rotational speed, at a Mach number of 0.7 and a blade angle of 59.0 degrees. Data for tilt angles of 0.0, 3.0, and 5.0 degrees are shown.

These data indicate that blade strain increases significantly with increased tilt angle, as expected. There is some residual strain for the zero tilt angle condition, probably due to several causes. There may be a small angular error



in the physical rotor shaft alignment to the tunnel centerline, and the pylon/nacelle may be introducing a small degree of non-uniformity to the tunnel flow. Also, blade response may be induced by the small amount of tunnel turbulence present.

Note, in Figure 8, that a strain peak occurs at or near 8000 RPM. This is due to the first mode/2-P critical speed crossover. The calculated first mode critical speed is indicated in Figure 7 to be lower, at about 7000 RPM. The measured critical speed will be discussed in the next section.

#### 4.3 Spectral Analysis

Spectral analysis of the strain gage signals is a useful tool for identifying the harmonic P-order and non-P-order (modal) responses of the blade. Spectral analyses were conducted for all of the steady state runs, the data for which were stored permanently on computer disk. For this study, spectral plots were made from these data for selected test runs, for gages BG1-1, BG1-3, BG5-2 and BG5-3. These data represent respectively, inboard bending and shear on blade number 1, and mid-blade bending and shear on blade number 5.

Figure 9 shows typical samples of the spectral plots, giving strain amplitude as a function of frequency for a rotational speed of 7300 RPM, a Mach number of 0.7 and a blade angle of 59.0 degrees. The tilt angle for this run was 5.0 degrees. The plots show significant P-order response, while at the same time showing low amplitude modal response. Note that the shear strain spectra for the two blades are quite similar, showing the consistency of the test data.

The 1-P blade loads dominate, as was expected, since the aerodynamic loading is due primarily to pure angular inflow. The 2-P loads are of significant amplitude, probably due to the fact that this condition is near the 2-P/first mode critical speed. The source of the 2-P excitation is not known at this time. The 2-P response may be evidence of non-linear effects, due to blade sweep and flexibility. Further study of these data, and the test data which exist for other Prop-Fan models, would be helpful in clarifying the cause of this phenomena.

It is seen from the spectra in Figure 9, that non-p-order peaks are of very low magnitude. These peaks, and their underlying broadband humps, were used to define the modal responses. The low level seen for the modal responses is due to the small amount of turbulence in the wind tunnel, which is the source of random excitation for the blades.

#### 4.4 Modal Frequencies and Comparisons to Predictions

Blade modal frequencies for rotating operating conditions were identified using the blade strain signal spectra, described previously. Campbell diagrams illustrating the blade modal response were generated and are shown in Figure 10. Blade modal response frequency is plotted as a function of rotational speed, for data from the inboard bending, mid-blade bending, and shear gages. Also shown on these plots are the calculated frequencies (see Section 3.3), and the holographically measured frequencies at zero RPM, as supplied by NASA-Lewis. Calculations of modal frequency, as a function of RPM, were

performed using the CTRIA3 NASTRAN model. The CQUAD4 calculations and holographic measurements were performed for the zero RPM condition.

Inboard bending gage. The modal frequency test data indicated for the inboard bending gage clearly identify the first mode. Data for the higher order modes, however, contain much scatter. The inboard gage responds primarily to the first bending mode, with little response to the other modes, which accounts for the lack of clarity in the higher modes. Also, as was noted earlier, the modal responses indicated by the spectral data were of small magnitude, and thus difficult to identify, which could add to the data scatter.

It was observed that the measured first mode is a stronger function of rotational speed than the CTRIA3 model calculated curve. At the higher speeds, the test response frequencies for the first mode were higher than predicted. This indicates FEA modelling deficiencies.

Calculations of modal frequency as a function of RPM, using the improved CQUAD4 model, would be helpful in verifying the improvement in modelling centrifugal effects in the structural analysis. Also, the addition of aeroelastic effects in the structural analysis would improve the prediction of modal response frequencies.

Mid-blade bending gage. The modal responses indicated by the mid-blade bending gage are more consistent than the inboard gage data. The mid-blade gage is located in a position on the blade that is predicted to respond more readily to higher mode excitation. The test data indicate five response modes, whereas the calculations show only four modes over the same frequency range. The cause of the third experimental mode is not clear. These responses are of very low amplitude, as are the inboard gage data.

Correlation between test and prediction indicates that the measured second, and higher order mode frequencies are substantially lower than the CTRIA3 calculated values, although they have similar slopes. Again, the measured first mode has a steeper slope and higher frequencies than the calculations.

Shear gage. The shear gage modal response is similar to that seen for the mid-blade bending gage, except that it gives only weak indications of a mode in the 550 hz region. As before, the measured first mode response frequencies are higher than the calculated values. The higher mode test data show lower frequency values than the predictions. These results again indicate the need for improvement in the CTRIA3 structural model, in order to more accurately represent the response behavior of the blade.

#### 4.5 P-Order Vibratory Strains

A computer code, developed by Hamilton Standard, was used to search the spectral data stored on disk, to identify the strain peaks, and determine their values. These "peak values" were also stored on disk for tabulating and plotting. The only peaks saved were above a minimum strain level. In this study, the minimum value was 0.5 micro-strain. Appendix II is a listing of the P-order values of vibratory strain, tabulated according to reading number, along with selected operating parameters.

For this study, with the Prop-Fan operating in an environment of pure angular inflow (except for nacelle and pylon effects), the dominant 1-P blade responses are of primary interest.

Effect of rotational speed. The 1-P data have been summarized in Figures 11 through 16. Here, micro-strain is plotted as a function of rotational speed for the three gages on blade number 5.

These figures display test data for operation from 0.36 through 0.85 Mach number. The combinations of Prop-Fan shaft tilt angle and blade angle used for each Mach number condition are given in Table VI. The test data generally show the 1-P vibratory strain increasing with rotational speed for the inboard bending gage and the mid-blade bending gage. The inboard gage strain amplitudes are consistently higher.

The shear gage data behave in a similar manner, up to 0.7 Mach number. At that point, the 1-P vibratory strains tend to decrease with increasing rotational speed. This may be an effect of compressibility, due to a shift in the chordwise aerodynamic center location. This would modify the torsional loading, while not affecting the bending loads. It should be noted that, although the mid-blade bending gage is located very close to the shear gage, it does not show this drop-off.

Effect of Mach number. The effect of Mach number on 1-P strain data is shown in Figure 17. Here, 1-P micro-strain measured by the inboard bending gage is given for the rotor operating at about 7000 RPM, at a tilt angle of 4 degrees. As indicated, some of the data were measured directly at 4 degrees tilt and some were interpolated from test data measured at other tilt angles.

The data show that 1-P micro-strain increases rapidly up to about 0.8 Mach number, and then levels off. The initial increase is due to dynamic pressure effects. The leveling may be due to other effects, which become more important than dynamic pressure at high speed. These stronger effects could include the decrease in angle of attack difference, between the advancing and retreating blades, with increased forward speed, and compressibility effects.

Effect of blade angle. The test data show that blade angle (rotor power) has little effect on 1-P strain.

#### 4.6 Shaft Tilt and the Excitation Factor

The effect of Prop-Fan rotor shaft tilt is shown in Figures 18 through 20, where 1-P and 2-P vibratory strain are plotted as functions of tilt angle. Each set of points has been fitted by a hyperbolic curve generated by a computer algorithm. The curves are nearly linear, however.

Figure 18 displays data for 0.6 Mach number operation at a blade angle of 57.0 degrees. The figure contains plots for test data at 5500, 6000, 6500 and 7000 RPM. The data shown in Figure 19 were taken during 0.7 Mach Number tests, for a blade angle of 59.0 degrees. Figure 20 displays data taken during 0.8 Mach number tests, for a blade angle of 61.0 degrees.

The test data trends show increasing vibratory strain with increasing tilt angle. This trend is expected since increasing the tilt angle increases the

difference in angle of attack between the advancing and retreating blades. The angle of attack difference is the source of the vibratory aerodynamic loading. There is a linear dependence on shaft tilt angle, away from the origin, for both 1-P and 2-P strains.

Excitation Factor. The linear dependence of 1-P blade strain on shaft tilt suggests the use of the term "Excitation Factor" for the analysis of data trends. Excitation Factor (EF) is defined as:

$$EF = \psi^2 (V_{eq} / 348)^2$$

where  $\psi$  is the tilt angle in degrees and  $V_{eq}$  is the equivalent sea level airspeed in knots. EF is proportional to Prop-Fan shaft tilt angle and dynamic pressure.

For a uniform, steady inflow to an untilted rotor, theoretically there is no aerodynamic excitation to induce a forced response of the blades. If the rotor shaft is tilted at some angle to this uniform flow, a sinusoidal variation in velocity at the blade will occur with a frequency of 1-P. This will produce a 1-P airload on the blade, that is some function of the mean flow velocity and density (dynamic pressure) and the shaft tilt angle.

For most operating conditions of interest, that is, away from critical speeds, it was shown above that blade stress is a linear function of shaft tilt angle. Past study has shown a linear dependence of blade stress on dynamic pressure, also. This allows the use of EF to normalize blade stress. In fact, this concept has been in use for many years. Other demonstrations of this concept for Prop-Fan data are given in References 2 and 3. Note that the quantity strain divided by EF is sometimes known as "strain sensitivity".

#### 4.7 Power Coefficient

The effect of power variation on blade strain can be studied through the use of the term "power coefficient". This term has been in use for many years, in application to propeller data analysis. The power coefficient is a non-dimensional function of the dynamic pressure, due to rotational speed at the blade tip, and diameter cubed. That is, everything else held constant, the power the rotor absorbs is proportional to the tip dynamic pressure and diameter cubed. Power coefficient is defined as:

$$C_p = \frac{2 \pi Q}{\rho n^3 D^5} = \frac{\pi^3 Q}{1/2 \rho V_{tip}^3 D^3}$$

where  $\rho$  = air density in  $\text{kg/m}^3$ ,  $Q$  = rotor torque in  $\text{n-m}$ ,  $n$  = rotational speed in revolutions per second,  $V_{tip}$  = blade tip rotational speed in  $\text{m/s}$ , and  $D$  = rotor diameter in  $\text{m}$ . Use of the power coefficient normalizes the effect of rotor size and speed in the data. In the range of linear aerodynamics, the power coefficient includes the effect of blade angle.

#### 4.8 Strain Sensitivity vs. Power Coefficient

A summary of the test data, normalized as described above, is given in Figure 21, where for each Mach number, the data for all blade angles, all RPM's and all tilt angles are shown in one plot. Figure 21 displays 1-P strain sensitivity plotted as a function of power coefficient, from the output of the inboard bending gage. This gage had the highest response amplitudes due to 1-P forced excitation.

These curves summarize the data for each Mach number tested. For Mach numbers of 0.6 or higher, the data collapse into a single curve. For the 0.36 Mach number condition, the effect of blade angle appears significant, with the data forming a different trend curve for each blade angle tested. Strain sensitivity decreases with increasing blade angle for constant power coefficient.

In general, the curves fitted to the data are parabolic, with strain sensitivity increasing somewhat as the power coefficient increases. For the windmilling points (zero power coefficient) at 0.6 Mach number and above, the strain sensitivity value is consistently about 60. The trends of strain sensitivity with power coefficient are remarkably similar over the Mach number range tested. Strain sensitivity increases somewhat with increasing Mach number, up to 0.8 Mach, and then decreases slightly.

#### 4.9 Comparison of 1-P Measurements to Predictions

Calculated strain sensitivities for six conditions are shown in Figure 21, in addition to the measured test data. These operating conditions correspond to those for six test runs (see Section 3.3). Calculations were made for all six cases using the CTRIA3 NASTRAN model. Calculations using the improved CQUAD4 model were made for the 0.8 Mach number (design point) case, only.

The blade angle used for the 0.36 Mach number case was 47.7 degrees. The calculated strain sensitivity for this case is considerably higher (88 percent) than the measured sensitivity, as shown in Table V.

For the higher Mach number conditions, the CTRIA3 calculations also significantly overpredicted the measured values (50 to 95 percent). The improved CQUAD4 model reduced the overprediction to about 33 percent at the design point condition (case 6A).

Overprediction of measured blade response was not evident in studies of the dynamic response of metal Prop-Fan blades (Reference 2, 3 and 4). A number of causes may be responsible. Non-linear effects, evident from the significant 2-P responses, discussed earlier, are not included in the prediction methodology. Also not included are twist magnification and other aeroelastic effects. Although beyond the scope of the present study, data from this and previous Prop-Fan model testing should be examined, to determine the extent of non-linear and aeroelastic effects. If important, these should be included in future improvements to the calculation procedure.

#### 4.10 Comparison to other Prop-Fan Models

Dynamic response test results for the SR-3C-3 were compared to results for other blade models, previously tested. This comparison was made with blade strain sensitivity data derived from other Prop-Fan tests conducted in the NASA-Lewis 8 X 6 wind tunnel, using the plotting format of Figure 21. This is given in Figure 22, which shows a set of plots, by Mach number, of blade strain sensitivity as a function of power coefficient. Comparisons are shown with the SR-2C composite material model, and the SR-3 and SR-5 solid titanium models, all of which were discussed in Reference 2.

The strain sensitivity of the swept composite SR-3C-3 model is generally lower than that of the straight composite SR-2C model. This indicates the benefit of blade sweep in reducing blade response. The benefit may disappear at extremely high blade sweep, noting that the highly swept SR-5 model strain sensitivity is generally higher than that for the moderately swept SR-3 model.

As shown in Figure 22, the composite material SR-2C and SR-3C-3 blades have greater strain sensitivities than the solid metal SR-3 and SR-5 blades. This may be due, in part, to differences in blade material stiffness and inertia properties. In addition, the non-linear effects discussed earlier may influence blade responses. Further studies are needed to define this behavior.

## 5.0 CONCLUSIONS

As a result of this study of SR-3C-3 model Prop-Fan blade dynamic response and stability, the following conclusions are made:

- 1) This composite blade was structurally adequate over its entire operating range.
- 2) The swept composite blade showed less response than the straight composite blade.
- 3) The trends of 1-P blade response were defined using non-dimensional data (strain sensitivity vs. power coefficient).
- 4) Composite blades have higher strain sensitivity than metal blades.
- 5) 1-P blade response was overpredicted 50 percent at the design point, and up to 95 percent at off-design conditions, using unimproved methods.
- 6) An improved finite element modelling method reduced overprediction of 1-P response to about 33 percent, at the design point operating condition.
- 7) High 2-P response levels suggest the existence of non-linear effects, not included in the prediction methodology.

## 6.0 RECOMMENDATIONS

Based on the conclusions of this study, the following recommendations are made:

- 1) The existing test data for all Prop-Fan models should be reviewed to determine the non-linear effects on blade response.
- 2) Non-linear effects should be included in the blade response prediction methodology.
- 3) The improved CQUAD4 FEA model should be used for additional calculations of SR-3C-3 blade modal and forced response.



## 7.0 REFERENCES

1. Gatzen, B.S.; "Prop-Fan Potential and Technology Summary", Presented at the Japan Society for Aeronautical and Space Sciences meeting, Tokyo, Japan, November, 1984.
2. Bansal, P.N.; Arseneaux, P.J.; Smith, A.F.; Turnberg, J.E. and Brooks, B.M.; "Analysis and Test Evaluation of the Dynamic Response and Stability of Three Advanced Turboprop Models", NASA CR-174814, August, 1985.
3. Smith, A.F.; "Analysis and Test Evaluation of the Dynamic Response and Stability of Three Advanced Turboprop Models at Low Forward Speed", NASA CR-175026, December, 1985.
4. Smith, A.F.; "Analysis and Test Evaluation of the Dynamic Stability of Three Advanced Turboprop Models at Zero Forward Speed", NASA CR-175025, December, 1985.
5. Turnberg, J.E.; "Unstalled Flutter Stability Predictions and Comparisons to Test Data for the SR-3C-X2 Model Prop-Fan", NASA CR-179512, October, 1986.
6. Swallow, R.J. and Aiello, R.A.; "NASA Lewis 8 X 6 Supersonic Wind Tunnel", NASA TM X-71542, May, 1974.
7. MacNeal, R.H.; "The NASTRAN Theoretical Manual", (Level 15.5), MacNeal Schwendler Corp., December 1972.
8. Smith, A.F. and Brooks, B.M.; "Dynamic Response of Two Composite Prop-Fan Models on a Nacelle/Wing/Fuselage Half Model", NASA CR-179589, October, 1986.

TABLE I

DESIGN CHARACTERISTICS OF THE SR-3C-3 MODEL PROP-FAN

<u>Parameter</u>	<u>Value</u>
Diameter, cm (in)	62.2 (24.5)
Number of blades	8
Activity Factor/blade, AF	235
Activity Factor, Total	1880
Airfoil series (NACA)	outboard 16
	inboard 65/CA
Integrated design lift coefficient, Cl	0.214
Blade aerodynamic tip sweep, degrees	34.5
Material	Carbon/Epoxy fiber composite
Fiber orientation (1), degrees	0, <u>+45</u>

Cruise Conditions:

Speed, Mach number	0.8
Altitude, km (ft)	10.7 (35,000)
Power loading, kW/m <sup>2</sup> (shp/ft <sup>2</sup> )	300 (37.5)
Tip rotational speed, m/s (fps)	244 (800)
Power coefficient, Cp	1.695
Advance Ratio, J	3.056
Cruise efficiency, percent	78.4
Cruise noise (2), dB	144.5

- (1) Zero degrees fiber orientation parallel to pitch change axis.
- (2) Maximum sideline noise at blade passage frequency.

TABLE II

STRAIN GAGE DESIGNATIONS FOR SR-3C-3 RESPONSE TESTS

Gage Description	Radial station cm	Blade number							
		1	2	3	4	5	6	7	8
Inboard Bending	11.9	BG1-1	BG2-1	BG3-1	-	BG5-1	BG6-1	-	-
Mid-blade Bending	24.6	BG1-2	BG2-2	-	-	BG5-2	BG6-2	-	-
Shear	26.0	BG1-3	-	-	-	BG5-3	-	-	-

Gages are designated BGx-y, where x = blade number and y = gage number.

TABLE III

## SCHEDULE OF TEST CONDITIONS

SR-3C-3 PROP FAN  
8' X 6' WIND TUNNEL TESTS  
NASA-LEWIS

RDG. NO.	MACH NO.	EQUIVALENT VELOCITY M/SEC	BLADE ANGLE DEG	TIPT ANGLE DEG	PROP SPEED RPM	POWER KW	POWER COEFFICIENT	TIP MACH
9	0.357	122.02	45.	0.09	5075.	0.35	0.01	0.591
10	0.360	122.39	45.	0.03	9021.	393.84	1.07	0.913
13	0.361	123.08	45.	8.15	5118.	1.33	0.02	0.598
14	0.360	122.55	45.	8.13	9021.	397.59	1.08	0.913
15	0.360	122.43	45.	8.09	8502.	315.21	1.02	0.869
16	0.359	122.44	45.	8.17	7018.	133.85	0.77	0.745
17	0.361	123.07	45.	8.04	6515.	89.28	0.64	0.706
18	0.361	122.84	45.	8.04	6002.	51.67	0.48	0.665
19	0.361	122.93	45.	8.09	5504.	21.26	0.25	0.626
20	0.362	123.23	45.	8.03	5128.	1.78	0.03	0.599
25	0.361	122.66	48.	0.21	4673.	1.54	0.03	0.564
26	0.362	123.13	48.	0.19	4693.	1.63	0.03	0.567
27	0.363	123.08	48.	0.27	9039.	500.80	1.37	0.915
36	0.361	122.90	48.	8.20	4427.	2.16	0.04	0.562
37	0.362	123.14	48.	8.22	4627.	2.16	0.04	0.562
38	0.361	122.74	48.	8.25	9044.	507.85	1.38	0.915
39	0.362	122.99	48.	8.17	8507.	409.85	1.34	0.870
40	0.362	122.97	48.	8.26	8028.	328.24	1.28	0.829
41	0.362	122.96	48.	8.17	7520.	253.80	1.20	0.787
42	0.361	122.76	48.	8.24	7009.	187.36	1.09	0.745
43	0.362	123.03	48.	8.13	6519.	133.73	0.97	0.706
44	0.361	122.77	48.	8.17	6013.	88.95	0.82	0.665
45	0.363	123.34	48.	8.17	5515.	52.07	0.62	0.638
46	0.362	123.12	48.	8.13	5023.	22.01	0.35	0.591
47	0.362	123.26	48.	15.07	4390.	1.75	0.04	0.546
48	0.362	123.17	48.	15.07	4522.	7.21	0.16	0.555
49	0.364	123.80	48.	15.11	5025.	34.04	0.54	0.592
50	0.363	123.30	48.	15.05	5509.	65.08	0.78	0.628
51	0.363	123.46	48.	15.15	6024.	105.61	0.97	0.668
52	0.363	123.35	48.	15.13	6505.	152.02	1.11	0.705
54	0.359	122.38	51.	0.18	3968.	1.51	0.05	0.515
55	0.359	122.37	51.	0.27	9003.	669.08	1.83	0.911
65	0.361	123.20	51.	15.11	3732.	1.55	0.06	0.501
66	0.362	123.22	51.	15.04	4009.	13.13	0.41	0.519
67	0.361	123.07	51.	15.06	4515.	39.97	0.87	0.554
68	0.362	123.32	51.	15.04	5015.	74.20	1.17	0.591
69	0.362	123.48	51.	15.05	5504.	115.56	1.38	0.627
70	0.361	123.06	51.	15.01	6007.	165.66	1.53	0.665
71	0.362	123.27	51.	15.14	6511.	226.95	1.64	0.706
73	0.588	193.05	55.	0.09	6012.	0.31	0.00	0.813
74	0.586	192.57	55.	0.16	9020.	470.19	1.37	1.024
80	0.588	193.37	55.	7.03	6047.	14.35	0.14	0.815
81	0.589	193.71	55.	6.99	5919.	1.74	0.02	0.807
82	0.587	193.27	55.	7.14	6506.	64.58	0.50	0.845
83	0.587	193.36	55.	7.03	7013.	129.99	0.80	0.879
85	0.597	194.46	57.	0.25	9005.	668.95	1.98	1.033
93	0.605	194.09	57.	0.10	5308.	1.56	0.02	0.783
94	0.603	195.90	57.	4.11	5256.	2.09	0.03	0.779
95	0.603	195.88	57.	4.09	5279.	2.10	0.03	0.780
96	0.598	194.63	57.	4.05	9001.	665.87	1.97	1.033

TABLE III

## SCHEDULE OF TEST CONDITIONS (continued)

SR-3C-3 PROP FAN  
8' X 6' WIND TUNNEL TESTS  
NASA-LEWIS

RUN. NO.	MACH NO.	EQUIVALENT VELOCITY M/SEC	BLADE ANGLE DEG	TILT ANGLE DEG	PROP SPEED RPM	POWER KW	POWER COEFFICIENT	TIP MACH
97	0.599	194.90	57.	4.13	8503.	534.74	1.88	0.996
98	0.599	195.01	57.	4.18	8004.	416.54	1.75	0.960
99	0.601	195.35	57.	4.16	7507.	314.21	1.60	0.925
100	0.599	195.10	57.	4.09	7002.	222.22	1.40	0.888
101	0.600	195.19	57.	4.20	6496.	143.38	1.13	0.854
102	0.601	195.45	57.	4.07	5998.	79.28	0.79	0.833
103	0.602	195.61	57.	4.08	5501.	24.02	0.31	0.792
104	0.602	195.80	57.	7.06	5211.	2.08	0.03	0.775
105	0.602	195.68	57.	7.08	5507.	31.39	0.41	0.793
106	0.601	195.57	57.	7.01	6001.	86.80	0.87	0.833
107	0.602	195.82	57.	7.01	6506.	154.75	1.21	0.857
108	0.698	217.88	57.	-0.01	9015.	464.00	1.46	1.102
111	0.698	217.81	57.	0.16	9015.	473.68	1.49	1.102
117	0.702	218.63	57.	0.04	6280.	2.18	0.02	0.920
118	0.698	217.90	57.	5.02	7403.	172.38	0.98	0.989
119	0.699	218.11	57.	5.09	7013.	110.68	0.74	0.964
120	0.700	218.32	57.	5.04	6510.	40.37	0.34	0.932
121	0.700	218.21	57.	5.05	6202.	2.58	0.02	0.913
125	0.601	194.54	59.	-3.16	8788.	-25.73	-0.08	0.602
126	0.606	195.56	59.	-0.06	4993.	-22.15	-0.39	0.606
127	0.605	195.49	59.	-2.75	4925.	-19.03	-0.35	0.605
128	0.605	195.67	59.	7.21	5023.	10.18	0.18	0.766
129	0.604	195.35	59.	7.27	5523.	60.95	0.79	0.795
130	0.605	195.61	59.	7.25	6023.	122.38	1.23	0.826
131	0.604	195.47	59.	-2.65	6512.	-6.77	-0.05	0.604
135	0.605	194.58	59.	0.01	5118.	0.62	0.01	0.771
144	0.600	193.72	59.	-0.14	8771.	679.31	2.08	1.030
145	0.606	194.96	59.	6.84	5059.	1.05	0.02	0.768
146	0.604	194.57	59.	6.88	5489.	42.51	0.57	0.792
147	0.605	194.77	59.	6.98	5987.	99.78	1.03	0.824
148	0.603	194.43	59.	6.94	6493.	169.84	1.38	0.855
149	0.696	216.03	59.	-0.05	8995.	499.77	1.61	1.096
150	0.697	216.27	59.	-0.14	8502.	382.66	1.46	1.062
151	0.699	216.62	59.	-0.01	8004.	280.38	1.29	1.038
152	0.700	216.68	59.	-0.10	7497.	191.06	1.07	0.995
153	0.701	216.85	59.	-0.01	6998.	114.44	0.79	0.963
154	0.703	217.25	59.	0.05	6495.	46.92	0.40	0.933
155	0.700	217.16	59.	-0.05	6119.	1.38	0.01	0.907
156	0.700	216.78	59.	3.04	6060.	1.78	0.02	0.903
157	0.701	217.03	59.	2.97	6065.	1.58	0.02	0.905
158	0.697	216.13	59.	3.00	9000.	511.42	1.65	1.097
159	0.698	216.38	59.	2.98	8500.	393.45	1.51	1.062
160	0.699	216.52	59.	2.94	7995.	290.19	1.34	1.027
161	0.699	216.61	59.	2.90	7506.	203.76	1.13	0.994
162	0.700	216.68	59.	3.00	6998.	122.81	0.84	0.961
163	0.700	216.76	59.	2.94	6501.	54.74	0.47	0.930
164	0.699	216.62	59.	5.06	7296.	177.96	1.08	0.980
165	0.699	216.65	59.	5.04	6994.	130.74	0.90	0.961
166	0.700	216.78	59.	4.96	6497.	60.90	0.52	0.930
167	0.700	216.78	59.	4.96	6013.	2.40	0.03	0.900

TABLE III

## SCHEDULE OF TEST CONDITIONS (continued)

 SR-3C-3 PROP FAN  
 8' X 6' WIND TUNNEL TESTS  
 NASA-LEWIS

REG. NO.	MACH NO.	EQUIVALENT VELOCITY M/SEC	BLADE ANGLE DEG	TILT ANGLE DEG	PROP SPEED RPM	POWER KW	POWER COEFFICIENT	TIP MACH
168	0.797	233.94	59.	-0.10	9000.	306.39	1.07	1.172
173	0.799	234.24	59.	0.06	7175.	1.86	0.01	1.053
174	0.794	233.57	59.	4.07	9001.	325.45	1.14	1.170
175	0.794	233.55	59.	4.00	8502.	225.95	0.94	1.135
176	0.795	233.71	59.	3.96	8004.	138.80	0.69	1.102
177	0.796	233.81	59.	3.94	7497.	59.49	0.36	1.070
178	0.796	233.92	59.	4.04	7101.	2.83	0.02	1.046
180	0.699	218.00	61.	0.25	8815.	475.72	2.29	1.086
188	0.706	219.07	61.	0.06	5267.	1.55	0.02	0.863
189	0.708	219.44	61.	0.04	5294.	5.32	0.08	0.866
190	0.702	218.73	61.	4.91	4998.	240.90	1.77	0.964
191	0.702	218.64	61.	5.00	4491.	173.29	1.47	0.932
192	0.702	218.74	61.	4.99	5992.	98.41	1.06	0.902
193	0.703	218.81	61.	4.07	5495.	34.46	0.48	0.873
194	0.702	218.72	61.	4.22	5195.	2.16	0.04	0.856
195	0.795	235.23	61.	0.12	9000.	554.30	1.91	1.171
201	0.805	236.61	61.	0.10	6158.	1.81	0.02	0.998
202	0.805	236.66	61.	0.06	6149.	1.60	0.02	0.997
203	0.798	235.62	61.	1.98	8990.	546.37	1.89	1.173
204	0.799	235.83	61.	2.06	8508.	421.41	1.72	1.140
205	0.800	236.04	61.	1.98	8005.	307.33	1.51	1.107
206	0.800	236.00	61.	2.03	7503.	212.41	1.27	1.075
207	0.802	236.29	61.	1.89	7008.	128.81	0.94	1.045
208	0.802	236.38	61.	2.06	6495.	53.11	0.49	1.015
209	0.801	236.31	61.	1.93	6086.	2.21	0.02	0.990
210	0.802	236.29	61.	2.06	6095.	2.11	0.02	0.992
211	0.801	236.20	61.	3.89	7193.	162.88	1.10	1.056
212	0.802	236.34	61.	4.01	6999.	129.26	0.95	1.045
213	0.802	236.37	61.	3.91	6500.	56.42	0.52	1.015
214	0.802	236.45	61.	3.94	6090.	2.64	0.03	0.992
215	0.800	236.01	61.	5.92	6025.	2.71	0.03	0.986
216	0.844	241.66	61.	-0.04	9000.	438.92	1.58	1.211
221	0.849	242.36	61.	-0.09	6622.	2.29	0.02	1.063
222	0.851	242.54	61.	-0.04	6628.	2.18	0.02	1.064
223	0.844	241.71	61.	3.92	7102.	78.87	0.58	1.087
224	0.845	241.98	61.	3.91	7005.	62.99	0.48	1.082
225	0.844	241.86	61.	3.94	6568.	2.62	0.02	1.056
226	0.844	241.85	61.	3.90	6573.	2.62	0.02	1.056
227	0.840	241.22	61.	3.96	9000.	453.73	1.63	1.208
230	0.789	234.46	63.	0.10	9005.	650.85	2.23	1.166
237	0.795	235.47	63.	0.08	5736.	-1.29	-0.02	0.965
238	0.799	235.89	63.	-0.05	5762.	-0.01	-0.01	0.971
239	0.794	235.34	63.	3.94	5738.	7.36	0.10	0.965
240	0.790	234.63	63.	4.00	6998.	192.03	1.40	1.034
241	0.791	234.74	63.	4.00	6502.	113.32	1.03	1.005
242	0.790	234.68	63.	4.00	5997.	43.11	0.50	0.975
243	0.790	234.63	63.	3.98	5640.	0.39	0.01	0.955
244	0.840	241.03	63.	0.10	9031.	547.42	1.96	1.208
250	0.846	241.79	63.	0.09	6202.	1.29	0.01	1.036
251	0.839	240.91	63.	2.03	9010.	535.55	1.93	1.206

TABLE III

## SCHEDULE OF TEST CONDITIONS (continued)

 SR-3C-3 PROP FAN  
 8' X 6' WIND TUNNEL TESTS  
 NASA-LEWIS

RUN. NO.	MACH NO.	EQUIVALENT VELOCITY M/SEC	BLADE ANGLE DEG	TILT ANGLE DEG	PROP SPEED RPM	POWER KW	POWER COEFFICIENT	TIP MACH
252	0.840	241.06	63.	1.93	8503.	407.32	1.75	1.173
253	0.840	241.08	63.	2.09	8009.	298.03	1.53	1.140
254	0.842	241.29	63.	2.02	7507.	201.97	1.26	1.109
255	0.843	241.43	63.	2.01	7008.	116.91	0.90	1.079
256	0.843	241.44	63.	1.99	6501.	44.26	0.43	1.049
257	0.842	241.42	63.	2.07	6168.	1.39	0.02	1.031
258	0.846	241.81	63.	3.95	7107.	127.43	0.94	1.088
259	0.846	241.76	63.	3.96	7032.	115.13	0.88	1.083
260	0.846	241.86	63.	3.92	6482.	35.37	0.34	1.031
261	0.846	241.93	63.	4.03	6231.	1.84	0.02	1.038
262	0.840	241.01	63.	0.01	9734.	731.36	2.09	1.258
263	0.891	247.28	63.	0.10	9994.	609.45	1.69	1.317
264	0.846	241.76	64.	0.03	5777.	1.40	0.02	1.012
265	0.846	241.40	64.	0.03	9083.	643.29	2.27	1.215
266	0.844	242.23	64.	4.05	6993.	161.85	1.26	1.084
267	0.849	242.30	64.	4.09	6501.	03.23	0.81	1.036
274	0.850	242.31	64.	4.13	6003.	15.50	0.19	1.028
275	0.850	242.27	64.	4.04	5889.	2.14	0.03	1.021
276	0.849	248.12	64.	0.17	6471.	2.91	0.03	1.094
277	0.898	247.79	64.	0.17	9996.	679.73	1.88	1.320
278	0.894	248.10	64.	0.10	9504.	571.68	1.85	1.288
279	0.897	248.54	64.	0.17	9010.	456.56	1.74	1.257
280	0.900	248.64	64.	0.17	8507.	344.27	1.56	1.224
281	0.901	249.27	64.	0.09	8005.	229.66	1.25	1.195
282	0.906	249.44	64.	0.14	7511.	135.84	0.90	1.166
283	0.907	249.32	64.	0.12	7003.	58.84	0.48	1.135
284	0.905	249.11	64.	-0.01	6554.	2.61	0.03	1.107
285	0.905	122.93	48.	0.06	4507.	0.08	0.00	0.952
286	0.361	122.93	48.	0.13	8999.	529.90	1.46	0.907
289	0.358	122.15	48.	7.99	4405.	0.23	0.01	0.543
291	0.359	122.63	48.	8.13	8995.	535.14	1.47	0.908
301	0.359	122.45	48.	8.04	8502.	440.84	1.44	0.866
302	0.357	121.88	48.	8.02	8000.	353.15	1.38	0.824
303	0.359	122.41	48.	8.04	7501.	276.01	1.31	0.782
304	0.356	121.71	48.	7.96	6999.	207.59	1.21	0.741
305	0.357	121.96	48.	8.03	6496.	149.79	1.09	0.700
306	0.357	122.08	48.	8.02	5998.	102.15	0.95	0.661
307	0.357	122.17	48.	7.98	5499.	62.97	0.76	0.624
308	0.359	122.61	48.	8.07	4996.	29.43	0.47	0.586
309	0.359	122.79	48.	8.07	4494.	3.50	0.08	0.550
310	0.359	123.04	48.	7.99	4299.	0.84	0.02	0.547
311	0.360	122.96	48.	14.91	6501.	167.13	1.22	0.703
312	0.360	122.77	48.	14.89	5994.	116.62	1.08	0.663
313	0.360	122.83	48.	14.83	5494.	74.81	0.90	0.624
314	0.360	122.83	48.	14.83	4996.	40.50	0.65	0.587
315	0.361	123.16	48.	14.89	4493.	13.00	0.29	0.551
316	0.361	123.19	48.	14.83	4212.	0.66	0.02	0.531
317	0.360	123.03	48.	14.88	9006.	558.42	1.53	0.909
318	0.358	122.02	48.	10.87	9000.	543.38	1.49	0.909
319	0.350	122.22	48.	10.87	4366.	1.06	0.03	0.542
320	0.359	122.72	48.	10.92				
321	0.359	122.72	48.	10.92				

TABLE III

## SCHEDULE OF TEST CONDITIONS (concluded)

SR-3C-3 PROP FAN  
8' X 6' WIND TUNNEL TESTS  
NASA-LEWIS

RIG. NO.	MACH NO.	EQUIVALENT VELOCITY M/SEC	BLADE ANGLE DEG	TILT ANGLE DEG	PROP SPEED RPM	POWER KW	POWER COEFFICIENT	TIP MACH
322	0.350	122.10	48.	10.99	9001.	542.68	1.49	0.909
323	0.358	122.09	48.	10.96	8502.	445.56	1.45	0.867
324	0.358	122.03	48.	10.83	7999.	358.09	1.40	0.824
325	0.360	122.81	48.	10.89	7501.	280.69	1.33	0.784
326	0.360	122.67	48.	10.92	7003.	213.28	1.24	0.743
327	0.360	122.69	48.	10.84	6500.	155.40	1.13	0.702
328	0.359	122.41	48.	10.94	5999.	106.32	0.98	0.682
329	0.358	122.12	48.	10.84	5495.	65.97	0.79	0.623
330	0.359	122.68	48.	10.84	4996.	32.97	0.53	0.587
331	0.360	122.88	48.	10.88	4493.	6.77	0.15	0.551
332	0.361	123.24	48.	10.90	4373.	1.21	0.03	0.543
333	0.700	217.17	58.	0.04	6016.	1.77	0.02	0.902
334	0.696	216.57	58.	0.12	9000.	517.66	1.65	1.099
335	0.700	217.28	58.	2.99	6016.	2.29	0.02	0.902
336	0.694	216.32	58.	3.07	9005.	532.60	1.69	1.098
337	0.695	216.54	58.	3.17	8503.	409.82	1.54	1.063
338	0.698	216.92	58.	3.08	7999.	300.58	1.36	1.029
339	0.699	217.08	58.	3.06	7501.	210.65	1.16	0.996
340	0.700	217.33	58.	2.95	6999.	129.86	0.88	0.963
341	0.701	217.58	58.	3.00	6501.	59.58	0.50	0.933
342	0.702	217.71	58.	3.04	6037.	2.41	0.03	0.905
343	0.698	217.00	58.	5.05	7491.	216.08	1.19	0.995
344	0.699	217.21	58.	4.96	7000.	137.89	0.93	0.963
345	0.699	217.14	58.	5.01	6497.	66.30	0.56	0.931
346	0.700	217.31	58.	5.01	5983.	2.18	0.02	0.900
347	0.696	216.60	58.	5.06	9000.	543.23	1.72	1.099
348	0.696	216.67	58.	5.14	8505.	425.65	1.60	1.064
349	0.840	241.69	66.	0.13	8536.	668.73	2.80	1.177
350	0.845	242.28	66.	0.09	8605.	673.34	2.76	1.186
351	0.852	243.19	66.	0.18	5216.	1.90	0.04	0.990
352	0.885	247.41	66.	-0.10	9232.	703.90	2.43	1.261
353	0.898	248.95	66.	0.04	5704.	2.08	0.03	1.056

\*\*\* END FILE \*\*\*



TABLE IV

HAMILTON STANDARD COMPUTER CODES USED FOR  
BLADE DYNAMIC RESPONSE ANALYSIS

Code Designation	Description
HS/H039	Potential flow field analysis, used to determine the influence of the nacelle on the inflow to the rotor.
HS/H045	Lifting line, quasi-static performance strip analysis, 2-D airfoil section data, Goldstein wake induction, azimuthal variations.
HS/H337	Lifting line, quasi-static performance strip analysis, 2-D airfoil section data, skewed wake induction, azimuthal variations.
HS/F194	Distributes airloads over finite element grid.
MSC/NASTRAN	Finite element analysis used for calculating vibratory mode shapes and frequencies, and dynamic responses of Prop-Fan model blades.
STRAINNP	Converts element stresses from MSC/NASTRAN to strains at the strain gage locations.

TABLE V RESULTS OF THE 1P RESPONSE CALCULATIONS

Case No.	RDG No.	Blade Angle 0.75R deg	Tilt Angle deg	Mach No.	Prop Speed RPM	Shaft Power kW	Equiv. Airspeed km/hr	Cp Power Coeff.	EF Excitation Factor	CALCULATED/MEASURED* Strain Sensitivity $\mu$ m/m/deg		
										Inboard Bending Gage	Mid-blade Bending Gage	Shear Gage
1	38	47.7	8.25	.361	9044	508	440	1.38	3.88	154/82	52/63	10/5.8
2	83	54.6	7.03	.587	7013	130	693	0.80	8.21	106/59	17/43	52/38
3	100	57.8	4.09	.599	7001	222	700	1.40	4.86	114/62	19/43	53/42
4	118	57.8	5.02	.698	7403	172	781	0.98	7.45	117/60	21/46	50/29
5	191	61.5	5.00	.702	6491	173	784	1.47	7.46	113/64	19/45	54/48
6	204	61.5	2.06	.799	8508	421	846	1.72	3.57	134/89	28/62	31/51
6A**	204	61.5	2.06	"	"	"	"	"	"	118/89	24/62	41/51

\*Measured inboard bending is averaged between gages BG1-1, 3-1 and 5-1

Measured mid-blade bending, gage BG5-2

Measured shear is averaged between gages BG1-3 and 5-3

Strain sensitivity is defined as micro-strain/EF

\*\*Case 6A includes CQUAD4 elements and K6ROT = 10,000 in MSC/NASTRAN

TABLE VISR-3C-3 MODEL 1-P VIBRATORY STRAIN TEST CONDITIONS

Measurements of 1-P vibratory blade strain data, at each Mach number tested, were acquired at the following combinations of shaft tilt angle and blade angle ( $\theta$  3/4), over the allowable RPM range. The data are plotted as 1-P micro-strain vs. RPM in the indicated figure.

<u>Figure</u>	<u>Mach number</u>	<u>Tilt Angle Deg.</u>	<u>Blade Angle Deg.</u>
11	0.36	8.0	44.5
		8.0	48.0
		15.0	48.0
		15.0	51.6
12	0.6	7.0	54.6
		4.0	57.8
		7.0	57.8
		7.0	59.1
		7.2	59.4
13	0.7	5.0	57.8
		5.0	58.4
		3.0	59.1
		5.0	59.1
		5.0	61.5
14	0.8	4.0	59.1
		2.0	61.5
		4.0	61.5
		4.0	62.5
15	0.84	2.0	62.5
		4.0	62.5
16	0.85	4.0	62.5
		4.0	63.7

ORIGINAL PAGE IS  
OF POOR QUALITY



FIGURE 1. SR-3C-3 MODEL PROP-FAN INSTALLED IN THE NASA-LEWIS 8X6 TUNNEL.

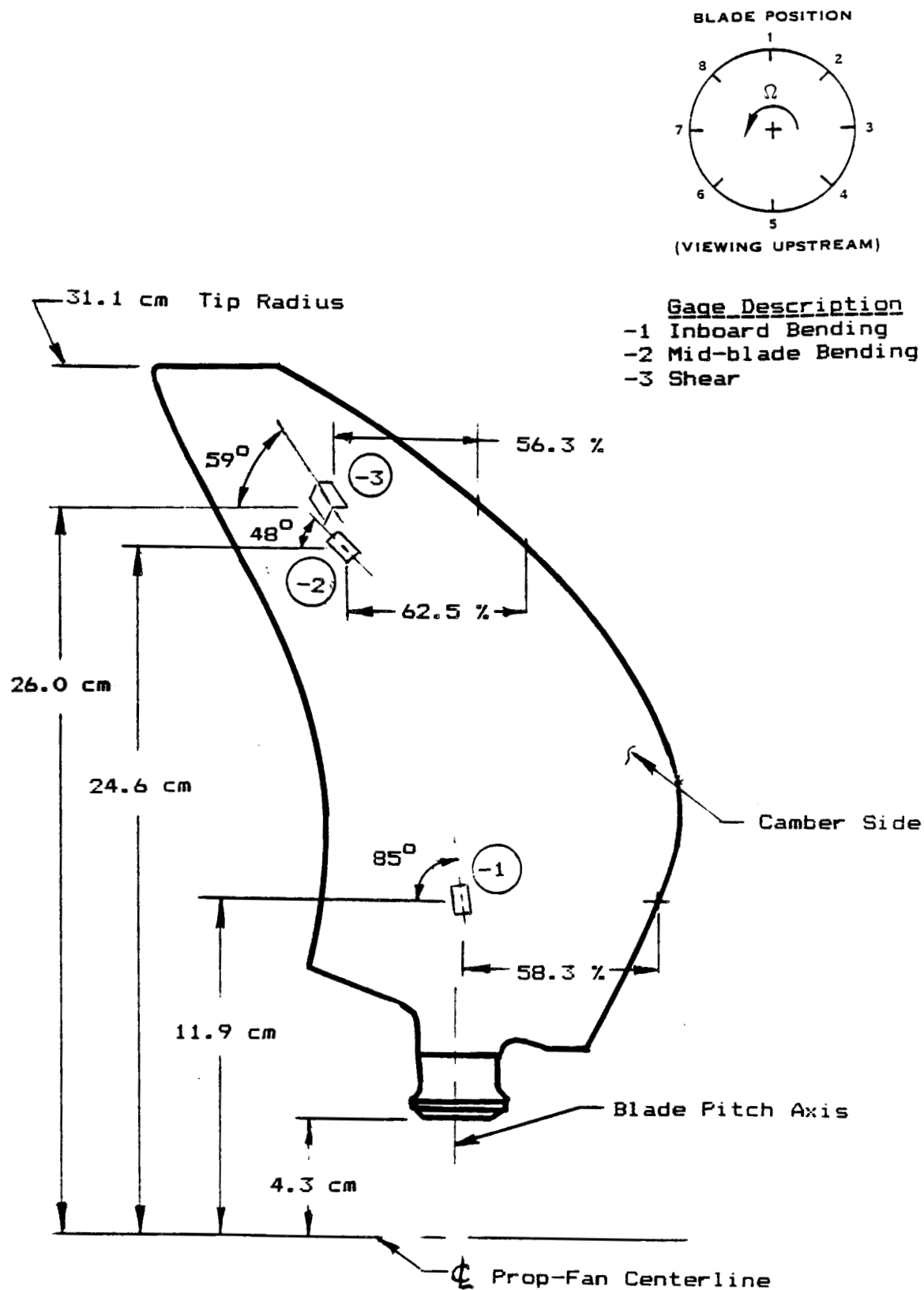


Figure 2 SR-3C-3 Prop-Fan Schematic showing the strain gage locations, NASA/Lewis 8 X 6 Wind Tunnel tests.

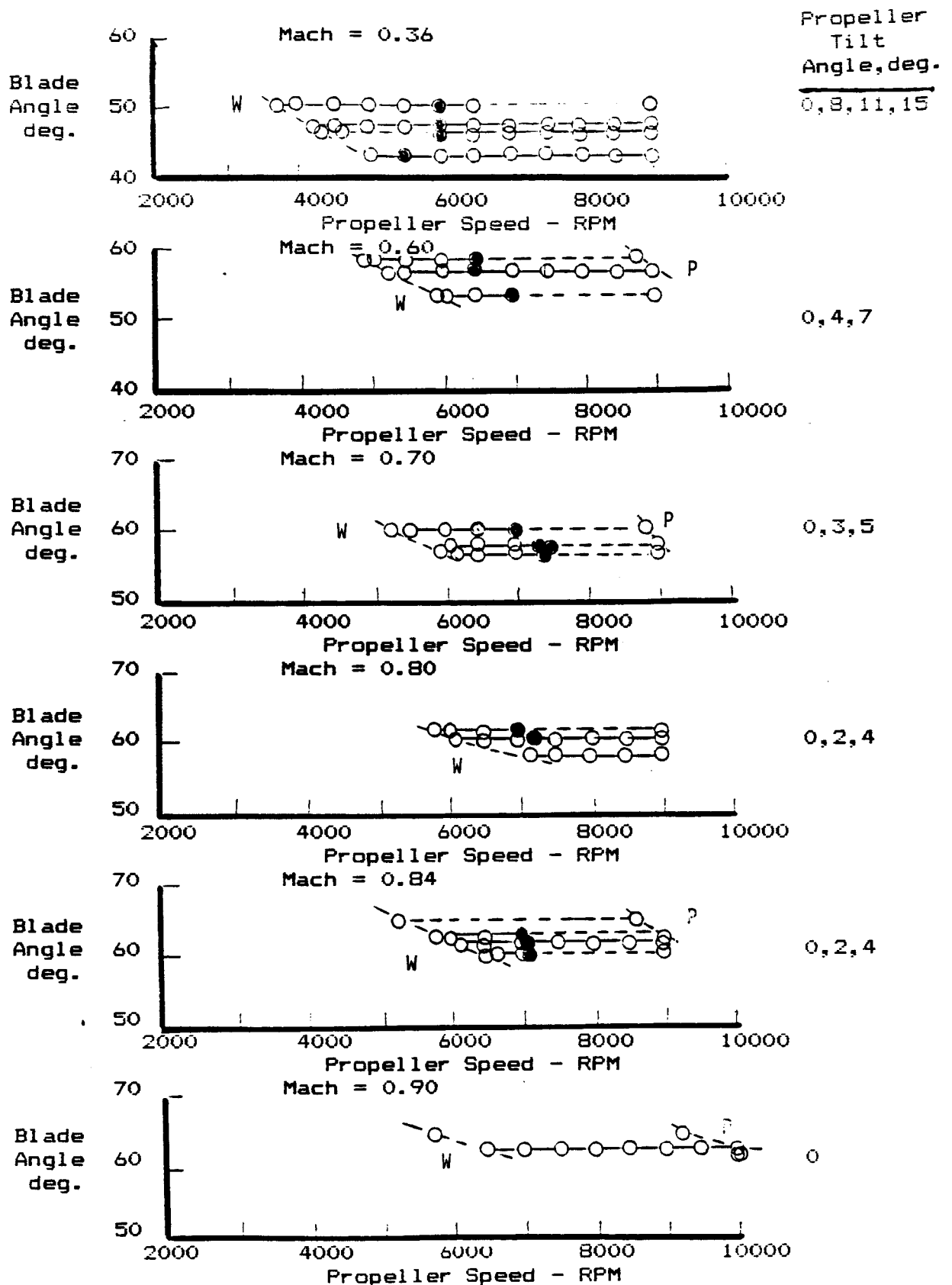
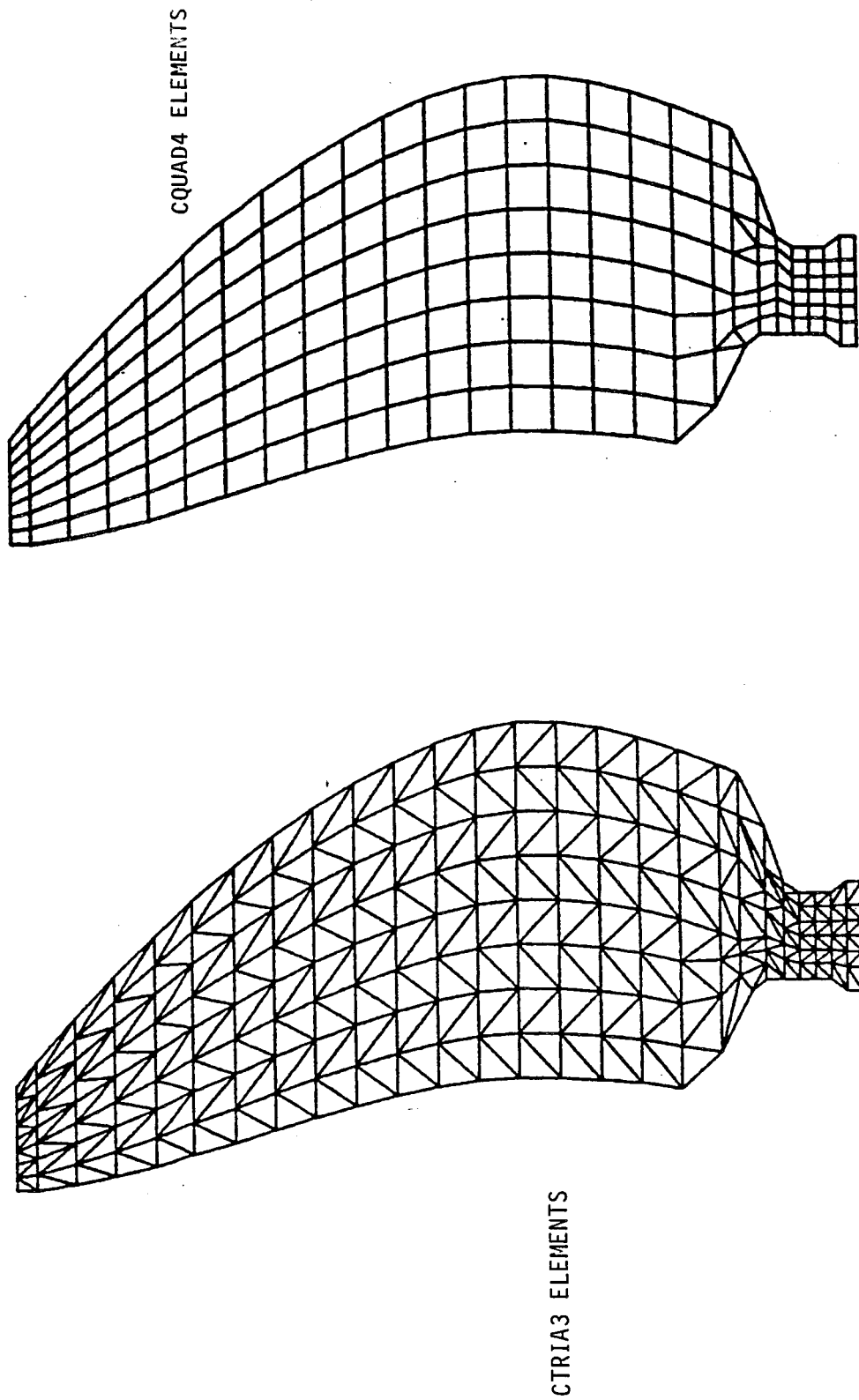


Figure 3 Test envelopes for the SR-3C-3 model Prop-Fan 8 X 6 wind tunnel tests at NASA/Lewis.

- = Strain Limit at Max Inflow Angle
- W = Windmill Speed
- P = Rq Power Limit



ORIGINAL NASTRAN MODEL

MODIFIED NASTRAN MODEL

Figure 4 SR-3C-3 FINITE ELEMENT MODELS

# 1P DYNAMIC ANALYSIS

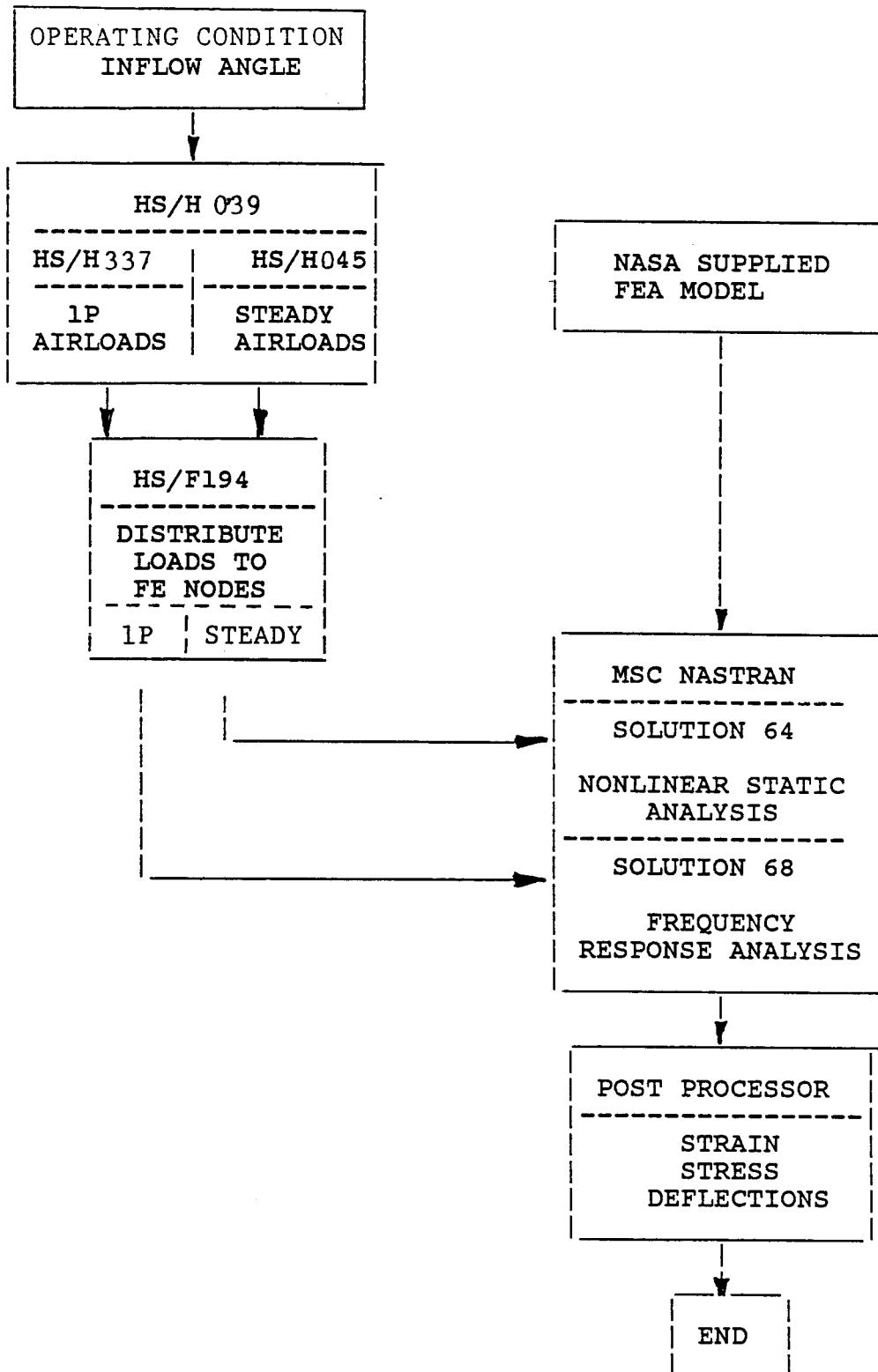


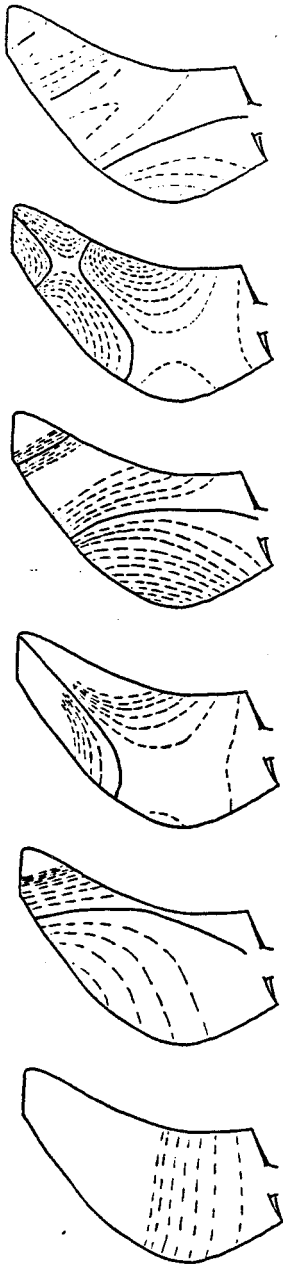
FIGURE 5. DYNAMIC RESPONSE PREDICTION METHOD



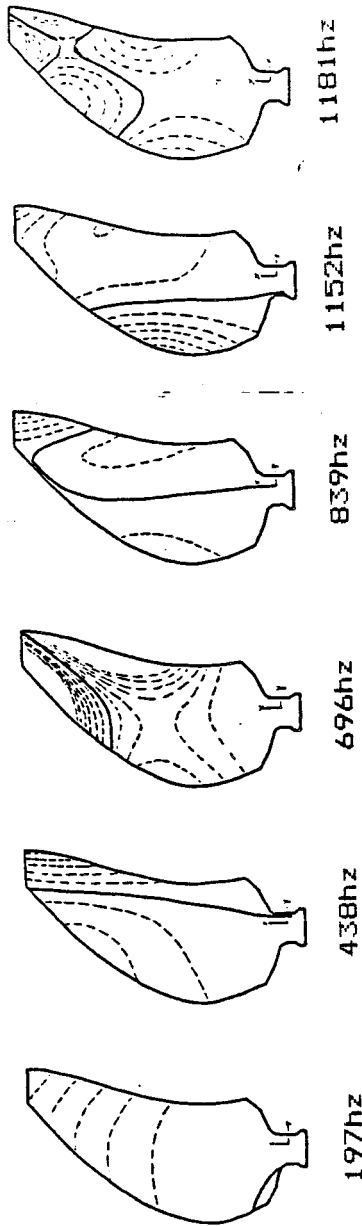
---MODE---

1 2 3 4 5 6

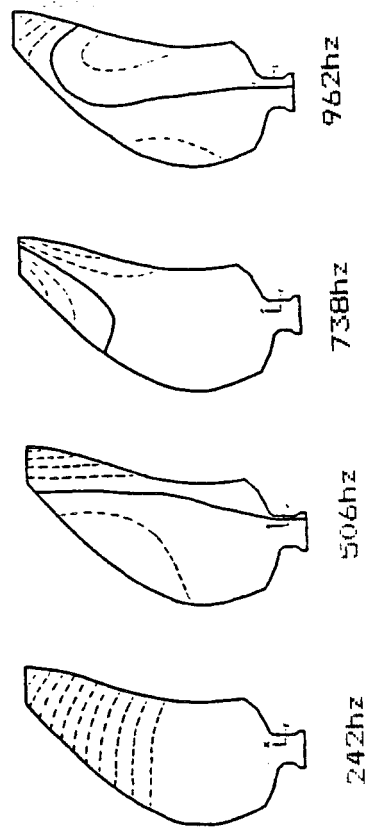
Holographic  
Patterns  
Non-Rotating



Calculated  
Patterns  
Non-Rotating



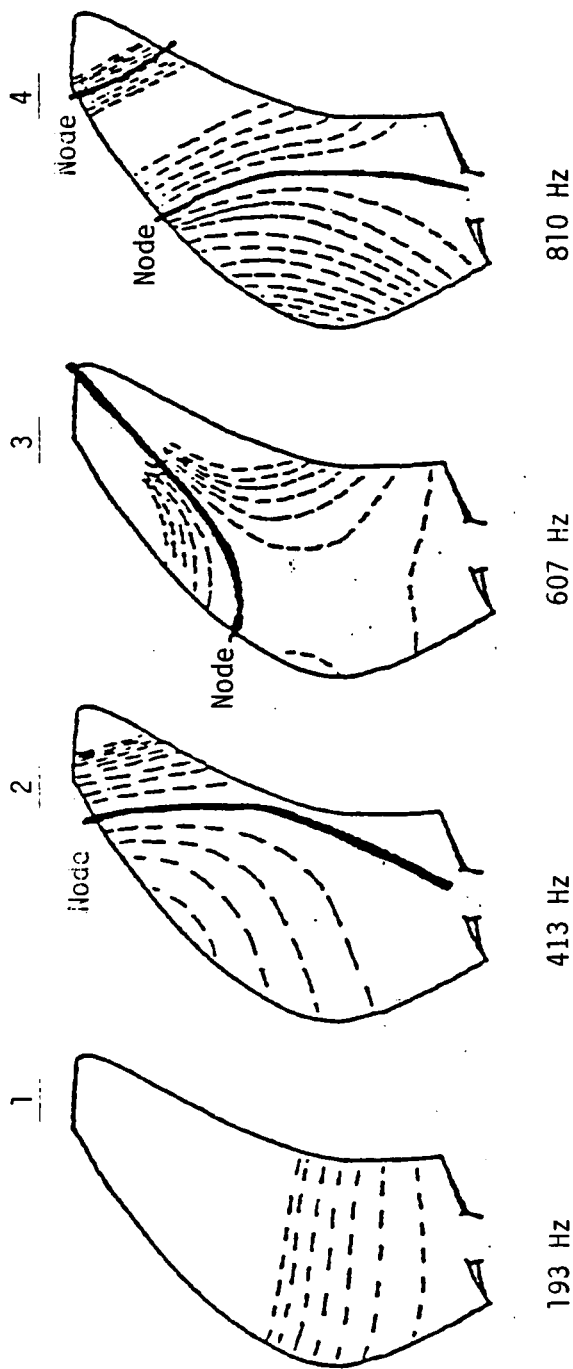
Calculated  
Patterns  
8600 RPM



-----Constant Displacement Contour

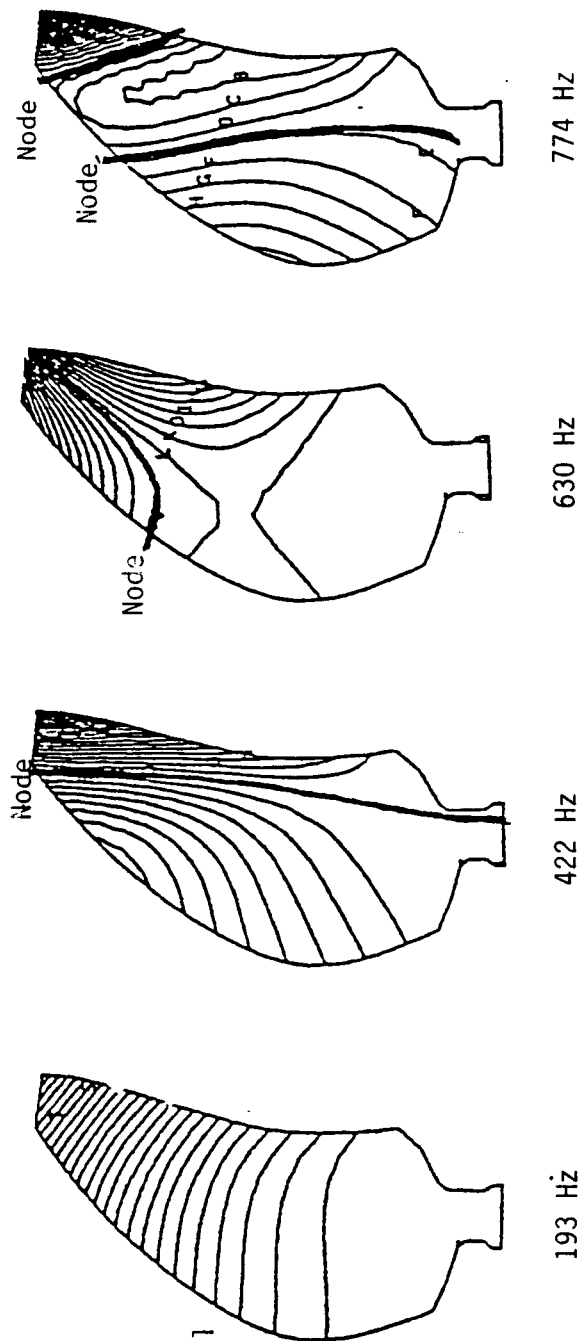
——Node Line

Figure 6A. Calculated and Measured Mode Shape Patterns and Frequencies, NASA/Lewis SR-3C-3 Model Prop-Fan Tests.



Holographic  
Patterns  
Non-Rotating

41



NASTRAN  
Calculated  
CQUAD4 Model

Note: Stiffness  
'adjusted' to match  
1st mode frequency

CALCULATED AND MEASURED MODE SHAPE  
PATTERNS AND FREQUENCIES

SR-3C-3

Figure 6B

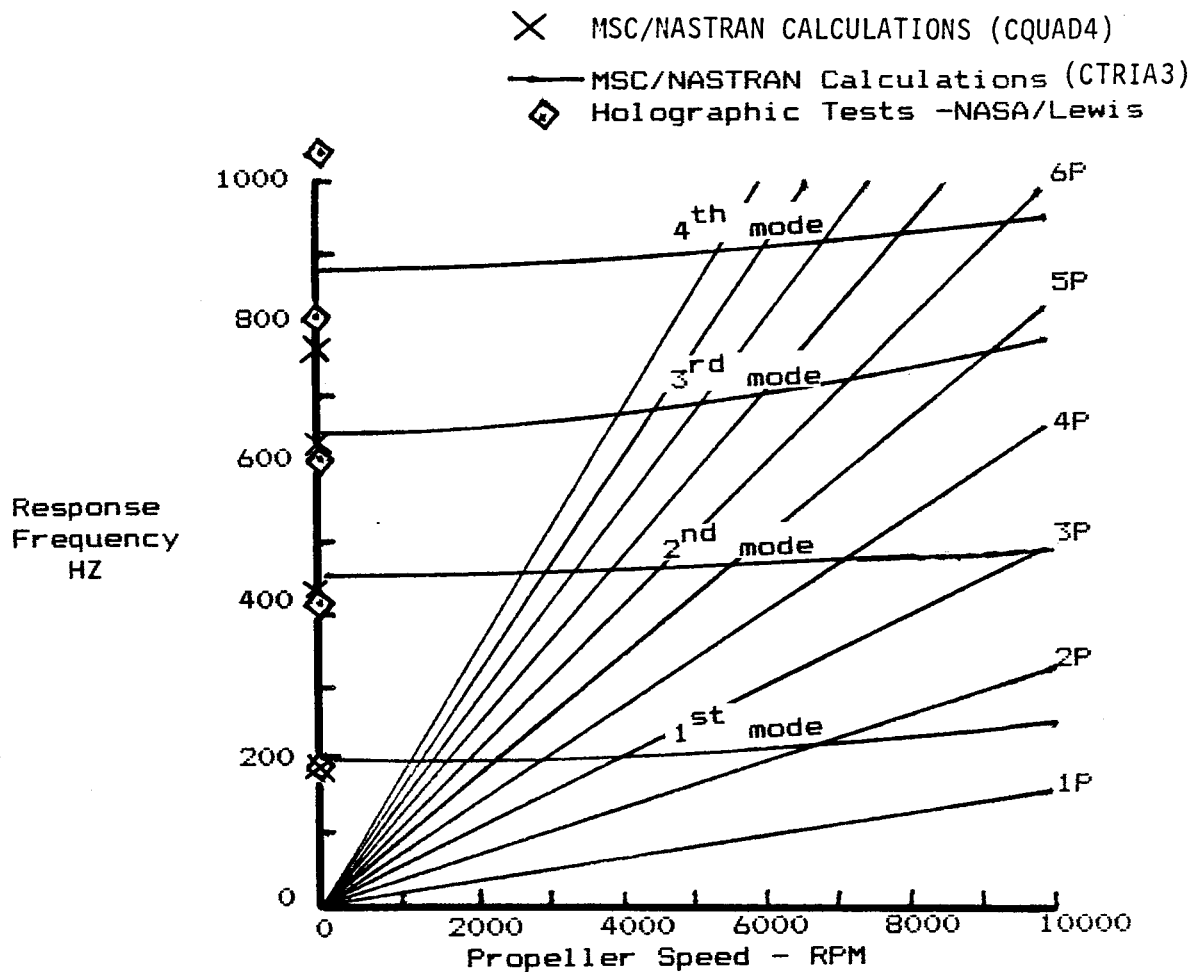


Figure 7 SR-3C-3 model Prop-Fan blade, natural frequencies

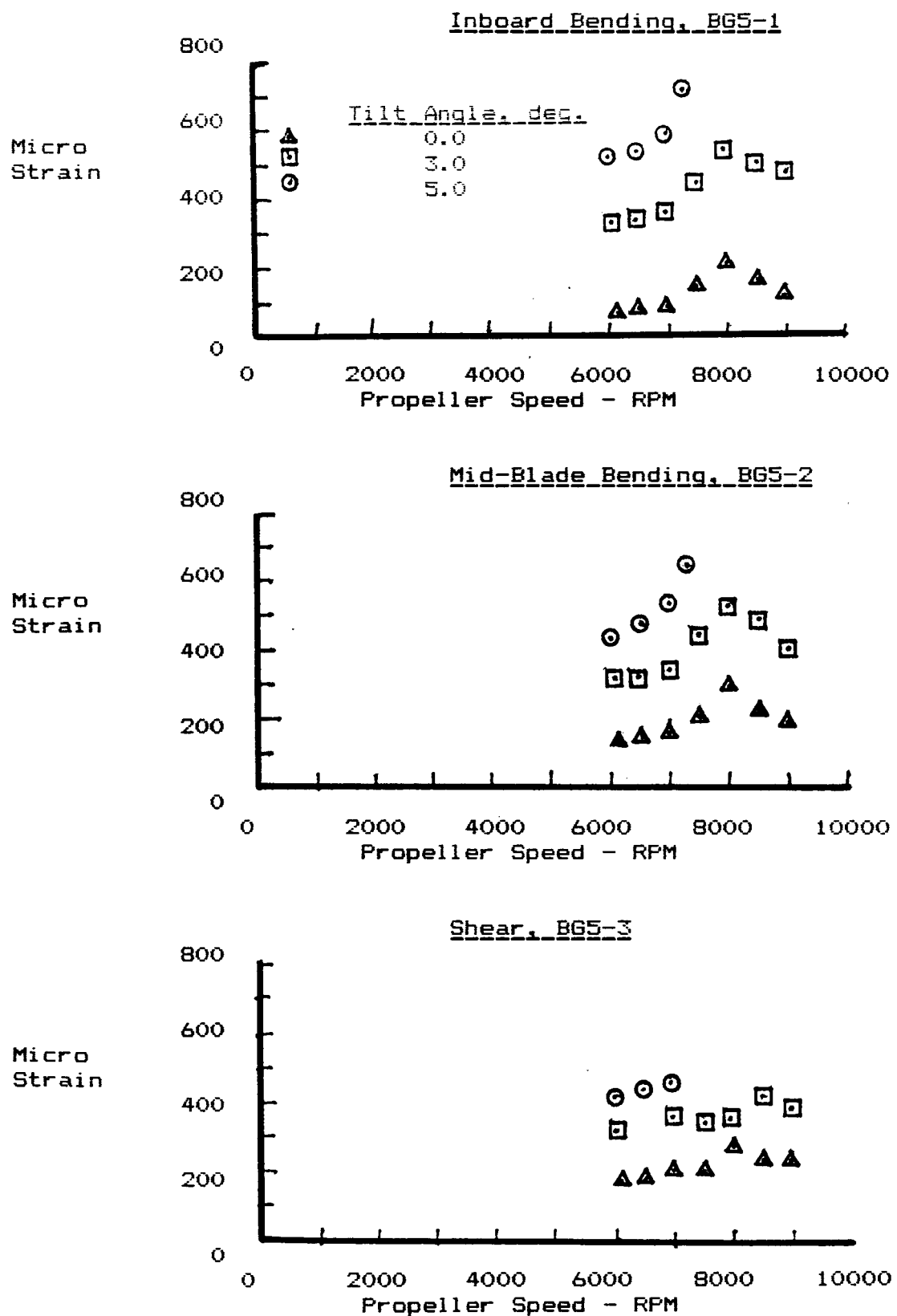


Figure 8 Total Vibratory strain vs propeller speed for the SR-3C-3 model Prop-Fan blade response tests, NASA/Lewis. Mach Number = 0.7, Blade Angle = 59.0 Deg.

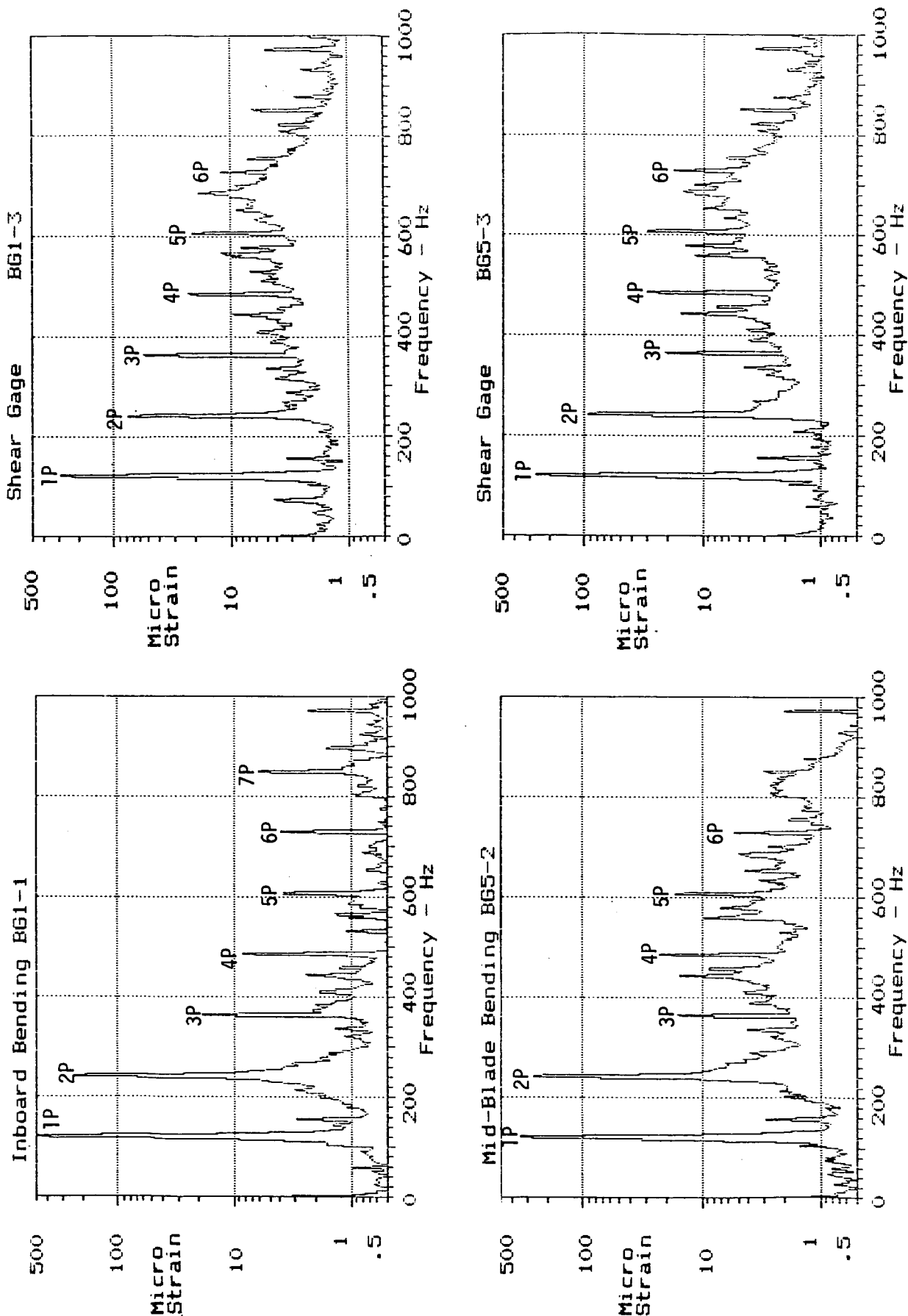
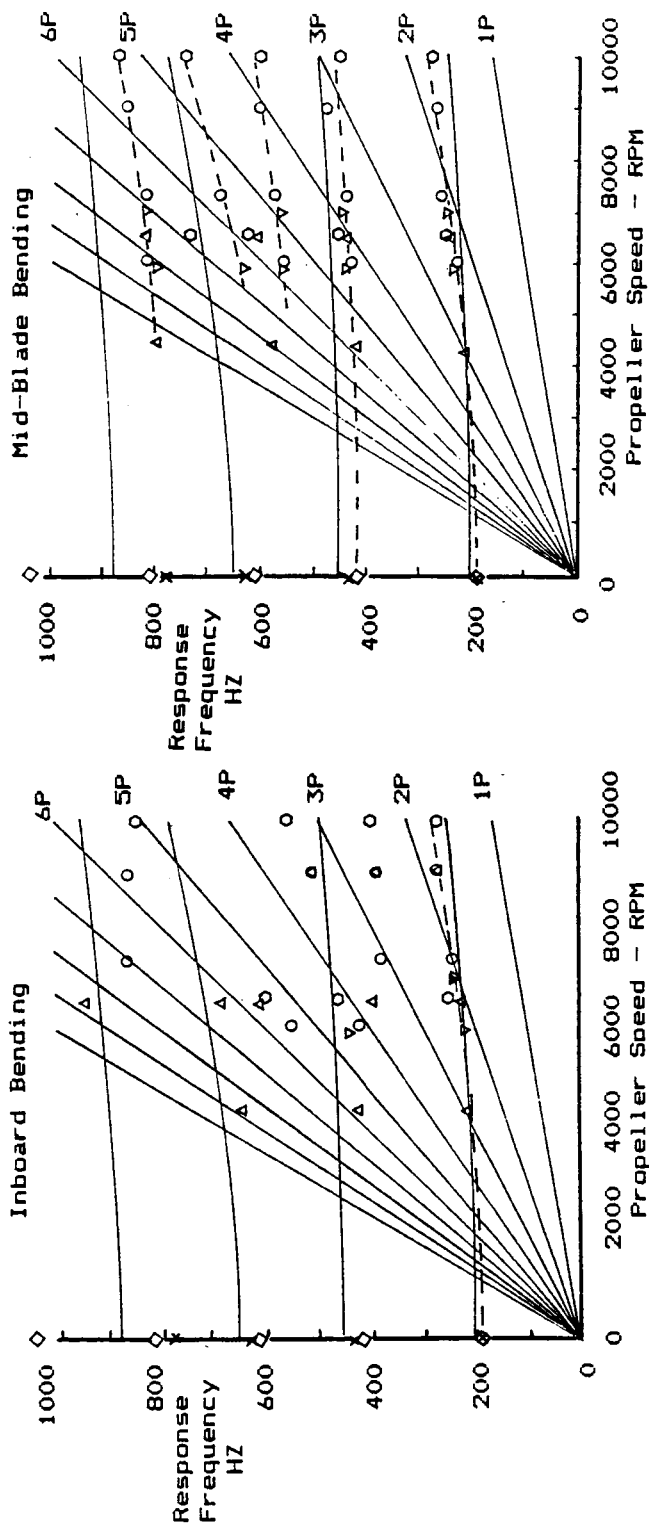


Figure 9 Spectral plots for the SR-3C-3 Prop-Fan tests, NASA/Lewis 8 X 6 Wind Tunnel, 7300 RPM, 59.0 degree blade angle, 5 degree tilt.



X Finite Element Calc.-CQUAD4  
 Finite Element Calc.-CTR1A3  
 Holograph test - NASA

Mach	8 X 6
0.7	Wind
0.36	Tunnel
0.85	Tests
0.9	

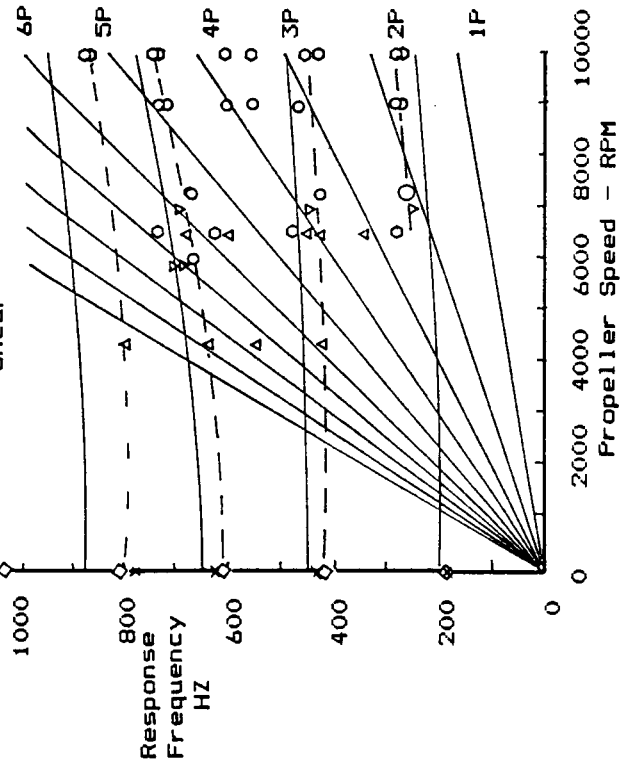


Figure 10 SR-3C-3 Prop-Fan modal Response Frequencies  
 NASA/Lewis 8 X 6 wind tunnel tests.

ONCE PER REV.  
VIBRATORY STRAIN

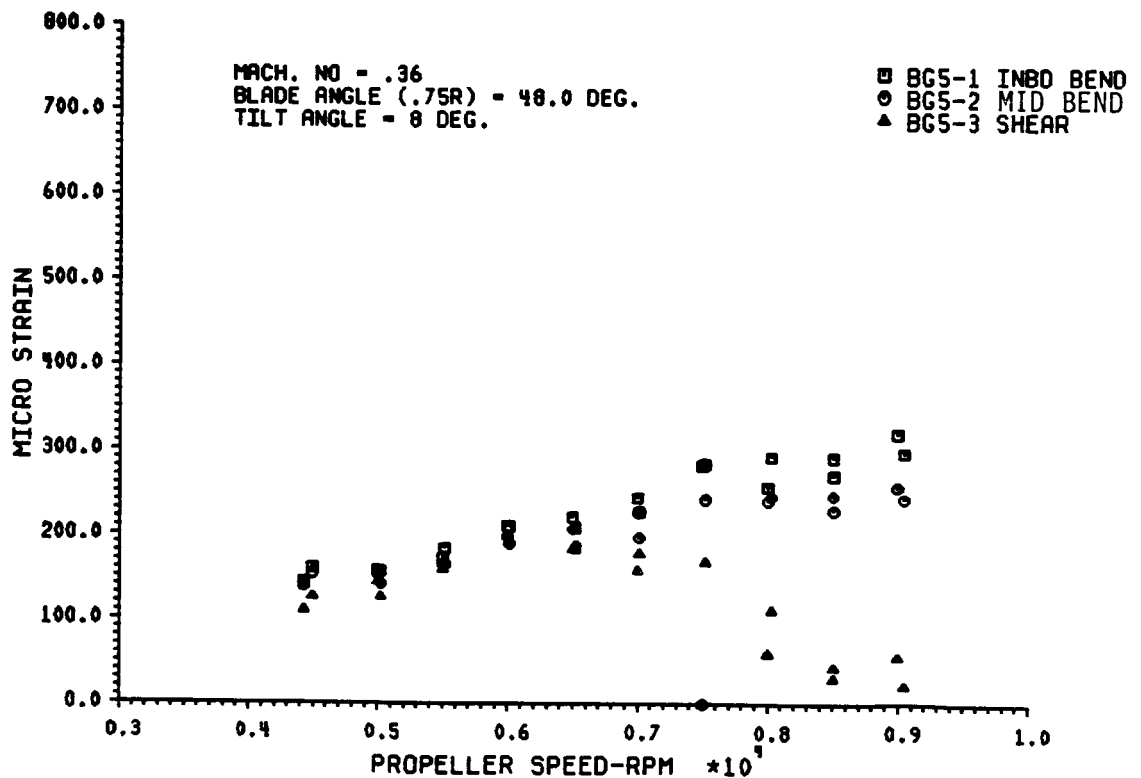
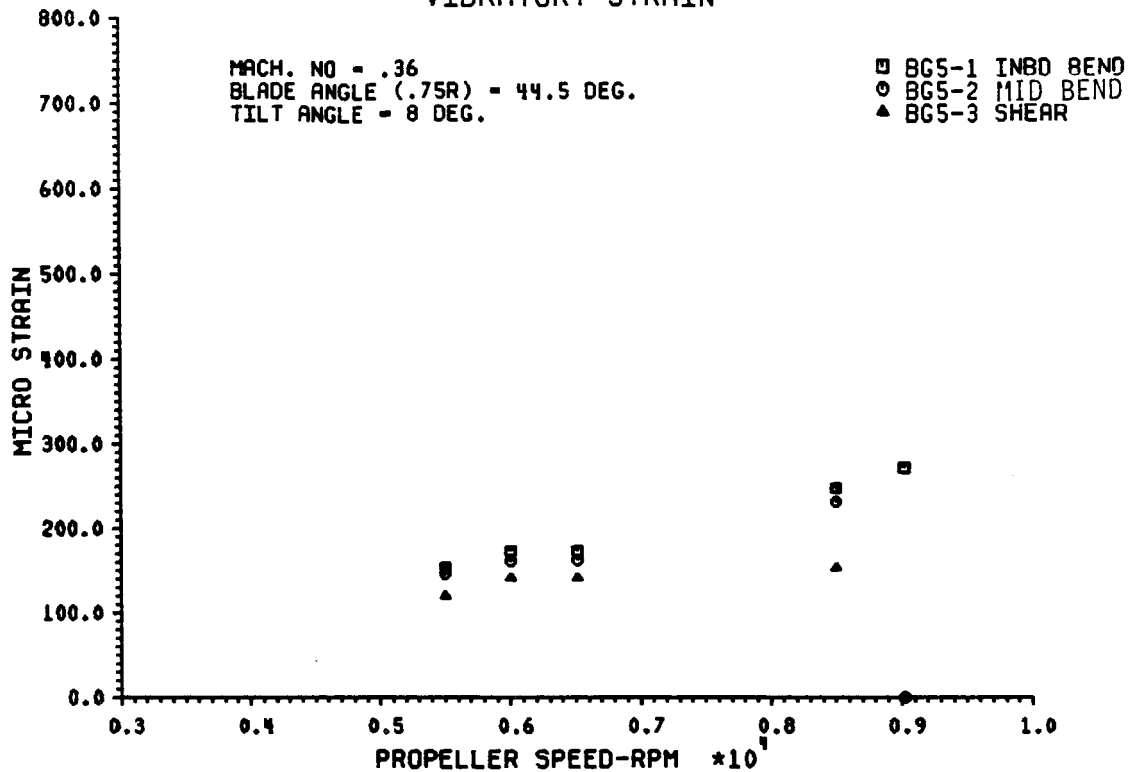


Figure 11 SR-3C-3 BLADE DYNAMIC RESPONSE TO  
ANGULAR INFLOW - 0.36 MACH

# ONCE PER REV. VIBRATORY STRAIN

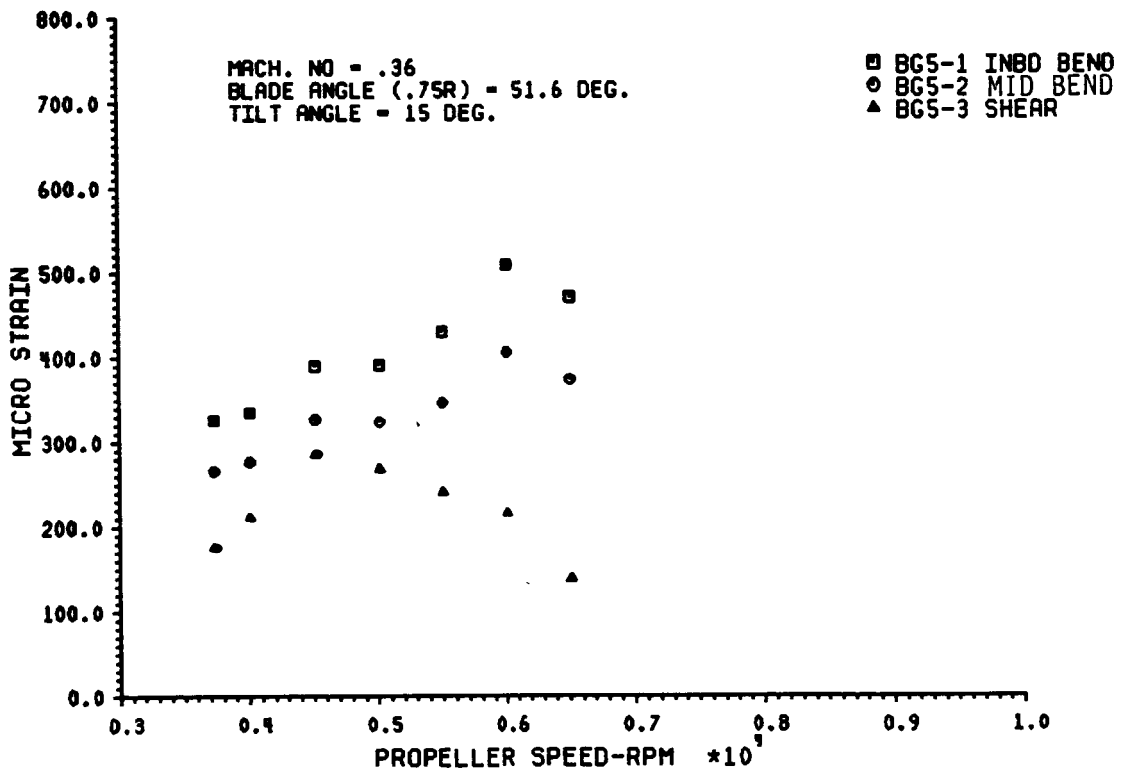
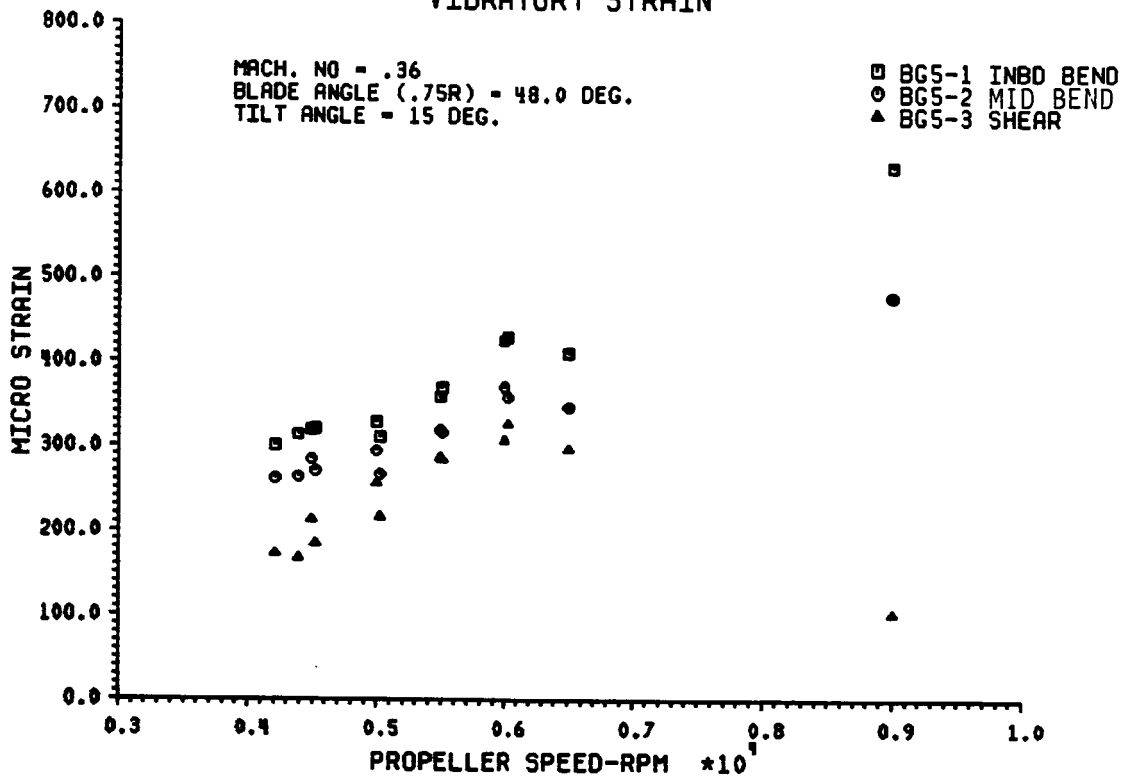


Figure 11 SR-3C-3 BLADE DYNAMIC RESPONSE TO  
ANGULAR INFLOW - 0.36 MACH



ONCE PER REV.  
VIBRATORY STRAIN

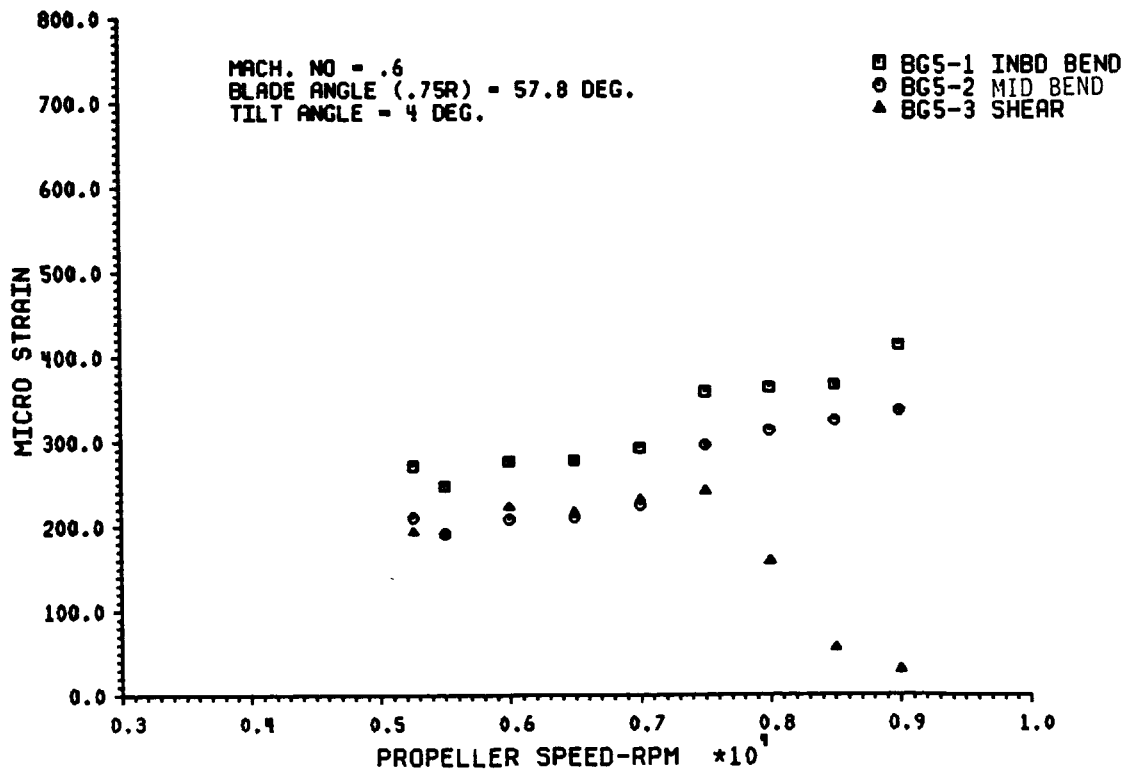
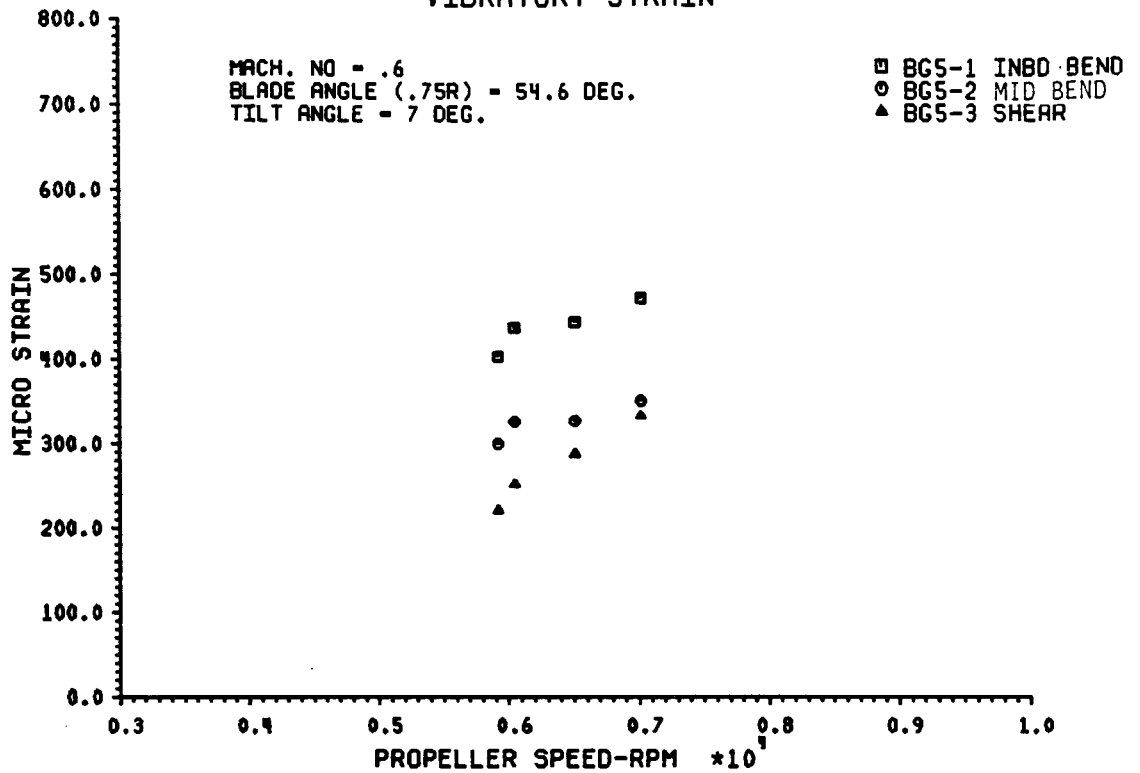


Figure 12 SR-3C-3 BLADE DYNAMIC RESPONSE TO  
ANGULAR INFLOW - 0.6 MACH

# ONCE PER REV. VIBRATORY STRAIN

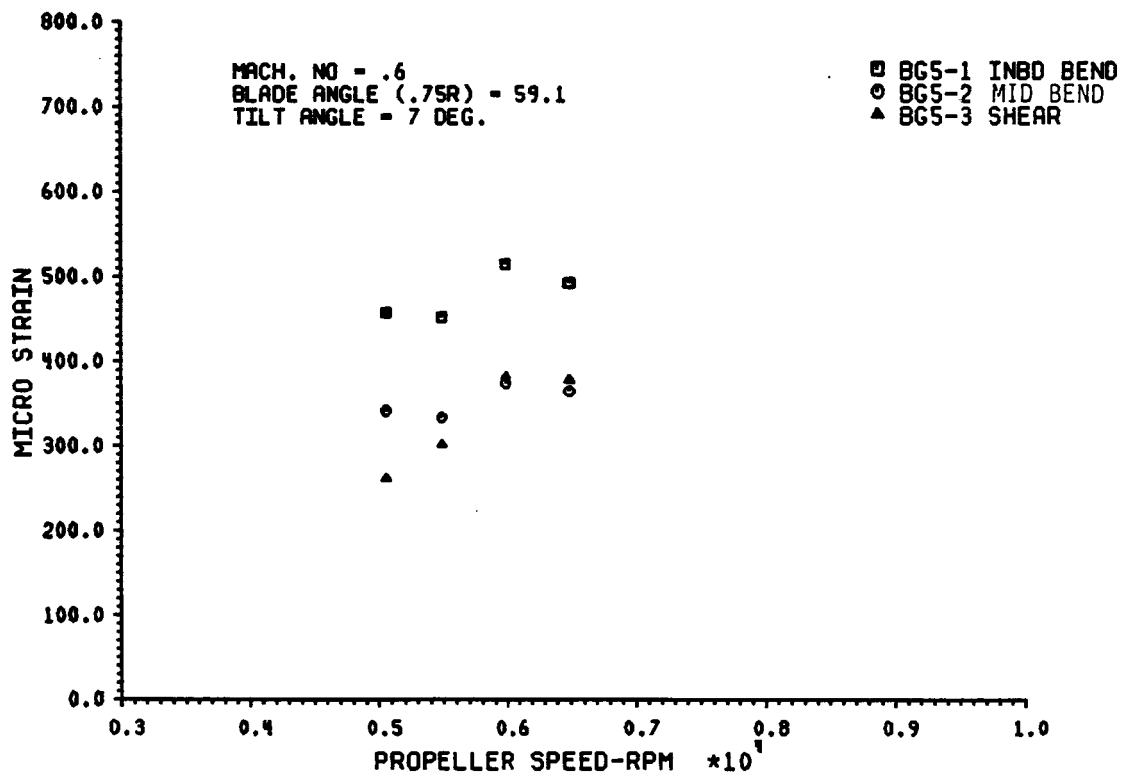
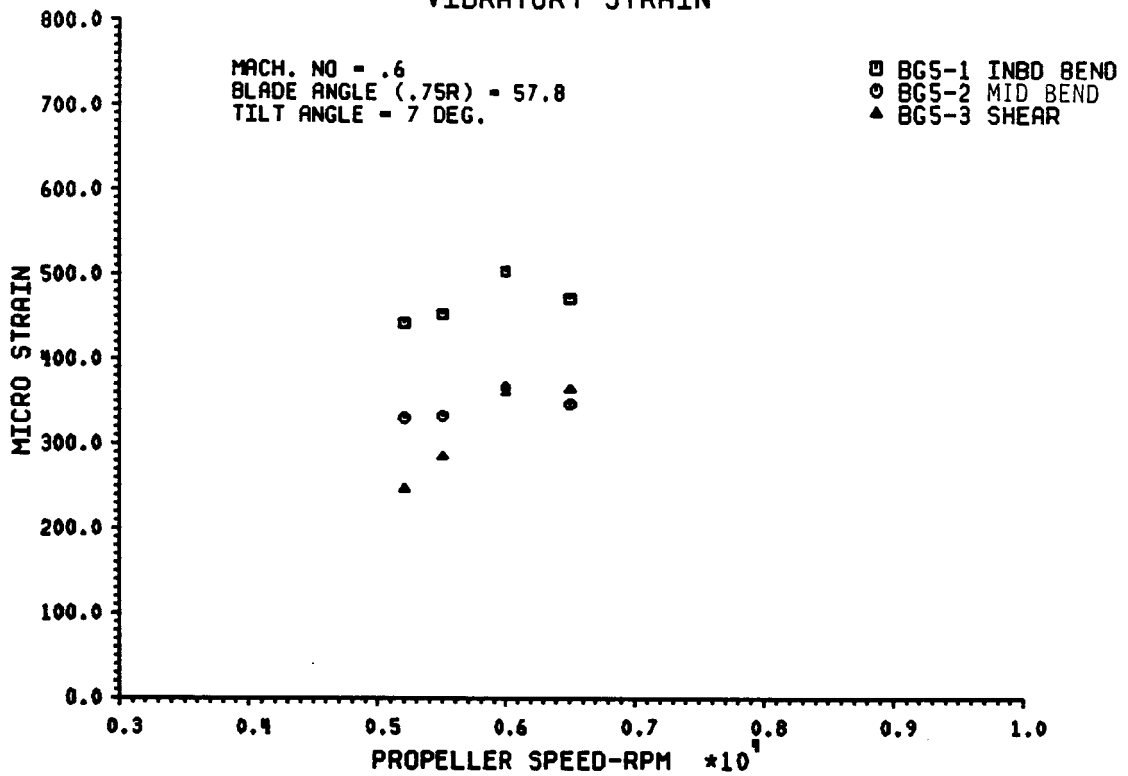


Figure 12 SR-3C-3 BLADE DYNAMIC RESPONSE TO  
ANGULAR INFLOW - 0.6 MACH

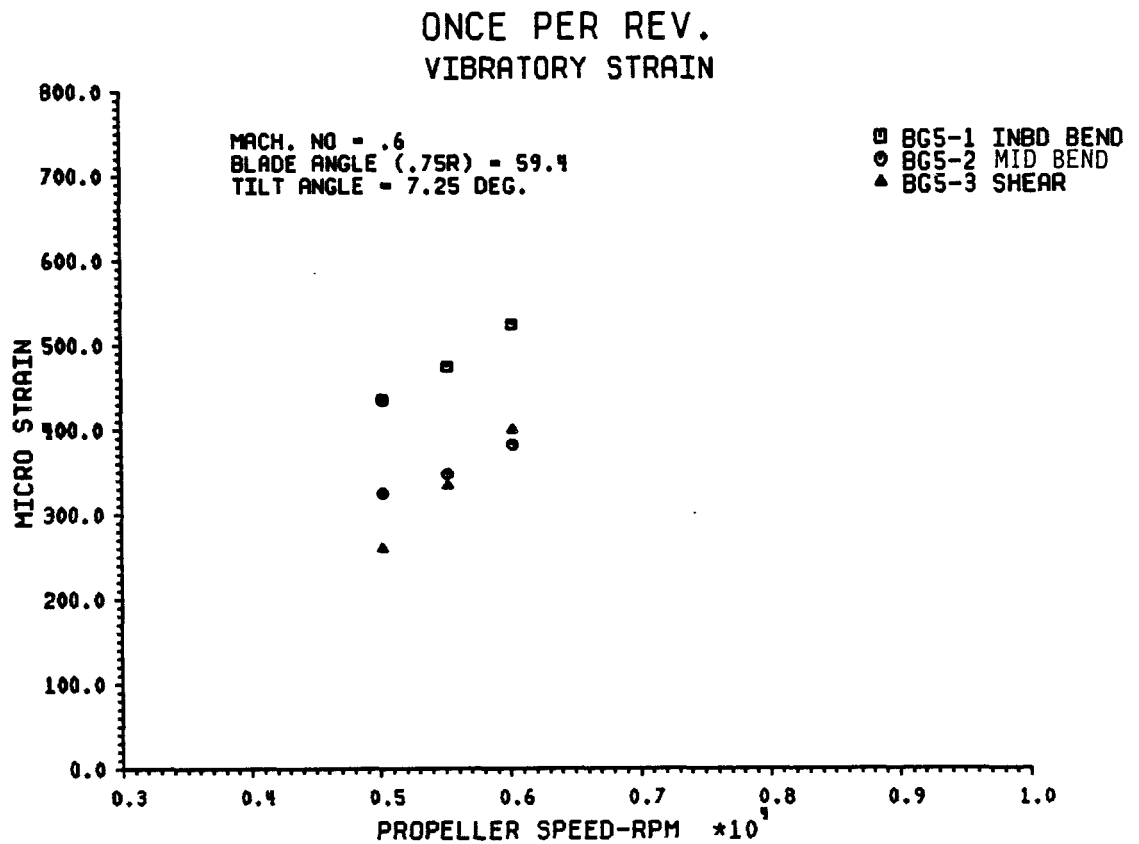


Figure 12 SR-3C-3 BLADE DYNAMIC RESPONSE TO  
ANGULAR INFLOW - 0.6 MACH

ONCE PER REV.  
VIBRATORY STRAIN

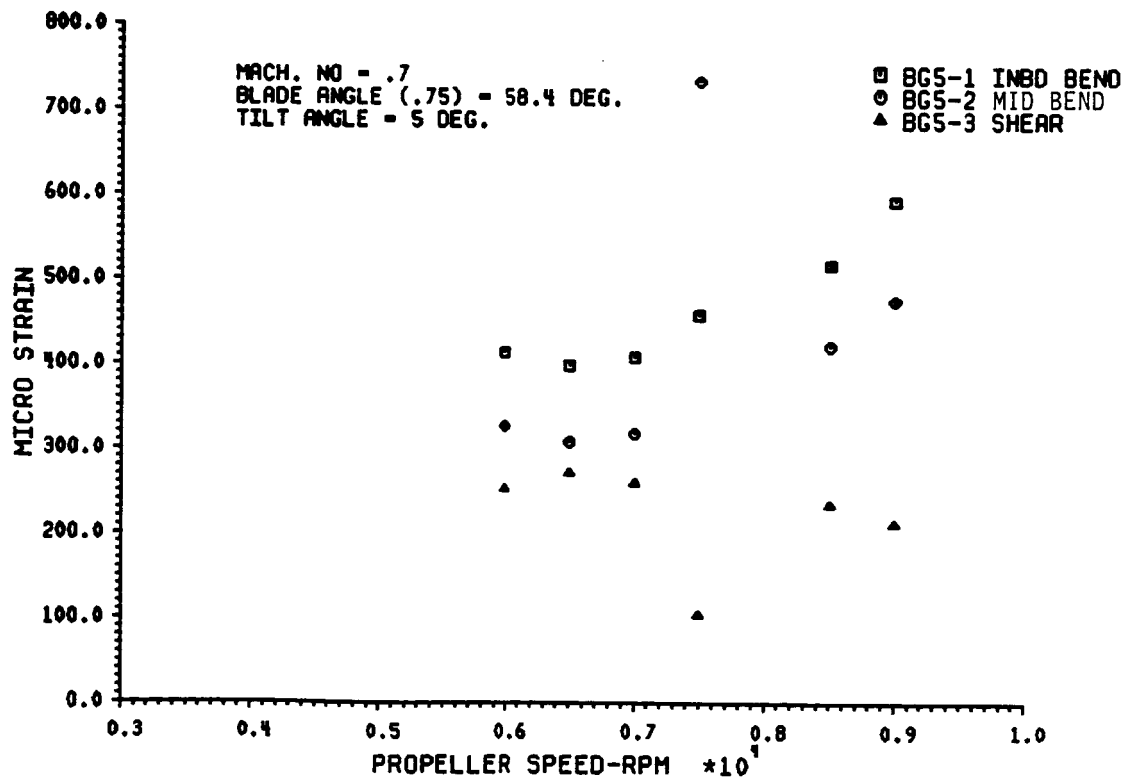
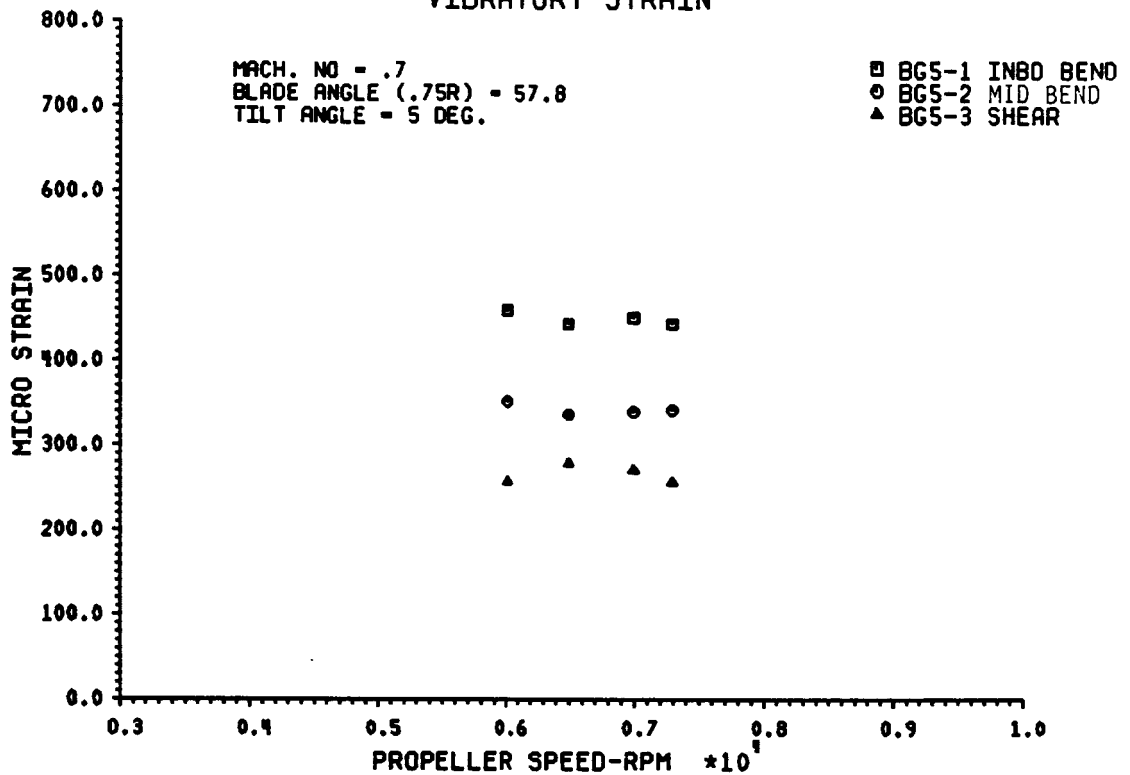


Figure 13 SR-3C-3 BLADE DYNAMIC RESPONSE TO  
ANGULAR INFLOW - 0.7 MACH

# ONCE PER REV. VIBRATORY STRAIN

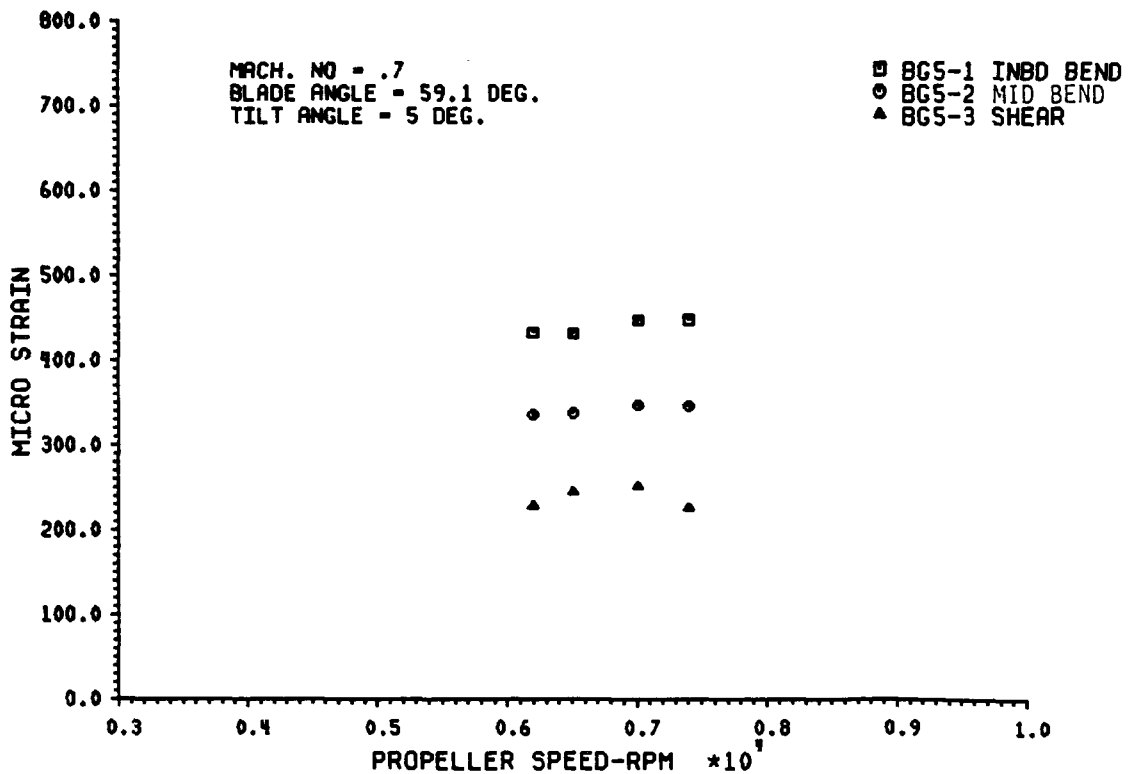
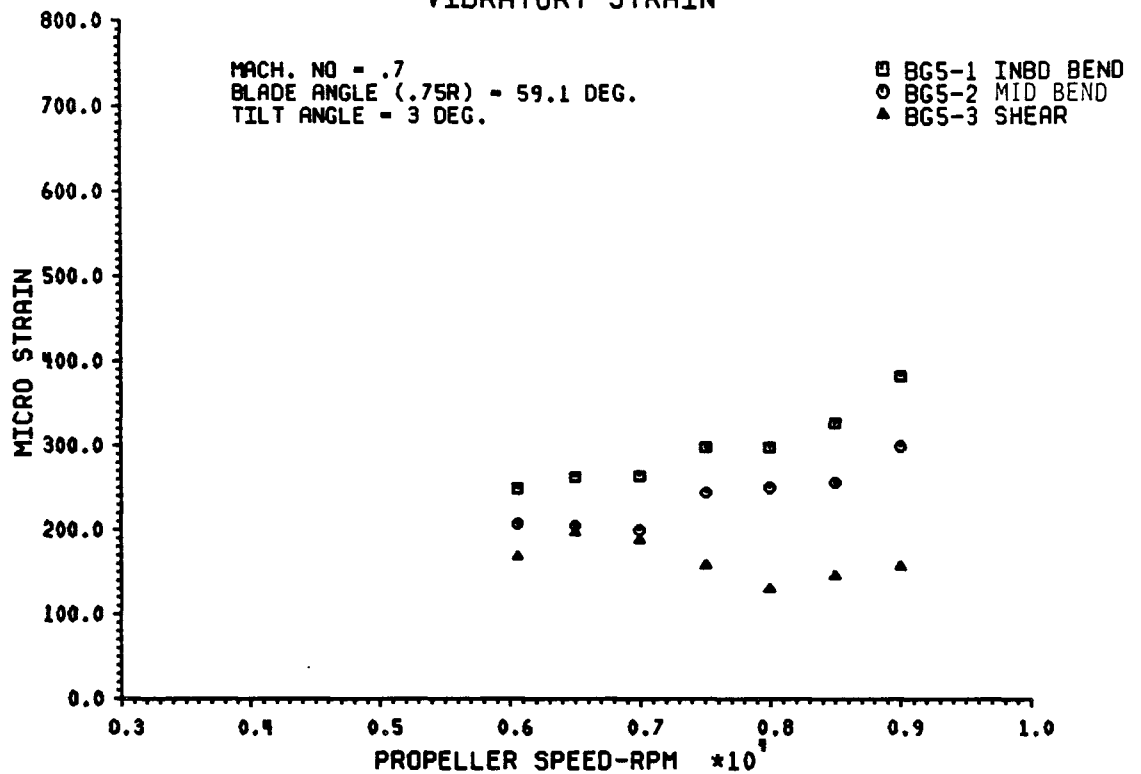


Figure 13 SR-3C-3 BLADE DYNAMIC RESPONSE TO  
ANGULAR INFLOW - 0.7 MACH

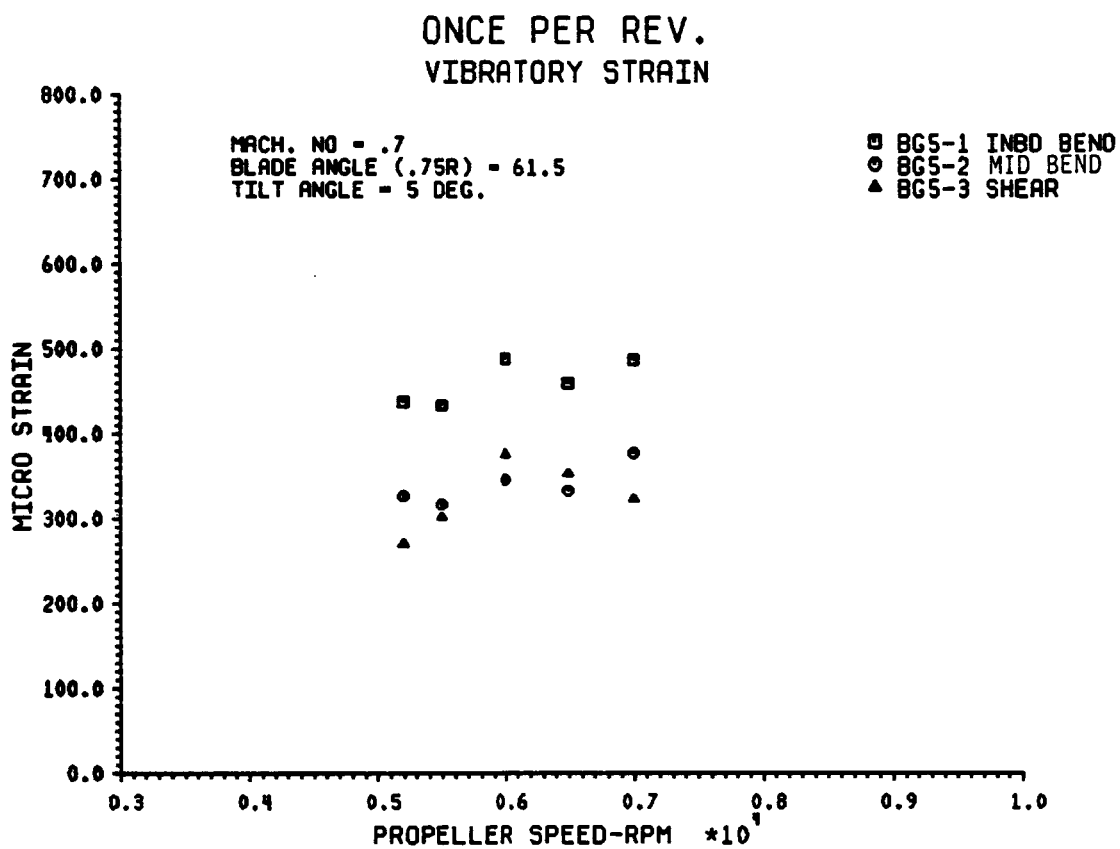


Figure 13 SR-3C-3 BLADE DYNAMIC RESPONSE TO  
ANGULAR INFLOW - 0.7 MACH

# ONCE PER REV. VIBRATORY STRAIN

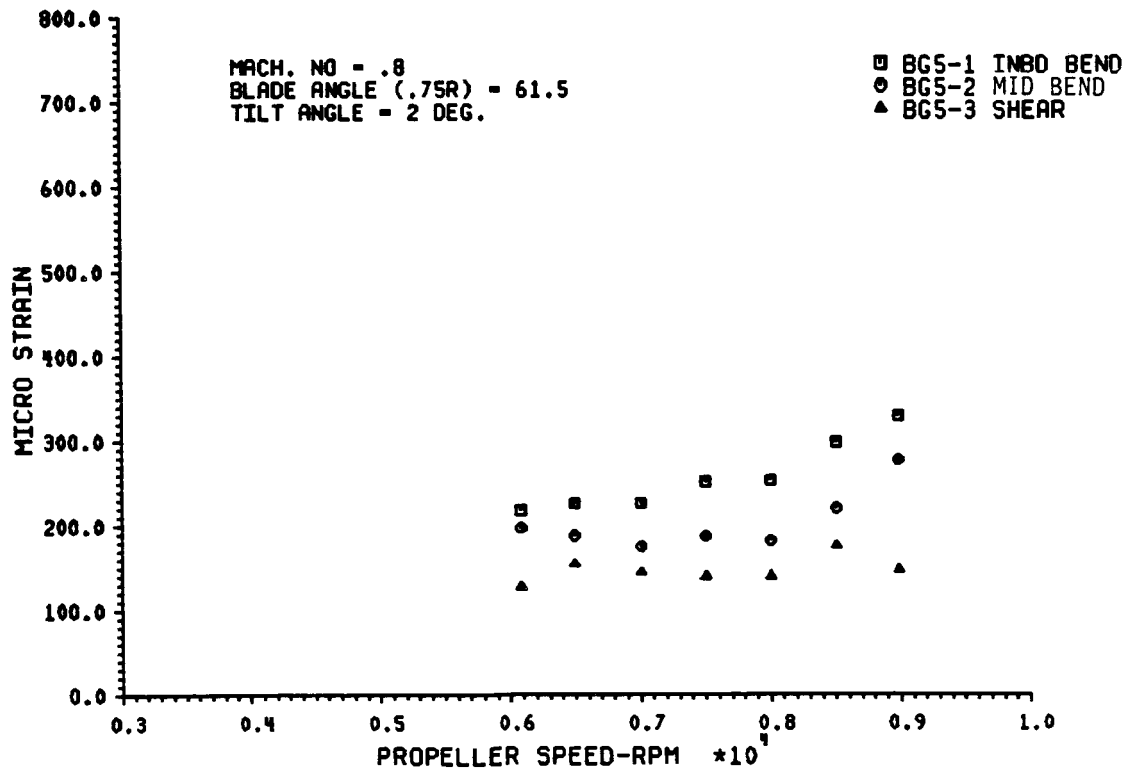
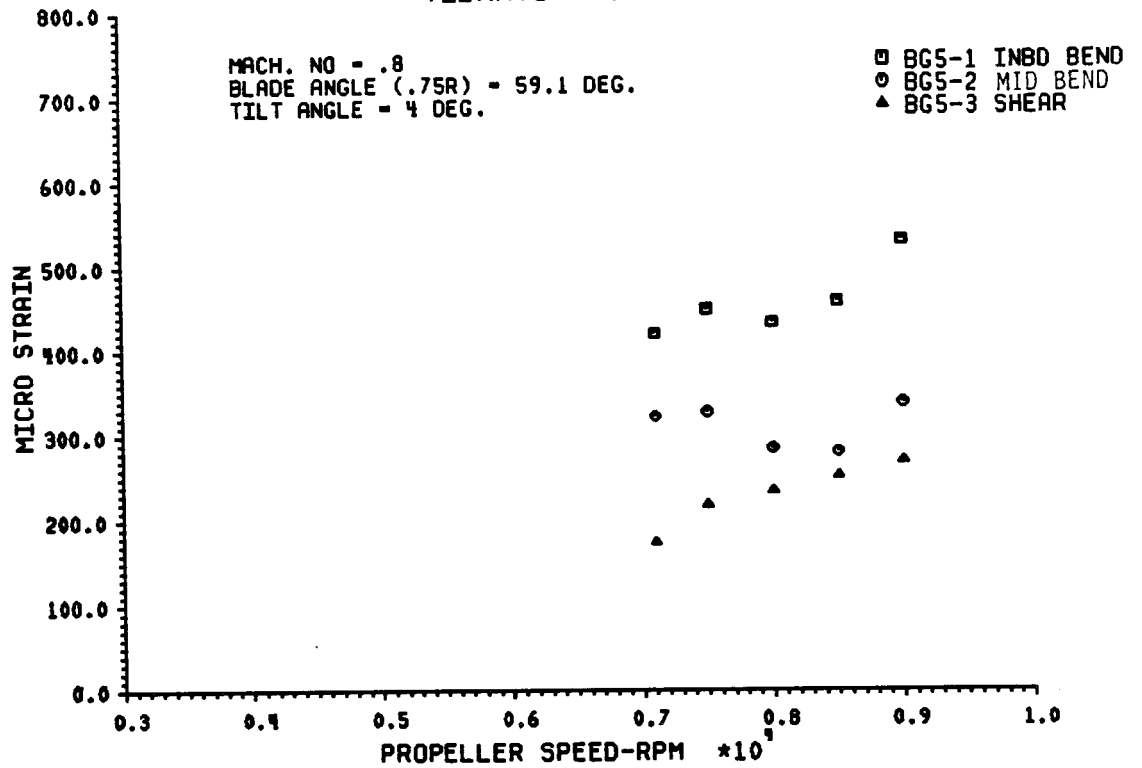


Figure 14 SR-3C-3 BLADE DYNAMIC RESPONSE TO  
ANGULAR INFLOW - 0.8 MACH

# ONCE PER REV. VIBRATORY STRAIN

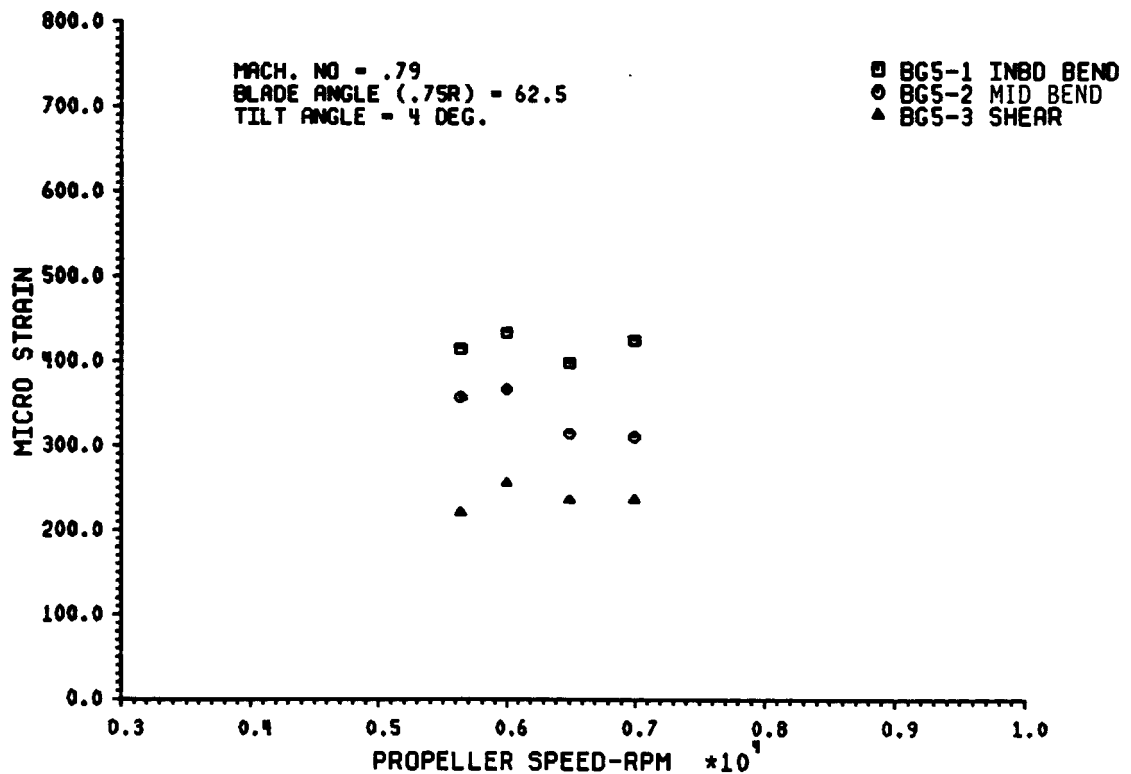
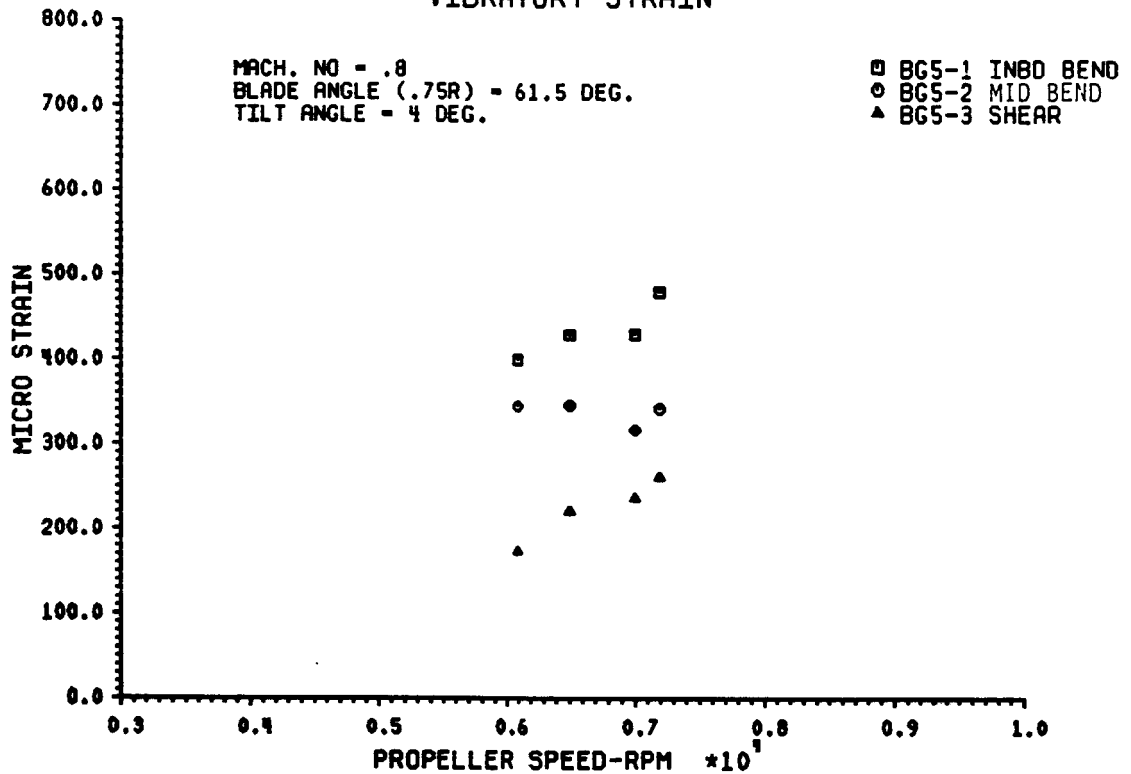


Figure 14 SR-3C-3 BLADE DYNAMIC RESPONSE TO  
ANGULAR INFLOW - 0.8 MACH



# ONCE PER REV. VIBRATORY STRAIN

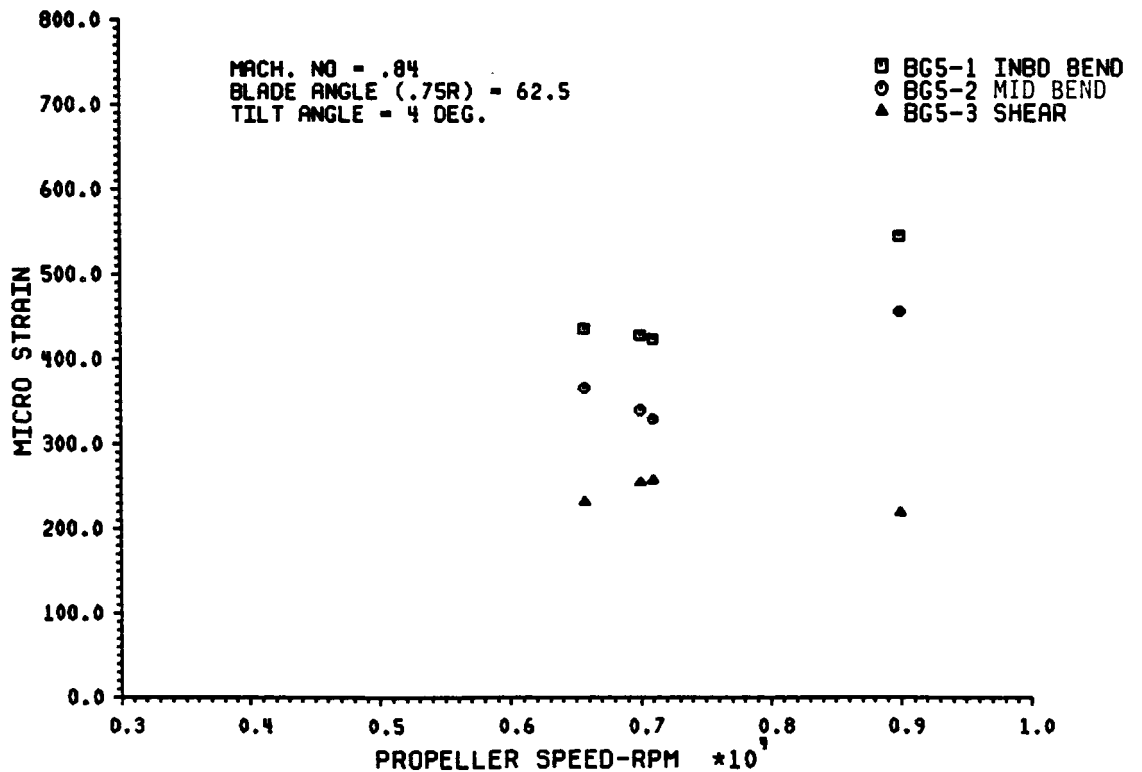
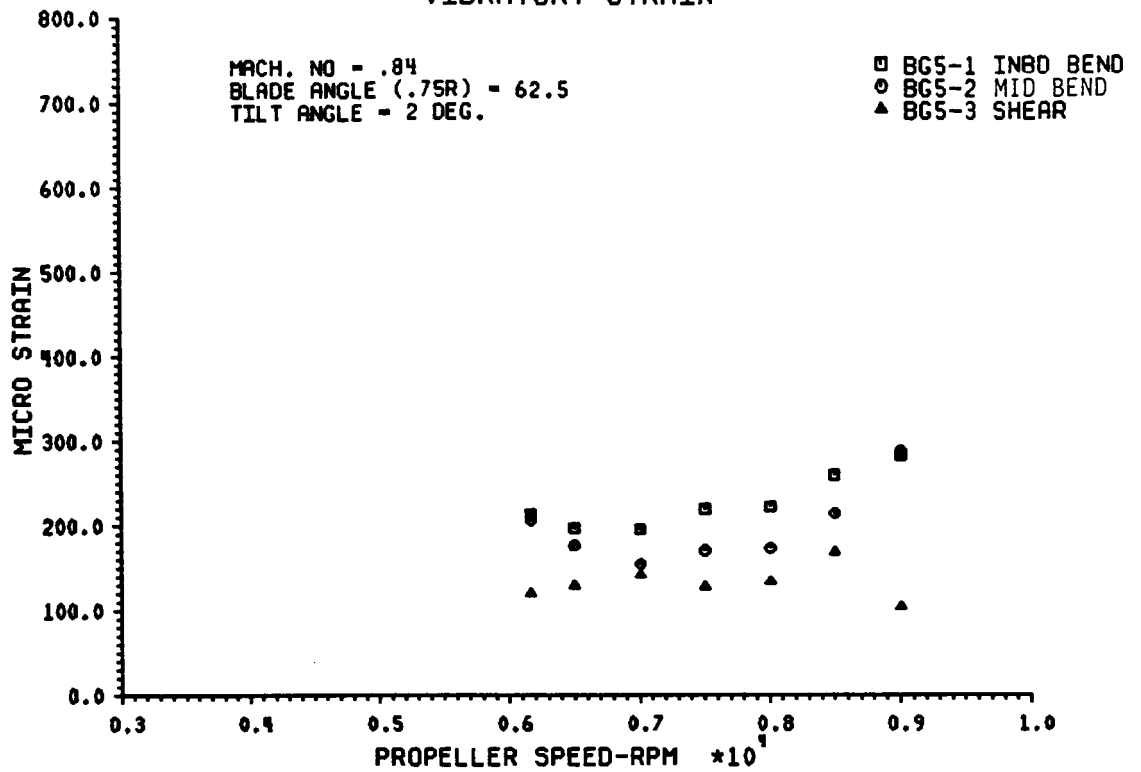


Figure 15 SR-3C-3 BLADE DYNAMIC RESPONSE TO  
ANGULAR INFLOW - 0.84 MACH

ONCE PER REV.  
VIBRATORY STRAIN

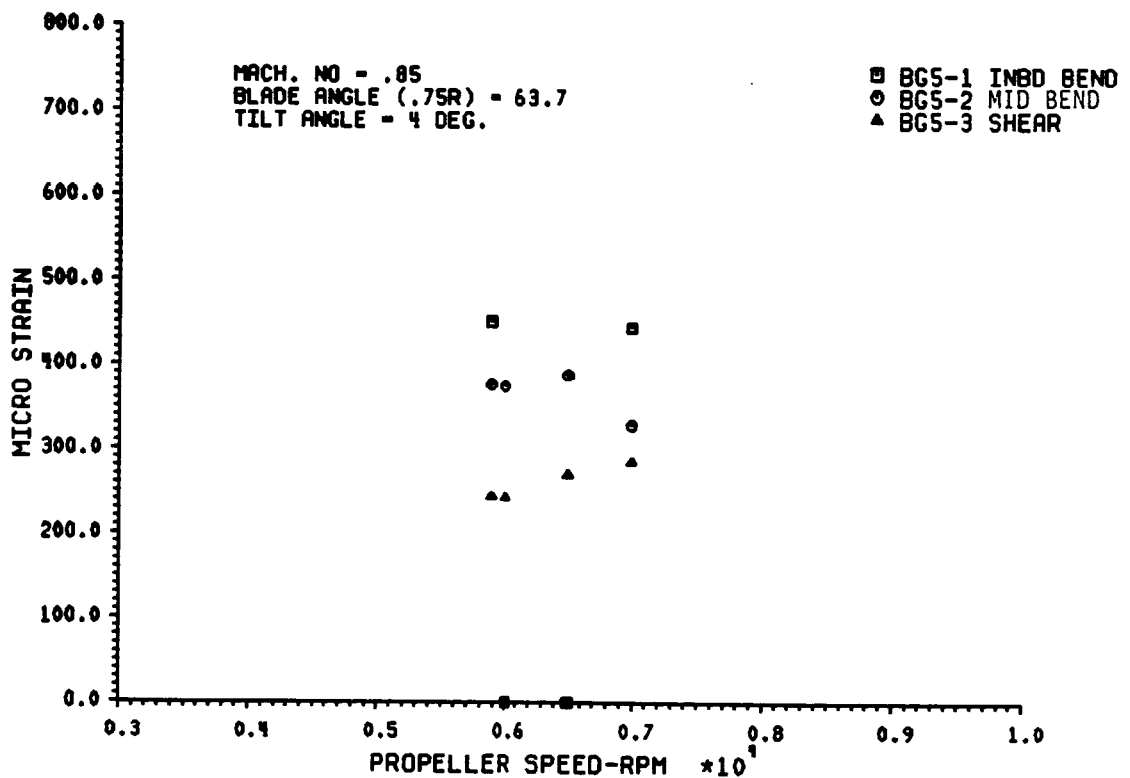
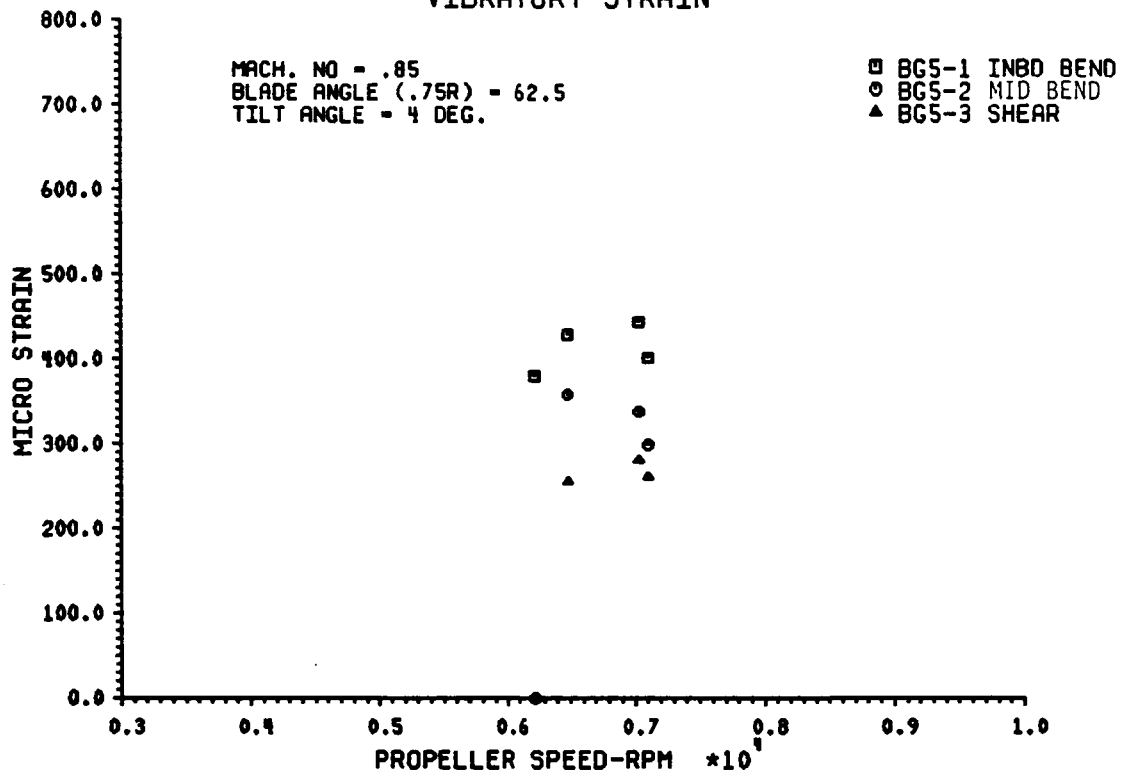


Figure 16 SR-3C-3 BLADE DYNAMIC RESPONSE TO  
ANGULAR INFLOW - 0.85 MACH

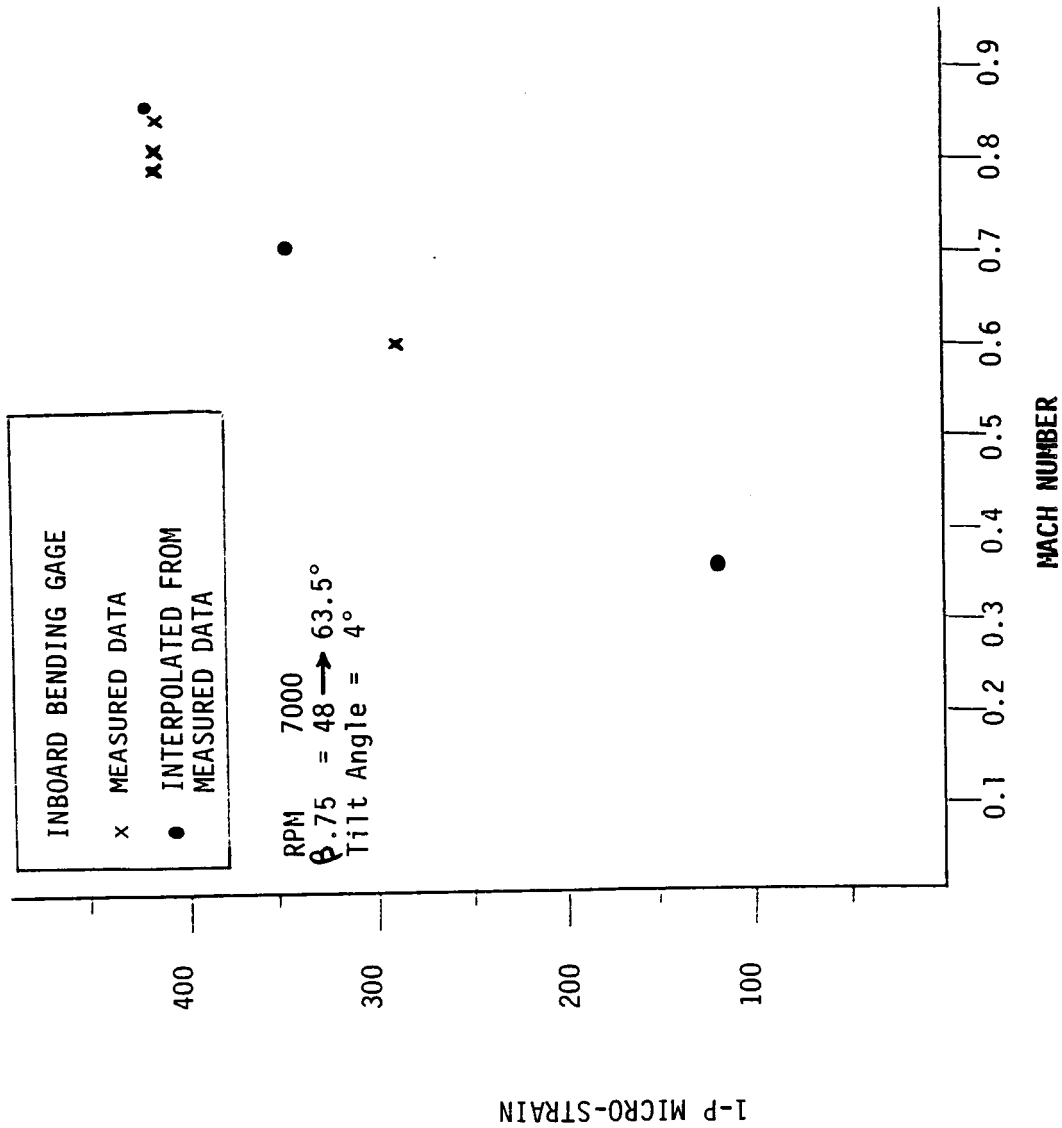


Figure 17 EFFECT OF MACH NUMBER ON SR-3C-3 1-P VIBRATORY STRAIN

SR-3C-3 MODEL PROP-FAN TESTS  
2.4 X 1.8 METER WIND TUNNEL  
NASA LEWIS

INBOARD BENDING STRAIN BG5-1

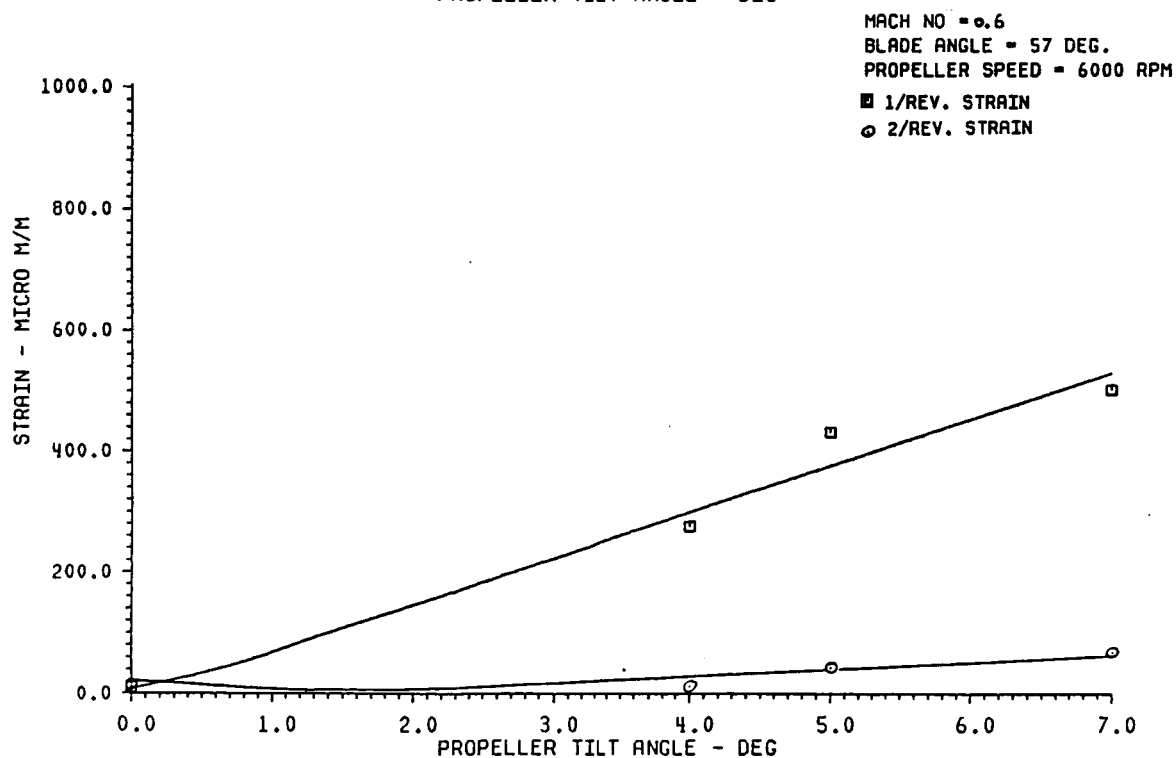
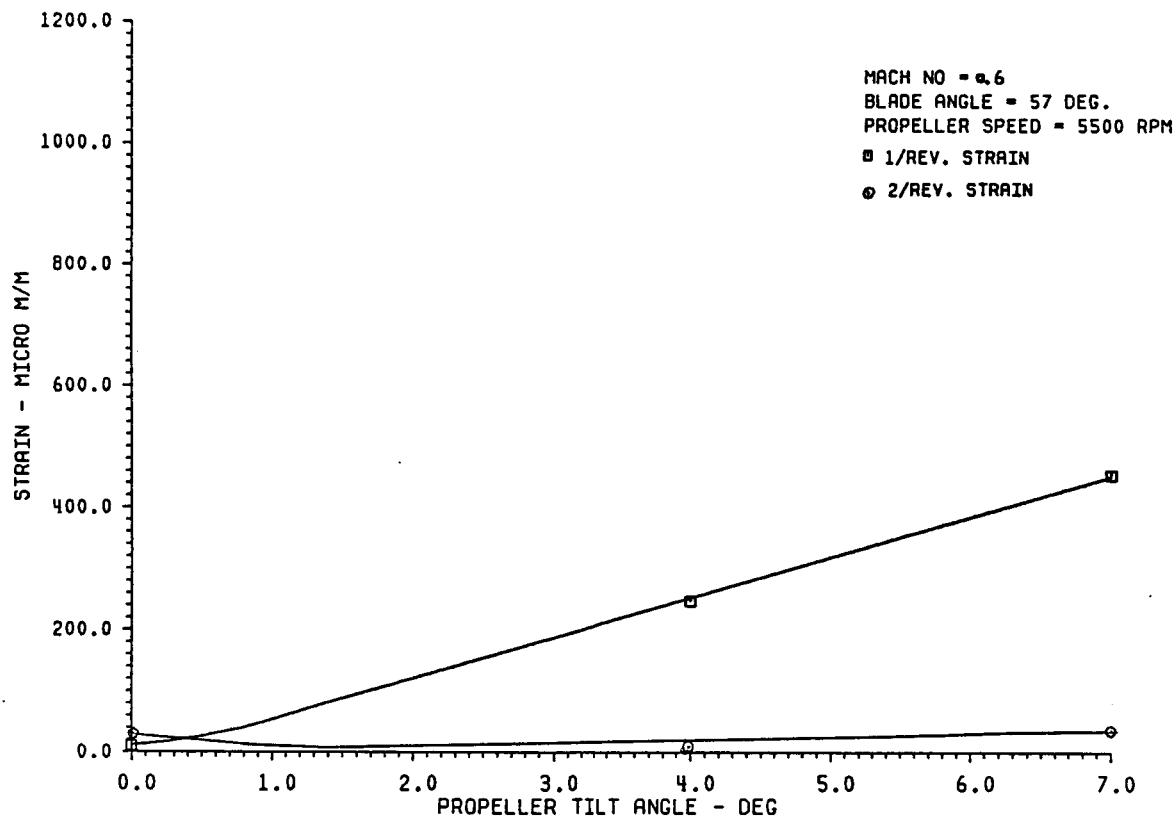


FIGURE 10. THE EFFECT OF PROPELLER TILT  
ON THE 1P AND 2P VIBRATORY STRAIN

SR-3C-3 MODEL PROP-FAN TESTS  
2.4 X 1.8 METER WIND TUNNEL  
NASA LEWIS

INBOARD BENDING STRAIN BG5-1

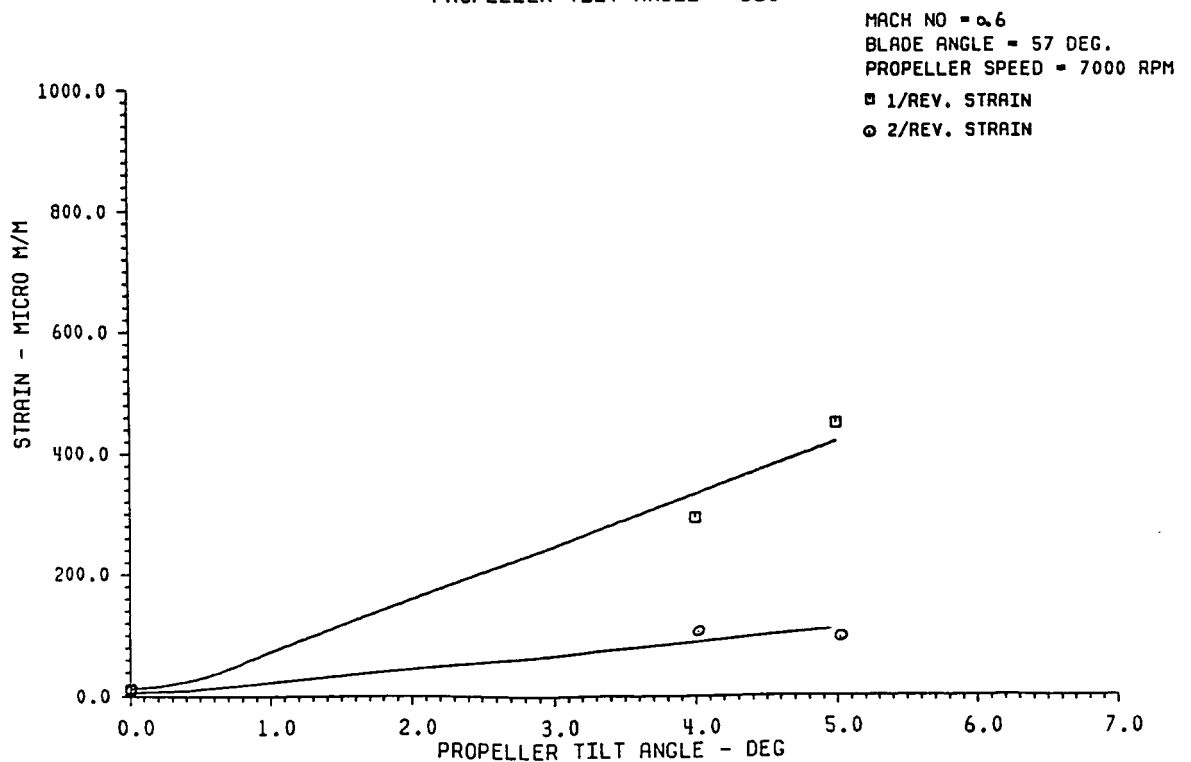
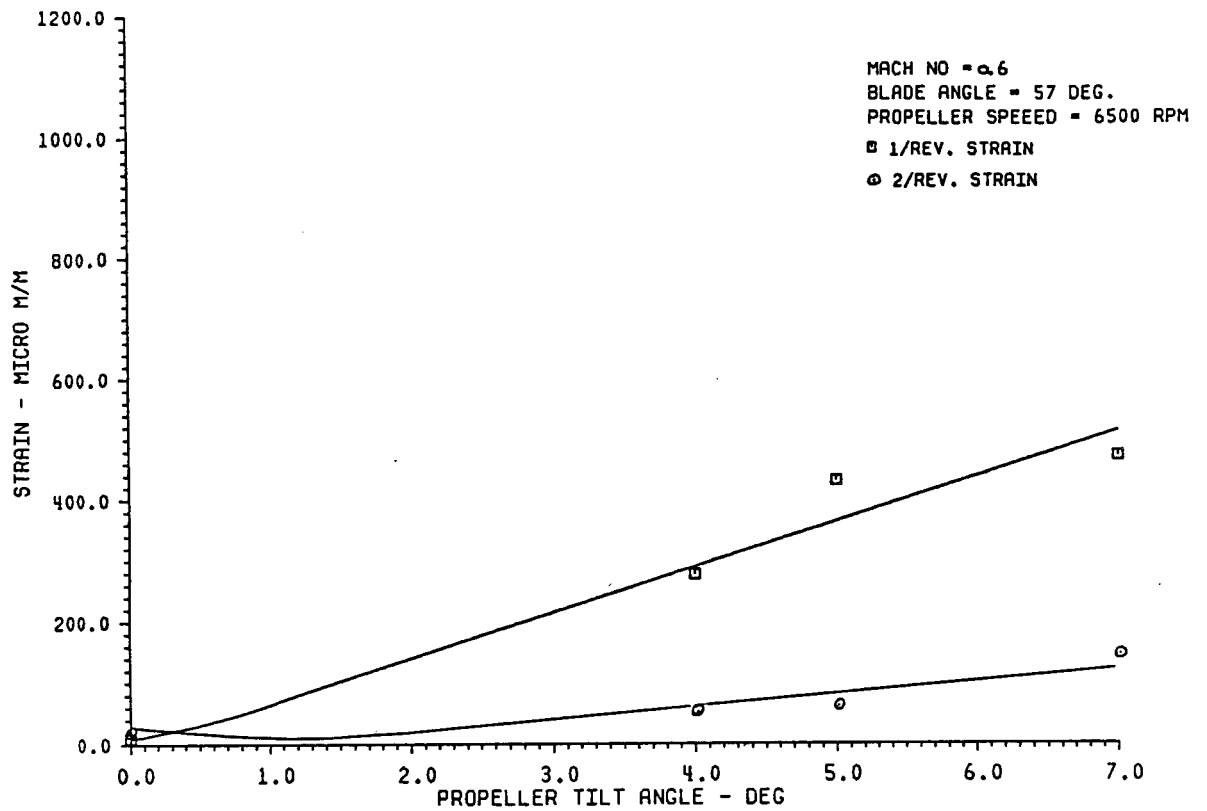


FIGURE 18. THE EFFECT OF PROPELLER TILT  
ON THE 1P AND 2P VIBRATORY STRAIN

SB-3C-3 MODEL PROP-FAN TESTS  
2.4 X 1.8 METER WIND TUNNEL  
NASA LEWIS

INBOARD BENDING STRAIN BG5-1

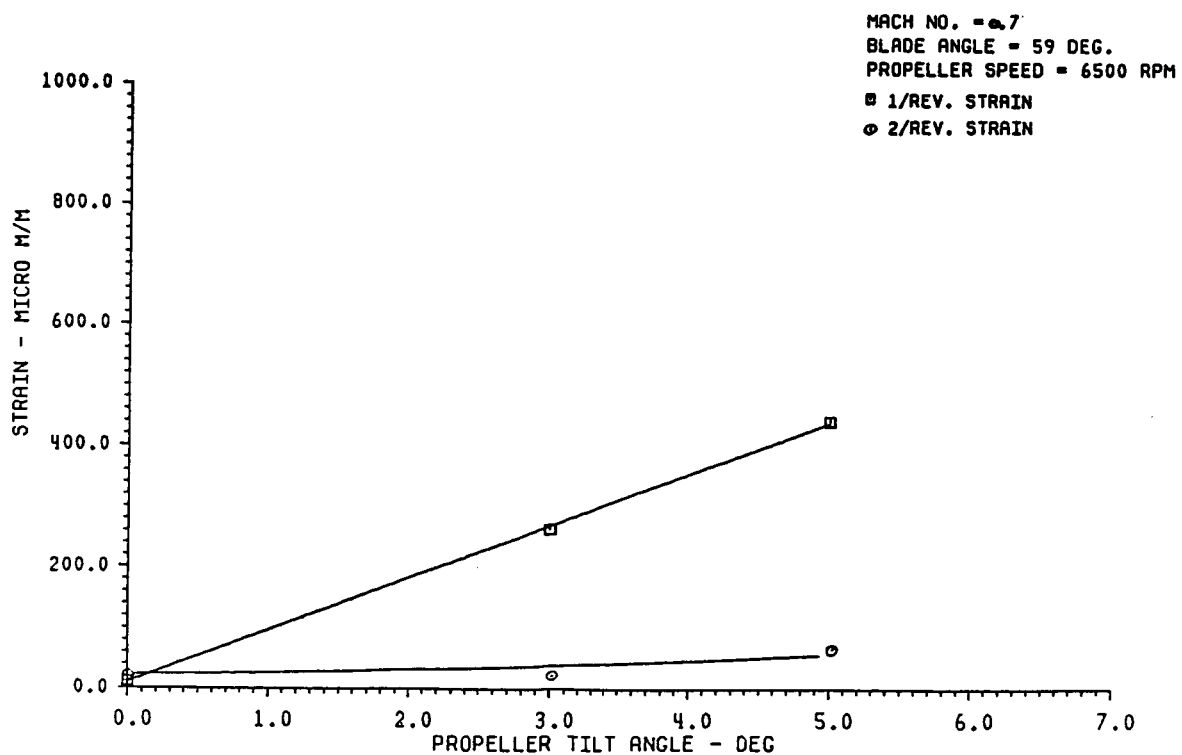
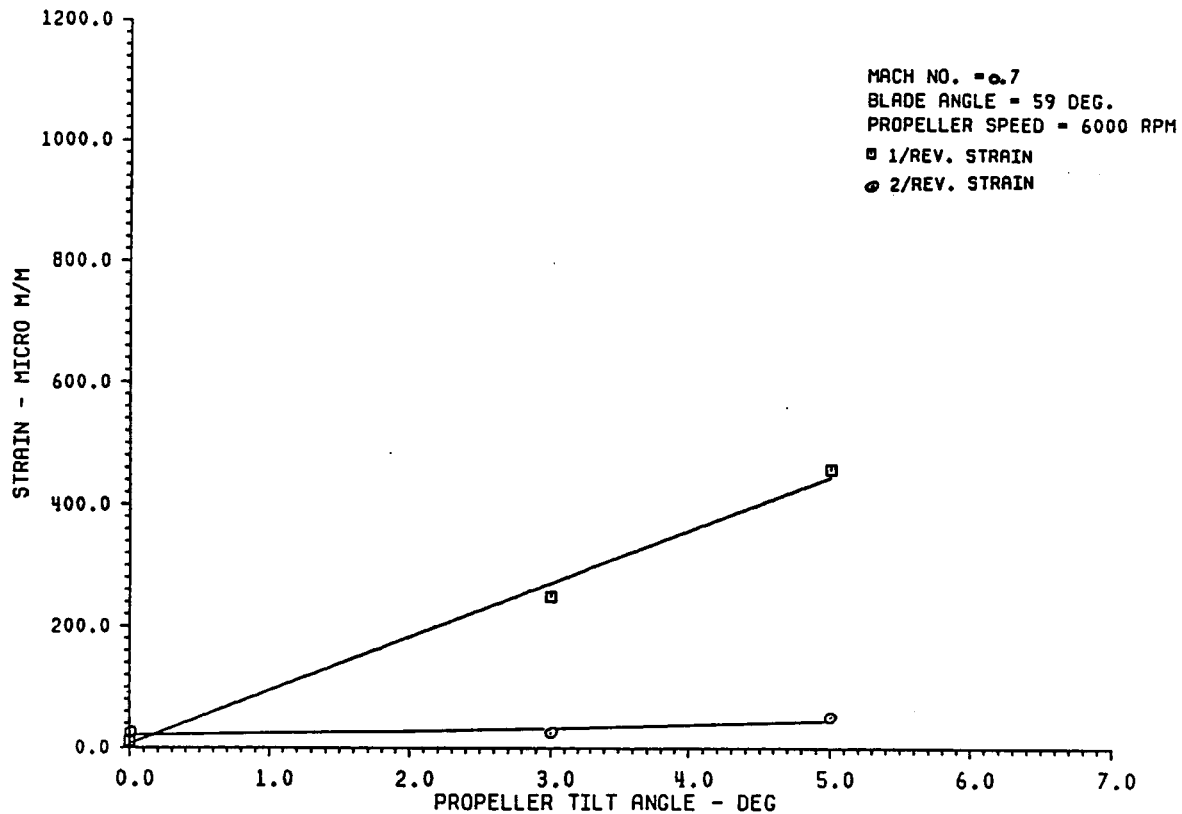


FIGURE 19. THE EFFECT OF PROPELLER TILT  
ON THE 1P AND 2P VIBRATORY STRAIN

SR-3C-3 MODEL PROP-FAN TESTS  
2.4 X 1.8 METER WIND TUNNEL  
NASA LEWIS

INBOARD BENDING STRAIN BG5-1

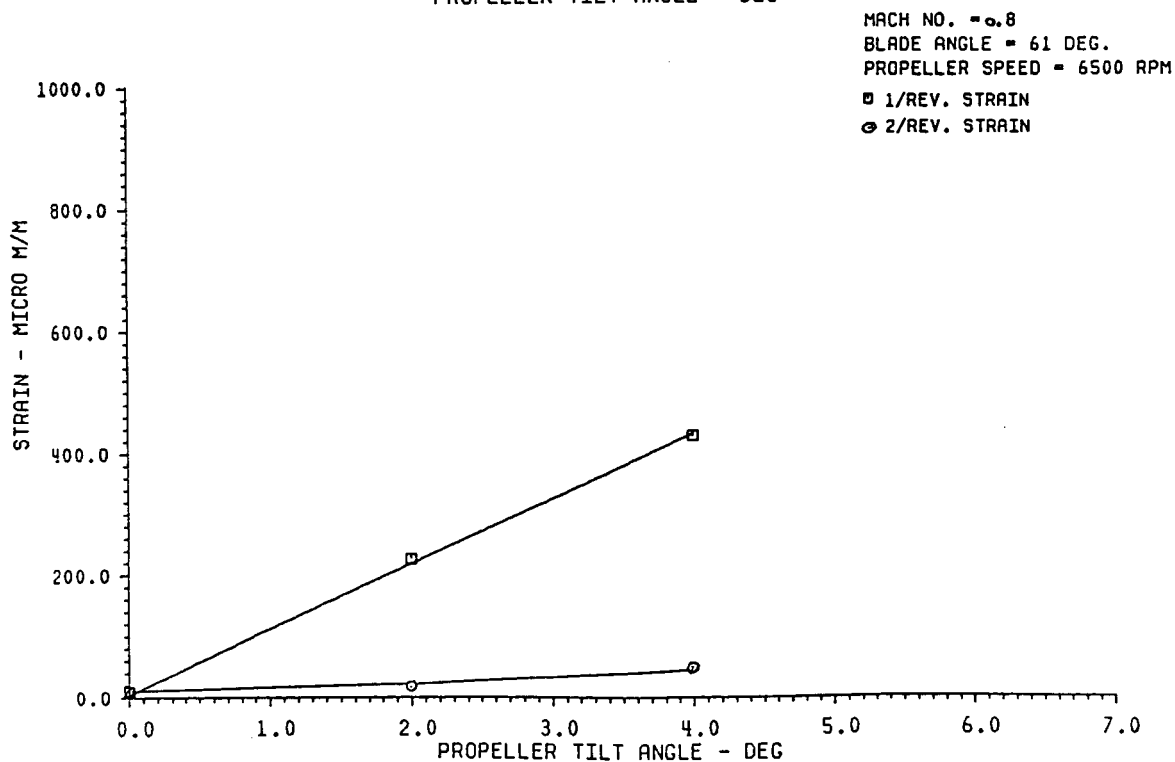
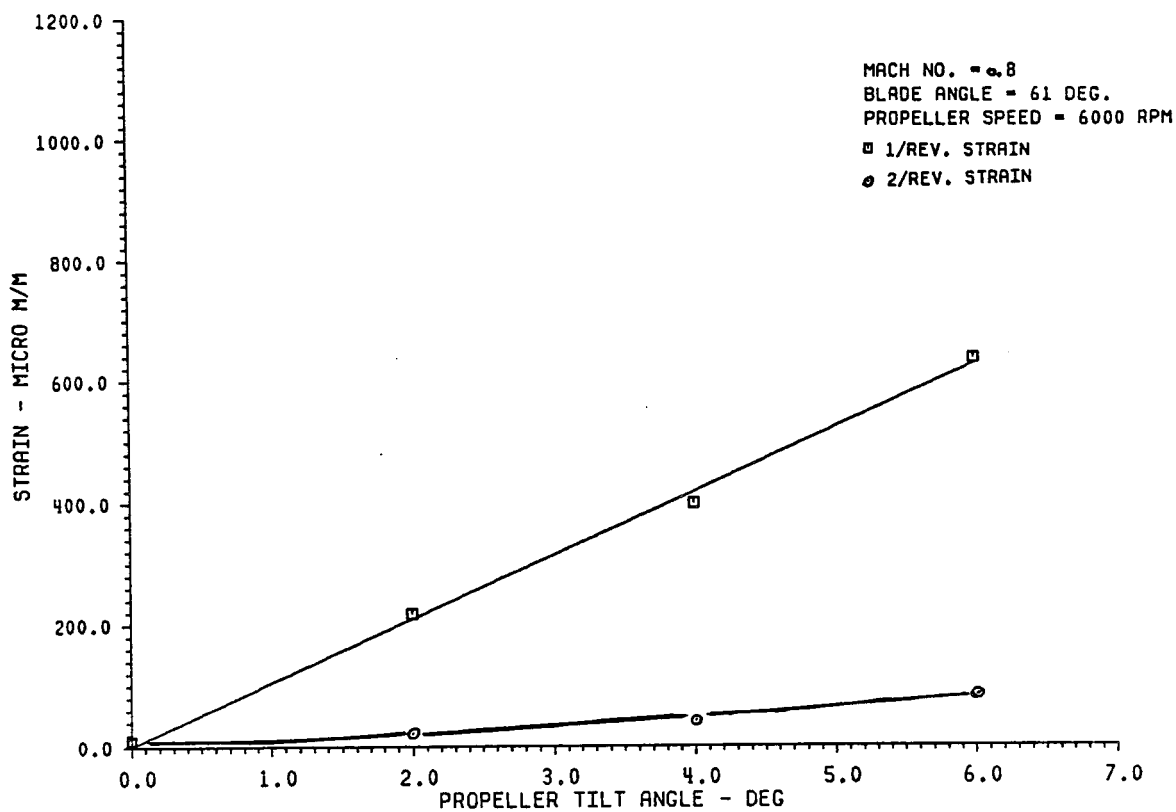


FIGURE 20. THE EFFECT OF PROPELLER TILT  
ON THE 1P AND 2P VIBRATORY STRAIN

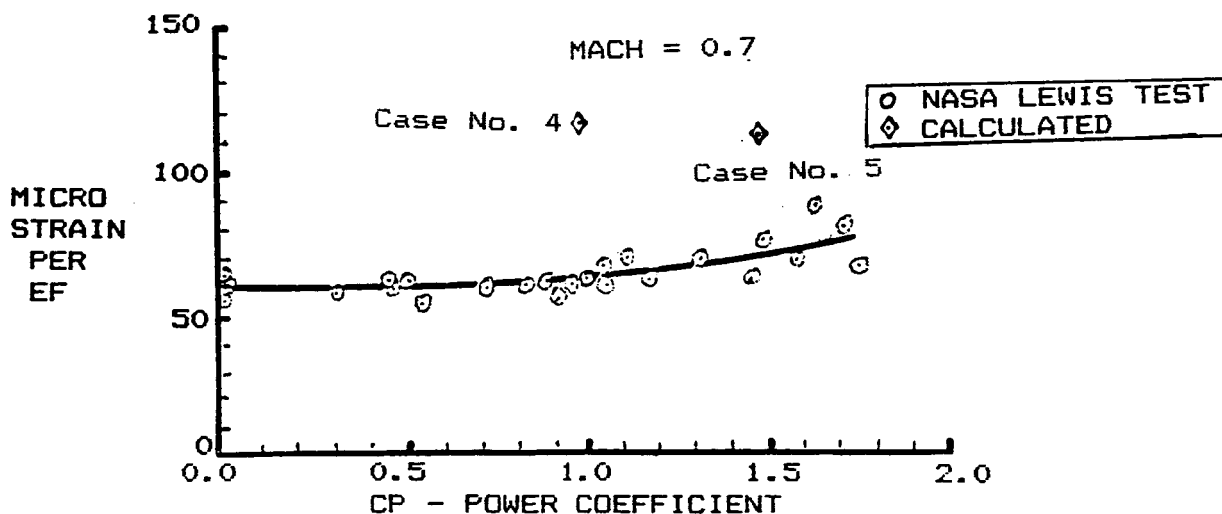
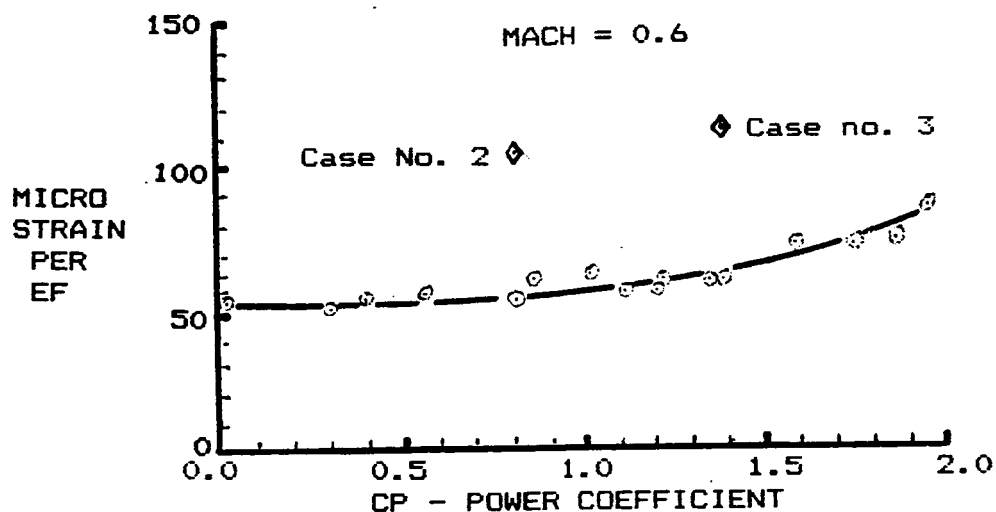
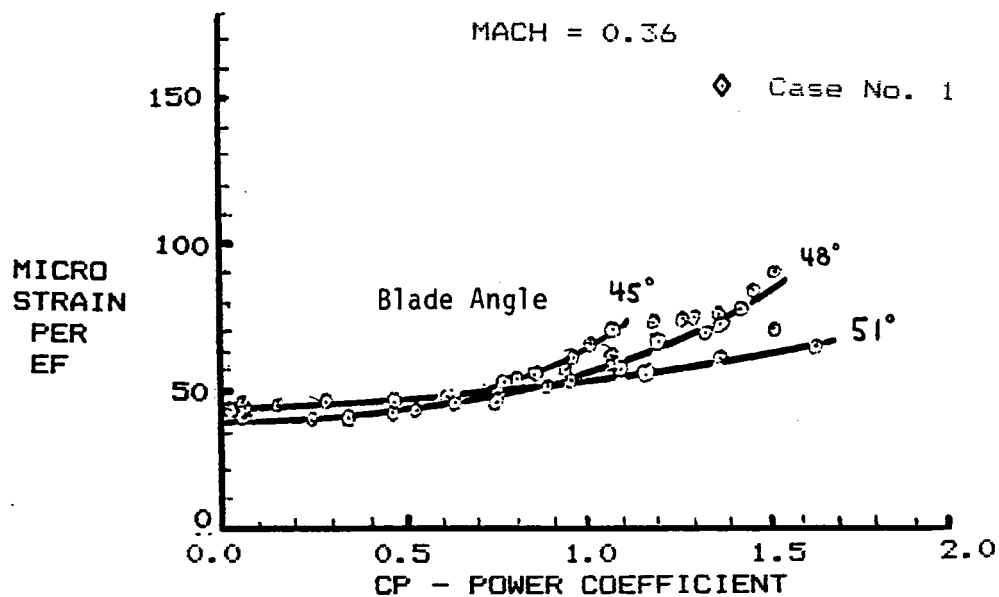


Figure 21 Strain Sensitivity vs. Power Coefficient for all Blade Angles, SR-3C-3 Prop-Fan tests at the 8 x 6 Wind Tunnel, NASA/Lewis. Inboard bending Gage BG5-1. 63



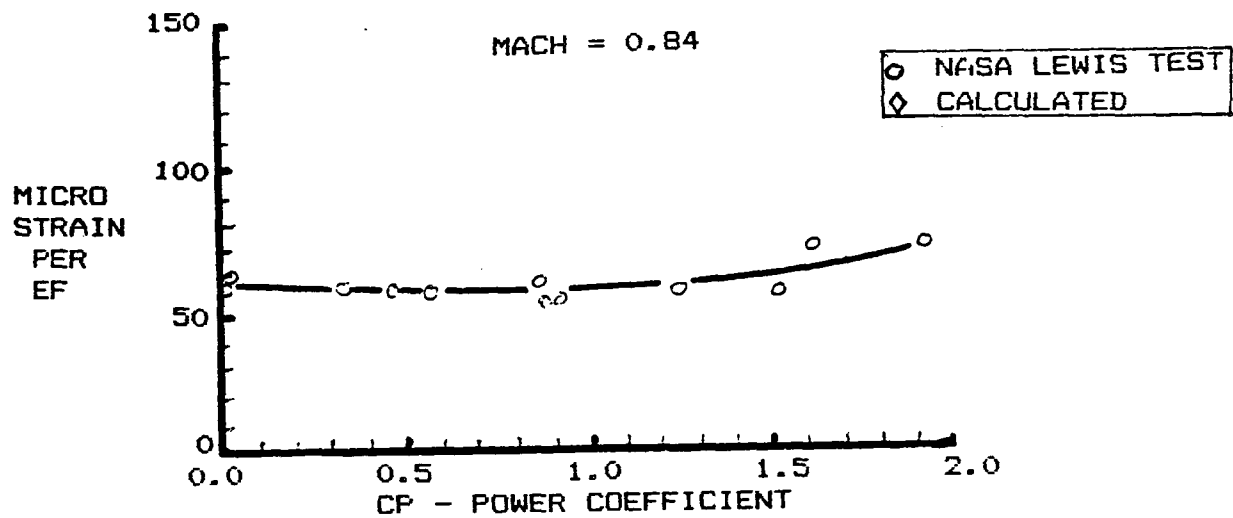
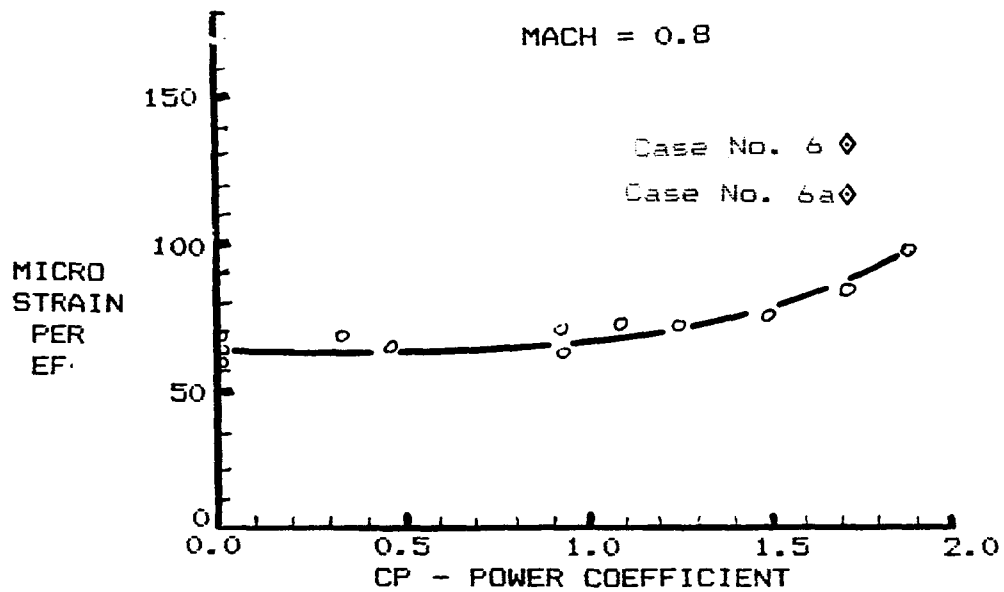


Figure 21  
(Concluded)

Strain Sensitivity vs. Power Coefficient for all Blade Angles, SR-3C-3 Prop-Fan tests at the 8 x 6 Wind Tunnel, NASA/Lewis. Inboard bending Gage BG5-1.

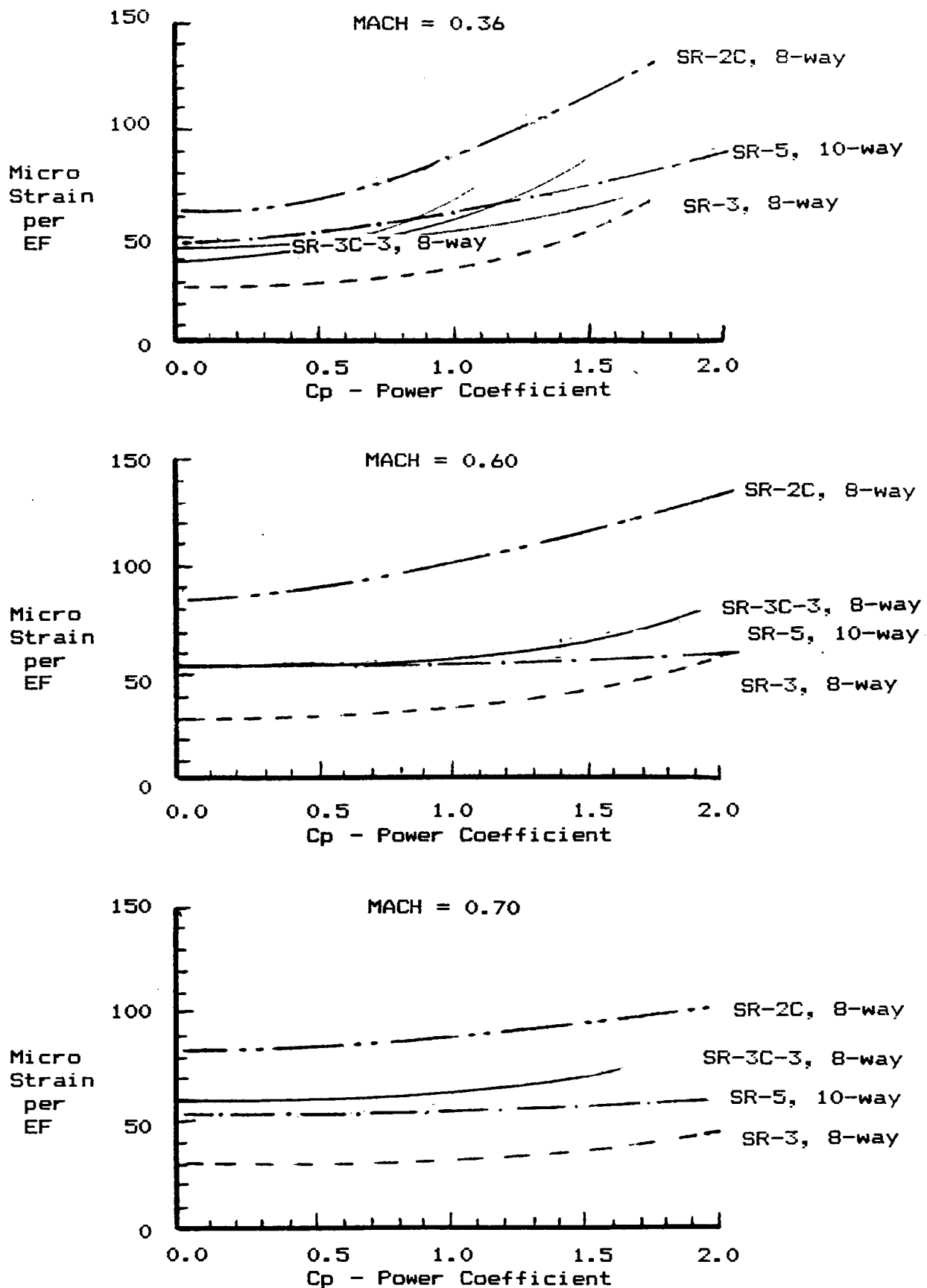


Figure 22 Strain Sensitivity vs. Power Coefficient for all Blade Angles, several Prop-Fan response tests at the 8 X 6 Wind Tunnel, NASA/Lewis. Inboard Bending Gages.

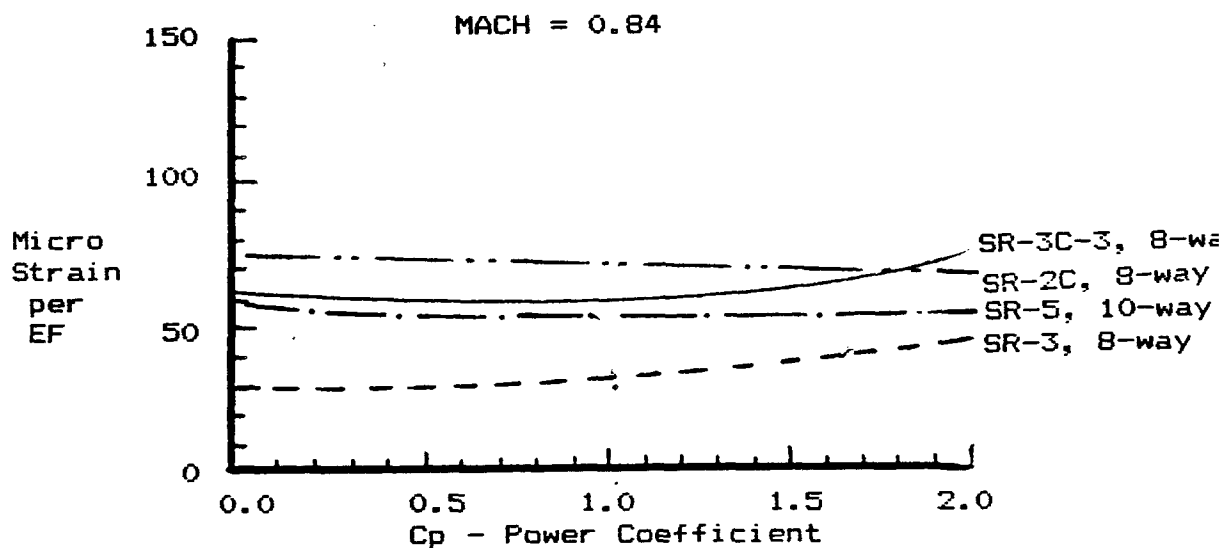
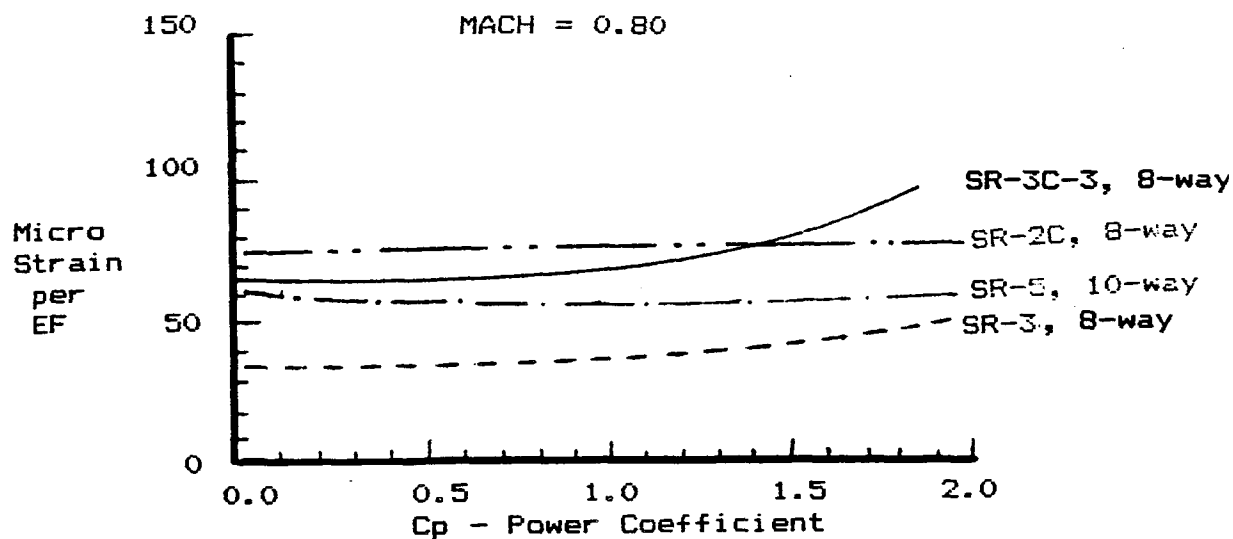


Figure 22 (Concluded) Strain Sensitivity vs. Power Coefficient for all Blade Angles, several Prop-Fan response tests at the 8 X 6 Wind Tunnel, NASA/Lewis. Inboard Bending Gages.

APPENDIX I

Peak Total Strain Tabulation.

ORIGINAL PAGE IS  
OF POOR QUALITY

PEAK DETECTOR SAMPLED DATA: XBAR + 2 * SIGMA												
PAGE 1 OF 6												
JOB I.D.: SR3 DATE: 12-SEP-84												
TITLE: SR3C-3 PROF-FAN TEST LERC JUL-83												
ROW#	BG1-1	BG1-2	BG1-3	BG2-2	BG2-1	BG5-2	BG3-1	BG5-1	BG5-3	BG6-1	BG6-2	
9	59.	144.	141.	76.	87.	66.	63.	60.	101.	54.	57.	
10	86.	166.	166.	77.	93.	84.	77.	81.	135.	57.	68.	
14	371.	363.	263.	317.	344.	322.	367.	371.	262.	381.	313.	
15	382.	378.	260.	333.	333.	389.	384.	402.	292.	394.	325.	
16	13.	42.	13.	12.	12.	11.	17.	15.	51.	12.	14.	
17	268.	303.	207.	242.	244.	240.	278.	259.	232.	277.	250.	
18	241.	284.	190.	205.	233.	220.	249.	219.	219.	244.	210.	
19	216.	264.	185.	218.	223.	204.	226.	210.	205.	226.	202.	
20	213.	260.	170.	184.	205.	204.	213.	203.	200.	218.	192.	
25	52.	145.	120.	80.	71.	59.	55.	55.	88.	45.	58.	
26	51.	146.	117.	83.	72.	65.	56.	58.	90.	45.	59.	
27	87.	174.	189.	92.	82.	114.	78.	81.	183.	15.	117.	
36	215.	258.	171.	189.	202.	213.	228.	213.	233.	222.	199.	
38	404.	353.	235.	336.	349.	344.	388.	390.	279.	49.	325.	
39	413.	389.	239.	327.	352.	368.	383.	383.	211.	51.	341.	
40	432.	371.	226.	341.	342.	377.	373.	395.	253.	46.	307.	
41	396.	369.	250.	305.	331.	371.	358.	402.	233.	46.	359.	
42	369.	340.	231.	385.	306.	309.	334.	335.	2539.	380.	316.	
43	321.	312.	231.	271.	288.	273.	311.	303.	284.	16.	296.	
44	271.	287.	202.	231.	244.	243.	281.	251.	265.	16.	246.	
45	260.	263.	194.	226.	219.	219.	267.	253.	269.	12306.	242.	
46	221.	257.	186.	222.	218.	204.	222.	209.	226.	17.	204.	
47	348.	352.	285.	324.	335.	357.	371.	365.	344.	17.	333.	
48	363.	353.	288.	330.	347.	352.	381.	366.	353.	16.	347.	
49	404.	370.	294.	359.	366.	363.	413.	408.	388.	15.	368.	
50	459.	427.	318.	393.	418.	409.	463.	456.	402.	16.	415.	
51	548.	484.	325.	469.	482.	473.	534.	528.	399.	17.	505.	
52	663.	550.	339.	549.	562.	571.	613.	632.	440.	15.	587.	
54	59.	123.	131.	66.	76.	66.	58.	61.	80.	49.	57.	
55	109.	196.	292.	140.	91.	146.	87.	90.	301.	17.	189.	
56	385.	353.	273.	326.	356.	348.	403.	392.	343.	18.	346.	
66	425.	400.	278.	366.	382.	394.	444.	431.	365.	16.	410.	
67	423.	424.	329.	407.	406.	476.	471.	466.	414.	16.	443.	
68	475.	435.	335.	401.	434.	473.	480.	488.	443.	31.	461.	
69	549.	488.	324.	472.	485.	486.	534.	544.	400.	18.	486.	
70	639.	559.	322.	512.	536.	547.	600.	609.	467.	1074.	557.	
71	737.	589.	365.	557.	609.	600.	667.	696.	437.	15.	606.	
73	74.	153.	151.	99.	91.	98.	75.	77.	126.	71.	96.	
74	122.	191.	211.	148.	123.	156.	128.	125.	227.	91.	145.	
80	512.	444.	323.	412.	480.	424.	498.	507.	394.	528.	436.	
81	502.	427.	314.	398.	471.	433.	499.	508.	393.	523.	434.	
82	536.	445.	370.	422.	486.	438.	519.	541.	417.	562.	463.	
83	679.	561.	396.	483.	550.	566.	607.	657.	463.	738.	591.	
85	139.	209.	225.	152.	116.	180.	128.	104.	229.	100.	134.	
93	93.	153.	143.	98.	90.	100.	84.	68.	134.	66.	97.	
94	322.	311.	246.	259.	322.	295.	332.	324.	317.	338.	263.	
96	505.	446.	312.	427.	444.	462.	497.	495.	344.	499.	420.	
97	515.	485.	306.	438.	443.	522.	518.	508.	297.	488.	465.	
98	539.	494.	308.	412.	444.	514.	467.	531.	370.	505.	442.	
99	551.	511.	347.	434.	434.	511.	459.	518.	431.	564.	518.	

JOB I.D.: SR3  
DATE: 12-SEP-84  
TITLE: SR3C-3 PROOF-FAN TEST LERC JUL-83

RD64	RG1-1	RG1-2	RG1-3	RG2-2	RG2-1	RG5-2	RG3-1	RG5-1	RG5-3	RG6-1	RG6-2
100	456.	401.	300.	323.	363.	381.	412.	417.	367.	483.	411.
100	456.	401.	300.	323.	363.	381.	412.	417.	367.	483.	411.
101	366.	319.	278.	294.	321.	311.	339.	331.	336.	379.	317.
102	329.	314.	266.	291.	321.	283.	339.	331.	336.	379.	317.
103	321.	299.	248.	274.	319.	287.	325.	323.	312.	330.	285.
104	522.	449.	350.	439.	494.	445.	521.	532.	403.	542.	454.
105	526.	431.	348.	417.	502.	426.	512.	531.	419.	550.	420.
106	565.	459.	400.	410.	507.	451.	544.	549.	474.	585.	480.
107	565.	446.	501.	563.	534.	524.	621.	637.	515.	710.	549.
108	149.	213.	244.	174.	137.	197.	185.	135.	272.	115.	183.
111	141.	208.	242.	163.	128.	193.	161.	136.	254.	114.	181.
117	100.	194.	188.	147.	108.	145.	100.	89.	183.	92.	143.
118	700.	639.	415.	486.	530.	602.	582.	671.	436.	771.	702.
119	558.	476.	376.	447.	493.	511.	529.	554.	427.	599.	520.
120	515.	468.	399.	425.	492.	468.	509.	526.	462.	547.	462.
121	505.	462.	371.	424.	479.	453.	504.	511.	407.	541.	443.
125	129.	205.	217.	169.	126.	193.	141.	130.	231.	98.	159.
126	59.	145.	138.	96.	77.	93.	68.	79.	126.	54.	93.
127	520.	413.	306.	415.	485.	442.	522.	523.	413.	553.	441.
128	519.	415.	313.	419.	480.	440.	516.	520.	429.	555.	434.
129	540.	408.	349.	417.	499.	420.	514.	537.	471.	571.	409.
130	598.	471.	393.	454.	519.	473.	529.	578.	529.	629.	515.
131	727.	562.	435.	550.	596.	591.	652.	677.	544.	759.	601.
135	69.	147.	142.	95.	84.	97.	77.	67.	131.	61.	92.
144	134.	203.	244.	147.	116.	180.	121.	103.	218.	91.	135.
145	528.	408.	410.	490.	446.	446.	522.	526.	417.	548.	447.
146	539.	433.	437.	414.	505.	436.	515.	544.	447.	566.	425.
147	580.	463.	487.	424.	513.	451.	557.	565.	512.	602.	492.
148	700.	571.	537.	539.	588.	570.	640.	664.	520.	734.	576.
149	159.	210.	260.	162.	131.	194.	161.	241.	241.	120.	156.
150	163.	238.	253.	179.	145.	229.	205.	163.	240.	134.	166.
151	177.	248.	252.	217.	167.	306.	228.	215.	279.	152.	205.
152	223.	301.	252.	231.	172.	211.	152.	144.	209.	146.	192.
153	164.	255.	217.	176.	114.	165.	112.	90.	210.	128.	185.
154	107.	209.	201.	142.	102.	154.	103.	85.	192.	102.	159.
155	95.	187.	201.	138.	94.	142.	97.	81.	186.	91.	145.
156	337.	349.	342.	292.	324.	320.	336.	336.	355.	355.	294.
158	474.	392.	407.	388.	412.	412.	464.	480.	390.	486.	393.
159	460.	413.	410.	403.	401.	490.	515.	498.	420.	488.	414.
160	454.	433.	358.	389.	418.	540.	540.	538.	361.	454.	392.
161	480.	483.	332.	343.	356.	448.	395.	449.	347.	497.	453.
162	355.	337.	370.	309.	336.	345.	361.	361.	367.	382.	350.
163	338.	339.	367.	309.	335.	320.	337.	343.	1594.	359.	316.
164	744.	666.	515.	474.	546.	653.	616.	720.	1640.	817.	737.
165	604.	515.	465.	434.	500.	544.	553.	587.	459.	648.	560.
166	534.	455.	490.	447.	490.	477.	519.	537.	441.	561.	454.
167	514.	456.	451.	434.	482.	440.	508.	519.	416.	538.	440.
168	157.	220.	264.	183.	140.	210.	174.	144.	230.	136.	178.
173	264.	324.	237.	245.	185.	212.	157.	137.	216.	194.	232.
174	610.	483.	602.	466.	567.	546.	660.	674.	531.	658.	498.

ORIGINAL PAGE IS  
OF POOR QUALITY

PAGE 3 OF 6

PEAK DETECTOR SAMPLED DATA: XBAR + 2 \* SIGMA

JOB I.D.: SR3 DATE: 12-SEP-84  
TITLE: SR3C-3 PROF-FAN TEST LERC JUL-83

RG#	RG1-1	RG1-2	RG1-3	RG2-2	RG2-1	RG5-2	RG3-1	RG5-1	RG5-3	RG6-1	RG6-2
175	584.	556.	636.	456.	531.	591.	644.	671.	545.	622.	512.
176	564.	500.	502.	427.	502.	614.	657.	691.	492.	611.	530.
177	659.	575.	502.	467.	519.	549.	528.	639.	421.	672.	556.
178	538.	444.	425.	438.	507.	498.	522.	566.	347.	607.	478.
180	226.	291.	311.	215.	190.	249.	203.	175.	338.	170.	195.
188	99.	186.	182.	140.	106.	148.	107.	83.	184.	96.	144.
190	782.	694.	511.	541.	614.	669.	646.	709.	529.	818.	739.
191	605.	503.	553.	463.	519.	515.	566.	588.	543.	637.	526.
192	538.	448.	513.	404.	501.	432.	520.	541.	520.	562.	461.
193	517.	437.	466.	440.	505.	431.	507.	526.	469.	544.	426.
194	522.	442.	440.	429.	500.	433.	520.	528.	452.	552.	434.
195	205.	254.	327.	213.	171.	264.	216.	190.	307.	186.	208.
201	140.	248.	238.	183.	129.	198.	131.	115.	197.	142.	215.
203	458.	432.	406.	395.	400.	432.	445.	468.	357.	460.	395.
204	440.	424.	461.	367.	392.	444.	454.	464.	422.	460.	396.
205	406.	385.	381.	349.	374.	481.	508.	500.	392.	452.	390.
206	474.	478.	350.	367.	372.	430.	377.	421.	353.	438.	374.
207	339.	329.	355.	293.	335.	327.	338.	349.	328.	373.	325.
208	326.	358.	371.	308.	328.	337.	336.	334.	324.	350.	335.
209	322.	330.	330.	326.	318.	353.	329.	326.	291.	348.	339.
211	731.	628.	530.	470.	565.	616.	618.	695.	451.	802.	685.
212	602.	502.	493.	433.	526.	507.	567.	602.	437.	651.	534.
213	540.	472.	447.	451.	523.	491.	538.	561.	386.	571.	491.
214	537.	501.	405.	481.	516.	519.	536.	549.	349.	566.	489.
215	762.	624.	505.	596.	700.	646.	737.	774.	426.	793.	638.
216	173.	234.	302.	201.	143.	250.	177.	169.	296.	151.	194.
221	151.	255.	224.	182.	130.	201.	124.	116.	204.	144.	205.
223	703.	590.	576.	517.	568.	591.	585.	664.	466.	757.	619.
224	631.	542.	549.	498.	544.	541.	559.	621.	456.	669.	549.
226	584.	531.	551.	536.	556.	557.	568.	600.	421.	610.	511.
227	682.	628.	635.	573.	630.	684.	699.	730.	497.	731.	600.
230	166.	270.	310.	201.	163.	251.	190.	191.	290.	142.	209.
237	101.	203.	222.	172.	116.	185.	107.	112.	225.	103.	186.
240	651.	606.	402.	434.	522.	544.	587.	622.	453.	711.	630.
241	518.	461.	380.	439.	507.	476.	520.	534.	437.	555.	446.
242	513.	362.	362.	473.	503.	493.	511.	526.	413.	547.	470.
243	508.	505.	348.	482.	506.	510.	523.	528.	401.	545.	486.
244	160.	212.	239.	187.	146.	223.	175.	170.	243.	139.	183.
250	116.	228.	214.	173.	120.	175.	111.	108.	186.	107.	195.
251	397.	484.	394.	398.	361.	458.	396.	414.	351.	420.	375.
252	388.	395.	406.	350.	345.	428.	384.	417.	375.	406.	390.
253	378.	411.	358.	364.	329.	458.	431.	455.	388.	413.	377.
254	388.	385.	322.	290.	292.	355.	332.	352.	324.	378.	335.
255	389.	352.	318.	342.	306.	304.	304.	313.	330.	325.	266.
256	292.	331.	294.	308.	294.	314.	302.	302.	286.	317.	301.
257	295.	352.	267.	316.	298.	330.	300.	304.	266.	315.	326.
258	756.	442.	502.	515.	571.	590.	600.	663.	476.	779.	641.
259	692.	600.	488.	489.	540.	563.	564.	621.	455.	722.	605.
260	523.	509.	441.	446.	507.	547.	544.	538.	408.	553.	485.
261	521.	500.	428.	472.	502.	491.	511.	528.	384.	548.	482.

PEAK DETECTOR SAMPLED DATA: XBAR + 2 \* SIGMA

JOB I.D.: SR3

DATE: 12-SEP-84

TITLE: SR3C-3 PROP-FAN TEST LERC JUL-83

RG#	RG1-1	RG1-2	RG1-3	RG2-2	RG2-1	RG5-2	RG3-1	RG5-1	RG5-3	RG6-1	RG6-2
262	124.	212.	255.	154.	114.	154.	133.	131.	218.	107.	147.
263	115.	219.	239.	151.	112.	156.	140.	131.	207.	105.	142.
264	94.	185.	204.	175.	102.	183.	103.	109.	202.	96.	167.
265	143.	232.	266.	190.	154.	236.	180.	171.	270.	128.	190.
266	829.	724.	510.	583.	637.	615.	630.	695.	510.	825.	701.
267	539.	518.	453.	478.	506.	476.	541.	4.	427.	571.	487.
268	276	533.	448.	489.	510.	514.	547.	4.	422.	564.	495.
269	277	533.	448.	489.	510.	514.	547.	4.	422.	564.	495.
270	276	533.	448.	489.	510.	514.	547.	4.	422.	564.	495.
271	277	533.	448.	489.	510.	514.	547.	4.	422.	564.	495.
272	276	533.	448.	489.	510.	514.	547.	4.	422.	564.	495.
273	277	533.	448.	489.	510.	514.	547.	4.	422.	564.	495.
274	276	533.	448.	489.	510.	514.	547.	4.	422.	564.	495.
275	277	533.	448.	489.	510.	514.	547.	4.	422.	564.	495.
276	276	533.	448.	489.	510.	514.	547.	4.	422.	564.	495.
277	277	533.	448.	489.	510.	514.	547.	4.	422.	564.	495.
278	276	533.	448.	489.	510.	514.	547.	4.	422.	564.	495.
279	277	533.	448.	489.	510.	514.	547.	4.	422.	564.	495.
280	276	533.	448.	489.	510.	514.	547.	4.	422.	564.	495.
281	277	533.	448.	489.	510.	514.	547.	4.	422.	564.	495.
282	276	533.	448.	489.	510.	514.	547.	4.	422.	564.	495.
283	277	533.	448.	489.	510.	514.	547.	4.	422.	564.	495.
284	276	533.	448.	489.	510.	514.	547.	4.	422.	564.	495.
285	277	533.	448.	489.	510.	514.	547.	4.	422.	564.	495.
286	276	533.	448.	489.	510.	514.	547.	4.	422.	564.	495.
287	277	533.	448.	489.	510.	514.	547.	4.	422.	564.	495.
288	276	533.	448.	489.	510.	514.	547.	4.	422.	564.	495.
289	277	533.	448.	489.	510.	514.	547.	4.	422.	564.	495.
290	276	533.	448.	489.	510.	514.	547.	4.	422.	564.	495.
291	277	533.	448.	489.	510.	514.	547.	4.	422.	564.	495.
292	276	533.	448.	489.	510.	514.	547.	4.	422.	564.	495.
293	277	533.	448.	489.	510.	514.	547.	4.	422.	564.	495.
294	276	533.	448.	489.	510.	514.	547.	4.	422.	564.	495.
295	277	533.	448.	489.	510.	514.	547.	4.	422.	564.	495.
296	276	533.	448.	489.	510.	514.	547.	4.	422.	564.	495.
297	277	533.	448.	489.	510.	514.	547.	4.	422.	564.	495.
298	276	533.	448.	489.	510.	514.	547.	4.	422.	564.	495.
299	277	533.	448.	489.	510.	514.	547.	4.	422.	564.	495.
300	276	533.	448.	489.	510.	514.	547.	4.	422.	564.	495.
301	277	533.	448.	489.	510.	514.	547.	4.	422.	564.	495.
302	276	533.	448.	489.	510.	514.	547.	4.	422.	564.	495.
303	277	533.	448.	489.	510.	514.	547.	4.	422.	564.	495.
304	276	533.	448.	489.	510.	514.	547.	4.	422.	564.	495.
305	277	533.	448.	489.	510.	514.	547.	4.	422.	564.	495.
306	276	533.	448.	489.	510.	514.	547.	4.	422.	564.	495.
307	277	533.	448.	489.	510.	514.	547.	4.	422.	564.	495.
308	276	533.	448.	489.	510.	514.	547.	4.	422.	564.	495.
309	277	533.	448.	489.	510.	514.	547.	4.	422.	564.	495.
310	276	533.	448.	489.	510.	514.	547.	4.	422.	564.	495.
311	277	533.	448.	489.	510.	514.	547.	4.	422.	564.	495.
312	276	533.	448.	489.	510.	514.	547.	4.	422.	564.	495.
313	277	533.	448.	489.	510.	514.	547.	4.	422.	564.	495.
314	276	533.	448.	489.	510.	514.	547.	4.	422.	564.	495.
315	277	533.	448.	489.	510.	514.	547.	4.	422.	564.	495.
316	276	533.	448.	489.	510.	514.	547.	4.	422.	564.	495.
317	277	533.	448.	489.	510.	514.	547.	4.	422.	564.	495.
318	276	533.	448.	489.	510.	514.	547.	4.	422.	564.	495.
319	277	533.	448.	489.	510.	514.	547.	4.	422.	564.	495.
320	276	533.	448.	489.	510.	514.	547.	4.	422.	564.	495.
321	277	533.	448.	489.	510.	514.	547.	4.	422.	564.	495.
322	276	533.	448.	489.	510.	514.	547.	4.	422.	564.	495.
323	277	533.	448.	489.	510.	514.	547.	4.	422.	564.	495.
324	276	533.	448.	489.	510.	514.	547.	4.	422.	564.	495.
325	277	533.	448.	489.	510.	514.	547.	4.	422.	564.	495.
326	276	533.	448.	489.	510.	514.	547.	4.	422.	564.	495.
327	277	533.	448.	489.	510.	514.	547.	4.	422.	564.	495.
328	276	533.	448.	489.	510.	514.	547.	4.	422.	564.	495.
329	277	533.	448.	489.	510.	514.	547.	4.	422.	564.	495.
330	276	533.	448.	489.	510.	514.	547.	4.	422.	564.	495.
331	277	533.	448.	489.	510.	514.	547.	4.	422.	564.	495.
332	276	533.	448.	489.	510.	514.	547.	4.	422.	564.	495.
333	277	533.	448.	489.	510.	514.	547.	4.	422.	564.	495.
334	276	533.	448.	489.	510.	514.	547.	4.	422.	564.	495.
335	277	533.	448.	489.	510.	514.	547.	4.	422.	564.	495.
336	276	533.	448.	489.	510.	514.	547.	4.	422.	564.	495.



PEAK DETECTOR SAMPLED DATA: XBAR + 2 \* SIGMA

JOB T.D.: SR3 DATE: 12-SEP-84  
 TITLE: SR3C-3 PROP-FAN TEST LENC JUL-83

ROW#	B61-1	B61-2	B61-3	B62-2	B62-1	B65-2	B63-1	B65-1	B65-3	B66-1	B66-2
342	390.	376.	317.	302.	319.	388.	356.	3.	350.	422.	384.
343	454.	386.	320.	380.	384.	405.	432.	3.	385.	457.	352.
345	398.	437.	301.	387.	375.	535.	491.	3.	370.	423.	396.
346	414.	410.	296.	313.	327.	422.	365.	3.	321.	445.	395.
347	327.	343.	305.	293.	315.	325.	327.	3.	350.	345.	330.
348	322.	332.	302.	286.	314.	301.	318.	3.	336.	340.	300.
349	319.	345.	294.	292.	304.	330.	320.	3.	330.	338.	300.
350	732.	654.	406.	546.	580.	757.	653.	3.	478.	806.	716.
351	563.	480.	380.	408.	483.	511.	523.	3.	434.	593.	487.
352	497.	448.	391.	420.	475.	429.	489.	2.	434.	530.	411.
353	487.	438.	360.	407.	458.	421.	491.	3.	419.	517.	422.
354	708.	558.	408.	543.	640.	625.	717.	3.	455.	739.	559.
355	708.	631.	490.	543.	628.	771.	770.	2.	553.	713.	653.
357	172.	265.	268.	214.	167.	233.	199.	3.	237.	159.	221.
358	175.	264.	266.	214.	163.	240.	218.	3.	239.	161.	226.
366	97.	209.	225.	168.	117.	177.	110.	3.	224.	97.	174.
367	148.	245.	247.	160.	130.	189.	190.	3.	177.	132.	148.
375	96.	191.	192.	161.	110.	152.	103.	3.	168.	98.	159.
376	540.	517.	454.	479.	506.	498.	540.	549.	420.	570.	488.
277	534.	519.	448.	488.	510.	516.	547.	554.	420.	564.	493.
278	140.	254.	198.	181.	122.	167.	145.	112.	173.	128.	183.
279	125.	224.	242.	151.	102.	150.	124.	118.	188.	103.	138.
280	143.	228.	237.	142.	114.	160.	126.	127.	193.	121.	159.
281	164.	292.	297.	161.	134.	187.	170.	152.	210.	139.	165.
282	155.	258.	275.	196.	154.	213.	189.	189.	222.	153.	241.
283	179.	252.	251.	257.	181.	339.	280.	275.	254.	180.	222.
284	301.	429.	233.	290.	248.	420.	240.	379.	234.	400.	438.
285	231.	303.	205.	222.	184.	192.	160.	384.	234.	401.	441.
286	131.	261.	207.	178.	126.	161.	117.	145.	184.	162.	215.
289	56.	130.	121.	66.	69.	60.	57.	64.	86.	53.	57.
291	85.	157.	204.	137.	86.	139.	75.	86.	231.	64.	122.
301	302.	361.	301.	353.	366.	356.	392.	403.	454.	411.	320.
303	410.	361.	249.	328.	352.	364.	388.	389.	297.	400.	349.
304	417.	367.	195.	333.	347.	376.	381.	390.	226.	398.	323.
305	416.	359.	196.	327.	335.	371.	363.	390.	243.	427.	344.
306	369.	335.	211.	300.	314.	350.	346.	353.	267.	394.	325.
307	337.	324.	223.	269.	288.	289.	321.	313.	269.	333.	285.
308	289.	294.	202.	235.	252.	260.	287.	266.	263.	281.	253.
309	246.	257.	194.	224.	239.	231.	259.	235.	234.	247.	215.
310	219.	241.	181.	202.	211.	204.	224.	209.	230.	231.	202.
311	216.	233.	162.	187.	197.	211.	224.	210.	202.	221.	199.
312	233.	160.	183.	160.	199.	214.	227.	209.	209.	217.	194.
314	591.	512.	316.	484.	493.	525.	549.	556.	404.	597.	528.
315	489.	427.	306.	400.	420.	439.	479.	477.	395.	497.	432.
316	418.	385.	306.	350.	369.	377.	422.	419.	400.	429.	371.
317	364.	281.	328.	338.	338.	371.	377.	370.	360.	387.	336.
318	360.	331.	267.	330.	326.	334.	377.	368.	343.	367.	316.
319	728.	599.	420.	595.	638.	634.	715.	739.	566.	752.	574.
320	545.	463.	346.	443.	471.	470.	518.	534.	482.	550.	437.

PEAK DETECTOR SAMPLED DATA: XBAR + 2 \* SIGMA

JOB I.D.: SR3 DATE: 12-SEP-04

TITLE: SR3C-3 PROF-FAN TEST LERC JUL-83

RG6#	RG1-1	RG1-2	RG1-3	RG2-2	RG2-1	RG5-2	RG3-1	RG5-1	RG5-3	RG6-1	RG6-2
321	268.	277.	202.	250.	249.	269.	292.	262.	255.	276.	357.
322	541.	457.	353.	447.	476.	464.	513.	539.	504.	550.	438.
323	540.	433.	303.	445.	473.	502.	527.	542.	389.	534.	445.
324	557.	461.	285.	467.	489.	569.	549.	599.	360.	570.	454.
325	566.	474.	292.	485.	485.	568.	521.	614.	360.	624.	524.
326	561.	489.	314.	451.	461.	510.	494.	532.	329.	590.	501.
327	480.	440.	270.	368.	402.	393.	437.	439.	329.	483.	424.
328	406.	382.	263.	335.	343.	355.	386.	371.	323.	395.	352.
329	338.	326.	261.	293.	294.	310.	332.	320.	318.	337.	311.
330	287.	278.	227.	261.	266.	277.	395.	283.	291.	302.	268.
331	273.	277.	209.	255.	263.	266.	289.	266.	262.	285.	261.
332	265.	265.	206.	252.	252.	266.	289.	261.	261.	279.	256.
333	84.	179.	190.	132.	95.	140.	99.	95.	174.	89.	142.
336	135.	212.	255.	171.	135.	208.	152.	156.	265.	117.	168.
342	406.	395.	316.	307.	330.	418.	368.	416.	350.	443.	399.
343	453.	387.	328.	379.	385.	406.	432.	445.	389.	458.	352.
345	396.	436.	299.	385.	372.	538.	490.	512.	375.	421.	394.
346	411.	408.	292.	307.	323.	424.	363.	406.	323.	444.	395.
347	330.	344.	313.	297.	320.	336.	333.	346.	353.	354.	337.
348	323.	334.	301.	284.	315.	303.	319.	316.	340.	338.	299.
349	320.	345.	294.	291.	303.	303.	319.	309.	332.	337.	299.
350	738.	655.	405.	546.	580.	580.	651.	806.	485.	806.	714.
351	562.	477.	385.	408.	483.	516.	523.	543.	440.	593.	487.
352	495.	445.	389.	421.	476.	433.	488.	505.	437.	531.	410.
353	485.	437.	361.	407.	458.	427.	490.	496.	424.	517.	421.
354	707.	556.	408.	541.	640.	631.	717.	762.	460.	740.	558.
355	704.	633.	492.	543.	628.	779.	772.	830.	556.	713.	654.
357	170.	264.	267.	216.	161.	237.	198.	194.	244.	160.	217.
358	176.	263.	263.	214.	165.	244.	216.	207.	245.	160.	228.
366	98.	209.	221.	166.	115.	178.	109.	103.	228.	96.	171.
367	148.	246.	247.	159.	129.	190.	187.	164.	183.	131.	147.
375	96.	193.	192.	162.	110.	153.	101.	96.	171.	98.	158.

STOP --

## APPENDIX II

P-order Strain Tabulation.

ORIGINAL PAGE IS  
OF POOR QUALITY

77

SR-3C-3 PROP FAN  
8' X 6' WIND TUNNEL TESTS  
NASA-LEWIS

P ORDER COMPONENTS  
PEAK STRAIN

REG. NO.	MACH NO.	BLADE ANGLE DEG	TILT ANGLE DEG	PROP SPEED RPM	BLADE GAGE	P ORDER COMPONENTS PEAK STRAIN				
						1	2	3	4	5
38	0.361	48.	8.25	9044.	BG1-1	329.	40.	****	****	****
					BG1-3	23.	26.	14.	10.	35.
					BG3-1	323.	35.	****	****	****
					BG5-1	297.	42.	****	****	****
					BG5-2	**** 143	**** 27	****	****	****
39	0.362	48.	8.17	8507.	BG5-3	**** 12	**** 14	****	****	****
					BG1-1	291.	73.	5.	****	28.
					BG1-3	44.	****	12.	72.	****
					BG3-1	284.	60.	****	****	****
					BG5-1	270.	70.	****	****	****
40	0.362	48.	8.26	8028.	BG5-2	229.	59.	22.	21.	7.
					BG5-3	44.	23.	24.	27.	23.
					BG1-1	307.	102.	13.	6.	12.
					BG1-3	97.	28.	14.	32.	****
					BG3-1	306.	60.	7.	****	****
41	0.362	48.	8.17	7520.	BG5-1	292.	84.	****	****	****
					BG5-2	245.	79.	16.	20.	18.
					BG5-3	111.	39.	15.	28.	****
					BG1-1	290.	113.	21.	****	****
					BG1-3	140.	38.	32.	****	****
42	0.361	48.	8.24	7009.	BG3-1	304.	66.	13.	****	****
					BG5-1	283.	134.	15.	****	****
					BG5-2	241.	136.	16.	7.	****
					BG5-3	168.	64.	9.	11.	****
					BG1-1	234.	113.	****	****	****
43	0.362	48.	8.13	6519.	BG1-3	134.	17.	13.	****	****
					BG3-1	248.	67.	****	****	****
					BG5-1	226.	89.	****	****	****
					BG5-2	196.	96.	****	****	****
					BG5-3	178.	29.	****	****	8.
44	0.361	48.	8.17	6013.	BG1-1	211.	91.	****	****	12.
					BG1-3	131.	11.	9.	****	****
					BG3-1	231.	62.	****	****	****
					BG5-1	208.	74.	4.	****	****
					BG5-2	186.	83.	****	****	****
45	0.363	48.	8.17	5515.	BG5-3	182.	9.	****	****	****
					BG1-1	216.	63.	5.	5.	****
					BG1-3	130.	10.	15.	****	****
					BG3-1	237.	48.	11.	****	****
					BG5-1	209.	47.	****	****	****
46	0.362	48.	8.13	5023.	BG5-2	189.	60.	6.	****	****
					BG5-3	190.	9.	10.	****	****
					BG1-1	193.	**** 13	****	****	****
					BG1-3	109.	**** 4	****	****	****
					BG3-1	210.	**** 25	11.	****	****

0.18 1.18 1.34 1.27 1.12 1.09 1.17 1.12 1.12 1.12

1.18 1.18 1.34 1.27 1.12 1.09 1.17 1.12 1.12 1.12

P ORDER COMPONENTS  
PEAK STRAIN

79

SR-3C-3 PROP FAN  
8'X6' WIND TUNNEL TESTS  
NASA-LEWIS

P ORDER COMPONENTS  
PEAK STRAIN

RNG. NO.	MACH NO.	BLADE ANGLE DEG	TILT ANGLE DEG	PROP SPEED RPM	BLADE GAGE	P ORDER COMPONENTS				
						1	2	3	4	5
68	0.362	51.	15.04	5015.	R65-2 R65-3 R61-1 R61-3 R63-1 R65-1 R65-2 R65-3	324. 269. 389. 286. 103. 391. 346. 241.	118. **** 125. 11. 103. 113. 155. 57.	61. 35. 32. 26. 44. 46. 17. 44.	4. 18. **** 11. 5. **** **** ****	**** **** **** **** **** **** **** ****
69	0.362	51.	15.05	5504.	R61-1 R61-3 R63-1 R65-1 R65-2 R65-3	427. 195. 440. 430. 405. 216.	169. 35. 139. 144. 198. 112.	12. 30. 22. 13. 11. 36.	**** **** **** **** **** ****	**** **** **** **** **** ****
70	0.361	51.	15.01	6007.	R61-1 R61-3 R63-1 R65-1 R65-2 R65-3	501. 176. 517. 508. 486. 119.	230. 84. 174. 182. 288. 124.	5. 41. 14. 12. **** 25.	5. **** 4. 7. **** ****	**** **** **** **** **** ****
71	0.362	51.	15.14	6511.	R61-1 R61-3 R63-1 R65-1 R65-2 R65-3	490. 373. 139. 437. 198. 440.	205. 237. 161. 70. 47. 44.	8. 11. 19. **** 42. 13.	**** **** **** **** 18. ****	**** **** **** **** **** ****
80	0.588	55.	7.03	6047.	R61-1 R61-3 R63-1 R65-1 R65-2 R65-3	436. 325. 252. 401. 173. 405.	50. 63. 47. 75. 58. 44.	7. 5. 29. **** 33. 13.	**** **** **** **** **** ****	**** **** **** **** **** ****
81	0.589	55.	6.99	5919.	R61-1 R61-3 R63-1 R65-1 R65-2 R65-3	299. 221. 440. 240. 442. 443.	65. 62. 91. 19. 75. 88.	5. 29. 4. 22. 14. 7.	**** **** **** **** **** ****	**** **** **** **** **** ****
82	0.587	55.	7.14	6506.	R61-1 R61-3 R63-1 R65-1 R65-2 R65-3	326. 288. 209. 208. 484. 471.	105. 12. 209. 35. 154. 162.	10. 11. **** **** **** ****	6. 24. **** **** **** ****	**** **** **** **** **** ****
83	0.587	55.	7.03	7013.	R61-1 R61-3 R63-1 R65-1 R65-2 R65-3	497. 208. 484. 350. 333. 14.	209. 35. 154. 215. 43. 8.	11. **** **** **** **** ****	**** **** **** **** **** ****	**** **** **** **** **** ****
93	0.405	57.	0.10	5308.	R65-2 R65-3 R61-1 R61-3 R63-1	27. 14. 22. 36. 14.	**** **** **** **** ****	**** **** **** **** ****	**** **** **** **** ****	**** **** **** **** ****

ORIGINAL PAGE IS  
OF POOR QUALITY

SR-3C-3 PROP FAN  
8'X6' WIND TUNNEL TESTS  
NASA-LEWIS

P ORDER COMPONENTS  
PEAK STRAIN

RING. NO.	MACH NO.	BLADE ANGLE DEG	TILT ANGLE DEG	PROP SPEED RPM	BLADE GAGE	P ORDER COMPONENTS PEAK STRAIN				
						1	2	3	4	5
94	0.603	57.	4.11	5254.	B65-2	210.	13.	9.	****	****
					B65-3	194.	35.	12.	****	****
					B61-1	285.	14.	****	****	****
					B61-3	143.	26.	16.	****	****
					B63-1	294.	10.	7.	****	****
96	0.598	57.	4.05	9001.	B65-1	271.	8.	7.	****	****
					B65-2	336.	11.	25.	42.	7.
					B65-3	30.	88.	35.	58.	34.
					B61-1	445.	53.	4.	****	****
					B61-3	66.	77.	34.	34.	20.
97	0.599	57.	4.13	8503.	B63-1	432.	91.	5.	****	****
					B65-1	413.	77.	4.	****	****
					B65-2	324.	96.	58.	26.	14.
					B65-3	56.	24.	77.	54.	24.
					B61-1	409.	71.	7.	****	5.
98	0.599	57.	4.18	8004.	B61-3	60.	41.	69.	69.	67.
					B63-1	374.	109.	****	****	****
					B65-1	366.	95.	6.	****	****
					B65-2	312.	121.	11.	24.	13.
					B65-3	159.	71.	20.	29.	49.
99	0.601	57.	4.16	7507.	B61-1	392.	111.	15.	6.	****
					B61-3	125.	31.	42.	60.	34.
					B63-1	363.	68.	7.	4.	****
					B65-1	363.	108.	****	****	****
					B65-2	295.	183.	9.	6.	36.
100	0.599	57.	4.09	7002.	B65-3	241.	83.	16.	12.	60.
					B61-1	373.	172.	8.	****	****
					B61-3	199.	66.	32.	10.	15.
					B63-1	363.	85.	7.	****	****
					B65-1	358.	161.	20.	****	****
101	0.600	57.	4.20	6496.	B65-2	224.	124.	14.	24.	****
					B65-3	231.	32.	19.	24.	****
					B61-1	306.	129.	5.	****	****
					B61-3	181.	23.	33.	13.	****
					B63-1	304.	84.	6.	****	****
102	0.601	57.	4.07	5998.	B65-1	292.	104.	5.	****	7.
					B65-2	210.	65.	****	12.	10.
					B65-3	217.	56.	4.	****	****
					B61-1	289.	56.	4.	4.	16.
					B61-3	164.	9.	13.	11.	****
103	0.602	57.	4.08	5501.	B63-1	289.	49.	5.	****	****
					B65-1	277.	51.	****	****	****
					B65-2	208.	27.	9.	5.	****
					B65-3	223.	****	****	8.	****
					B61-1	289.	29.	4.	****	****



SR-3C-3 PROP FAN  
8' X 6' WIND TUNNEL TESTS  
NASA-LEWIS

RIG. NO.	MACH NO.	BLADE ANGLE DEG	TILT ANGLE DEG	PROP SPEED RPM	BLADE GAGE	P ORDER COMPONENTS PEAK STRAIN				
						1	2	3	4	5
104	0.602	57.	7.06	5211.	B65-2	331.	42.	****	****	****
					B65-3	248.	69.	****	****	****
					B61-1	452.	53.	****	****	****
					B61-3	200.	57.	****	****	****
					B63-1	437.	26.	****	****	****
105	0.602	57.	7.08	5507.	B65-1	443.	33.	****	****	****
					B65-2	333.	47.	16.	****	****
					B65-3	286.	56.	15.	****	****
					B61-1	461.	55.	6.	****	****
					B61-3	230.	44.	21.	****	****
106	0.601	57.	7.01	6001.	B63-1	446.	34.	17.	****	****
					B65-1	453.	38.	****	****	****
					B65-2	367.	88.	26.	6.	5.
					B65-3	362.	29.	****	15.	10.
					B61-1	510.	99.	10.	5.	13.
107	0.602	57.	7.01	6506.	B61-3	297.	21.	12.	10.	13.
					B63-1	494.	73.	12.	****	****
					B65-1	504.	72.	14.	4.	****
					B61-1	501.	178.	8.	5.	****
					B61-3	309.	15.	15.	15.	15.
118	0.698	57.	5.02	7403.	B63-1	491.	139.	17.	4.	****
					B65-1	472.	142.	10.	****	5.
					B65-2	347.	170.	17.	10.	11.
					B65-3	365.	12.	13.	10.	11.
					B61-1	462.	209.	19.	5.	****
119	0.599	57.	5.09	7013.	B61-3	208.	76.	40.	16.	****
					B63-1	430.	114.	11.	****	****
					B65-1	448.	195.	10.	5.	****
					B65-2	346.	221.	22.	15.	14.
					B65-3	226.	80.	26.	19.	29.
120	0.700	57.	5.04	6510.	B61-1	450.	99.	****	****	****
					B61-3	230.	33.	29.	****	****
					B63-1	417.	61.	8.	****	****
					B65-1	447.	93.	8.	****	****
					B65-2	347.	113.	6.	10.	6.
121	0.700	57.	5.05	6202.	B65-3	252.	36.	16.	****	****
					B61-1	434.	56.	4.	****	5.
					B61-3	225.	23.	41.	28.	14.
					B63-1	405.	36.	7.	****	****
					B65-1	432.	60.	****	****	****
127	0.605	59.	-2.75	4925.	B65-2	338.	79.	7.	22.	9.
					B65-3	245.	29.	23.	24.	****
					B61-1	438.	55.	****	4.	****
					B61-3	204.	52.	41.	33.	****
					B63-1	411.	34.	4.	****	****

ORIGINAL PAGE IS  
OF POOR QUALITY

SR-3C-3 PROP FAN  
8'X6' WIND TUNNEL TESTS  
NASA-LEWIS

P ORDER COMPONENTS  
PEAK STRAIN

83

ORIGINAL PAGE IS  
OF POOR QUALITY

SR-3C-3 PROP FAN  
8'X6' WIND TUNNEL TESTS  
NASA-LEWIS

P ORDER COMPONENTS  
PEAK STRAIN

RNG. NO.	MACH NO.	BLADE ANGLE DEG	TILT ANGLE DEG	PROP SPEED RPM	BLADE GAUGE	P ORDER COMPONENTS				
						1	2	3	4	5
156	0.700	59.	3.04	6060.	R05-2	207.	33.	4.	14.	4.
					R05-3	169.	26.	****	11.	****
					R01-1	261.	26.	****	****	****
					R01-3	169.	38.	17.	23.	9.
					R03-1	263.	16.	****	****	****
158	0.697	59.	3.00	9000.	R05-1	249.	24.	4.	****	****
					R05-2	299.	77.	50.	29.	5.
					R05-3	158.	78.	50.	54.	27.
					R01-1	402.	61.	5.	6.	****
					R01-3	166.	53.	46.	23.	16.
159	0.698	59.	2.98	8500.	R03-1	394.	82.	6.	****	****
					R05-1	382.	88.	9.	****	****
					R05-2	256.	150.	6.	5.	14.
					R05-3	147.	97.	44.	18.	29.
					R01-1	352.	75.	****	****	****
160	0.699	59.	2.94	7995.	R01-3	156.	71.	10.	16.	30.
					R03-1	336.	133.	****	****	****
					R05-1	326.	137.	5.	****	****
					R05-2	250.	188.	4.	18.	6.
					R05-3	131.	85.	16.	25.	13.
161	0.699	59.	2.90	7506.	R01-1	321.	105.	10.	****	****
					R01-3	126.	59.	21.	36.	23.
					R03-1	309.	168.	5.	****	****
					R05-1	297.	175.	****	****	****
					R05-2	244.	133.	19.	8.	11.
162	0.700	59.	3.00	6998.	R05-3	159.	54.	18.	12.	23.
					R01-1	316.	143.	14.	8.	4.
					R01-3	150.	36.	28.	18.	14.
					R03-1	306.	60.	17.	****	****
					R05-1	297.	110.	15.	7.	****
163	0.700	59.	2.94	6501.	R05-2	200.	67.	11.	11.	5.
					R05-3	189.	24.	8.	9.	24.
					R01-1	276.	19.	****	****	****
					R01-3	205.	****	16.	22.	14.
					R03-1	272.	10.	****	****	****
164	0.699	59.	5.06	7296.	R05-1	263.	20.	4.	23.	5.
					R01-1	482.	241.	18.	8.	9.
					R01-3	280.	75.	54.	23.	21.
					R03-1	459.	144.	16.	****	****
					R05-1	443.	224.	10.	5.	****
165	0.699	59.	5.04	6994.	R05-2	341.	261.	16.	22.	17.
					R05-3	257.	96.	21.	30.	30.
					R05-2	339.	162.	16.	12.	20.
					R05-3	271.	54.	21.	10.	30.
					R01-1	456.	136.	****	****	****
					R01-3	297.	46.	26.	****	****
					R03-1	439.	91.	9.	****	****
					R05-1	450.	120.	7.	****	****

COVERED PAGE IS  
OF FLOOR QUALITY

85

ORIGINAL PAGE IS  
OF POOR QUALITY

SR-3C-3 PROP FAN  
8'X6' WIND TUNNEL TESTS  
NASA-LEWIS

RDG. NO.	MACH NO.	BLADE ANGLE DEG	TILT ANGLE DEG	PROP SPEED RPM	BLADE GAGE	P ORDER COMPONENTS PEAK STRAIN				
						1	2	3	4	5
192	0.702	61.	4.99	5992.	R65-2 R65-3 R61-1 R61-3 R63-1 R65-1 R65-2 R65-3	346. 377. 494. 380. 475. 489. 317. 303.	60. 20. 58. 16. 47. 46. 26. 57.	13. ***** 11. 19. 12. ***** 12. *****	17. 19. 4. 12. ***** ***** ***** *****	***** ***** ***** ***** ***** ***** ***** *****
193	0.703	61.	4.87	5495.	R61-1 R61-3 R63-1 R65-1 R65-2 R65-3	441. 299. 424. 434. 327. 271.	35. 54. 25. 25. 19. 70.	5. 31. 16. 5. ***** *****	***** ***** ***** ***** ***** *****	***** ***** ***** ***** ***** *****
194	0.702	61.	4.92	5195.	R61-1 R61-3 R63-1 R65-1 R65-2 R65-3	447. 264. 431. 438. 369. 162.	19. 22. 19. 16. 48. 24.	***** ***** ***** ***** ***** *****	***** ***** ***** ***** ***** *****	***** ***** ***** ***** ***** *****
203	0.798	61.	1.98	8990.	R61-1 R61-3 R63-1 R65-1 R65-2 R65-3	329. 277. 148. 337. 185. 321.	24. 33. 45. 53. 20. 20.	7. 16. ***** ***** ***** *****	23. 27. 7. 37. ***** *****	***** ***** ***** ***** ***** *****
204	0.799	61.	2.06	8508.	R61-1 R61-3 R63-1 R65-1 R65-2 R65-3	220. 176. 284. 133. 283. 253.	9. 9. 23. 13. 33. 151.	45. 51. 12. 8. ***** *****	21. 26. ***** ***** ***** *****	***** ***** ***** ***** ***** *****
205	0.800	61.	1.98	8005.	R61-1 R61-3 R63-1 R65-1 R65-2 R65-3	182. 140. 281. 142. 124. 281.	164. 77. 281. 35. 61. 89.	4. 11. 21. 41. 18. 12.	14. 24. 8. 6. 5. 14.	6. 9. 15. ***** ***** *****
206	0.800	61.	2.03	7503.	R61-1 R61-3 R63-1 R65-1 R65-2 R65-3	187. 140. 253. 152. 256. 226.	99. 36. 18. 33. 15. 37.	21. 15. 15. 6. 9. 6.	22. ***** ***** ***** ***** *****	***** ***** ***** ***** ***** *****
207	0.802	61.	1.89	7008.	R61-1 R61-3 R63-1 R65-1 R65-2 R65-3	145. 175. 145. 251. 176. 255.	22. 41. 14. 17. 14. 21.	***** ***** ***** ***** ***** *****	***** ***** ***** ***** ***** *****	***** ***** ***** ***** ***** *****
208	0.802	61.	2.06	6495.	R61-1 R61-3 R63-1 R65-1 R65-2 R65-3	188. 155. 155. 155. 155. 155.	30. 16. 16. 16. 16. 16.	***** ***** ***** ***** ***** *****	***** ***** ***** ***** ***** *****	***** ***** ***** ***** ***** *****

ORIGINAL PAGE IS  
OF POOR QUALITY

87

SR-3C-3 PROP FAN  
8'X6' WIND TUNNEL TESTS  
NASA-LEWIS

P ORDER COMPONENTS

RDG. NO.	MACH NO.	BLADE ANGLE DEG	TILT ANGLE DEG	PROP SPEED RPM	BLADE GAGE	PEAK STRAIN				
						1	2	3	4	5

227	0.840	61.	3.96	9000.	B65-2	455.	133.	53.	28.	14.
					B65-3	219.	90.	62.	33.	55.
					B61-1	574.	66.	9.	*****	*****
					B61-3	289.	127.	77.	24.	35.
					B63-1	569.	123.	*****	5.	*****
					B65-1	544.	105.	9.	*****	*****
240	0.790	63.	4.00	6998.	B61-1	449.	188.	7.	*****	5.
					B61-3	206.	44.	*****	*****	16.
					B63-1	447.	123.	10.	*****	*****
					B65-1	424.	150.	5.	*****	4.
					B65-2	310.	168.	15.	*****	9.
					B65-3	237.	55.	18.	*****	12.
241	0.791	63.	4.00	6502.	B65-2	314.	58.	8.	5.	15.
					B65-3	236.	33.	*****	*****	*****
					B61-1	423.	49.	7.	7.	*****
					B61-3	208.	25.	12.	20.	13.
					B63-1	423.	53.	13.	*****	*****
					B65-1	397.	51.	7.	*****	*****
					B65-2	366.	53.	15.	5.	7.
242	0.790	63.	4.00	5997.	B65-3	256.	37.	21.	15.	*****
					B61-1	463.	33.	9.	*****	*****
					B61-3	222.	27.	32.	21.	9.
					B63-1	462.	40.	8.	*****	*****
					B65-1	433.	40.	6.	*****	7.
					B65-2	357.	41.	15.	12.	8.
243	0.790	63.	3.98	5640.	B65-3	221.	40.	23.	9.	*****
					B61-1	443.	36.	*****	*****	*****
					B61-3	186.	38.	27.	*****	*****
					B63-1	446.	32.	*****	*****	*****
					B65-1	414.	31.	*****	*****	*****
251	0.839	63.	2.03	9010.	B65-2	288.	37.	34.	28.	*****
					B65-3	105.	36.	25.	25.	11.
					B61-1	310.	7.	8.	*****	*****
					B61-3	143.	49.	35.	*****	19.
					B63-1	303.	10.	*****	*****	*****
					B65-1	283.	9.	7.	*****	*****
					B65-2	215.	76.	40.	14.	11.
252	0.840	63.	1.93	8503.	B65-3	170.	56.	39.	15.	29.
					B61-1	289.	40.	*****	5.	*****
					B61-3	178.	54.	37.	19.	36.
					B63-1	283.	55.	4.	*****	*****
					B65-1	260.	81.	4.	*****	*****
					B65-2	174.	138.	18.	14.	9.
253	0.840	63.	2.09	8009.	B65-3	135.	87.	11.	19.	10.
					B61-1	250.	23.	5.	*****	*****
					B61-3	139.	12.	15.	44.	9.
					B63-1	257.	38.	5.	*****	*****
					B65-1	223.	127.	5.	*****	*****
					B65-2	171.	50.	7.	17.	15.
254	0.842	63.	2.02	7507.	B65-3	129.	27.	*****	18.	21.
					B61-1	241.	87.	7.	8.	5.
					B61-3	121.	28.	27.	21.	*****
					B63-1	251.	48.	4.	5.	*****

0.00 0.00 0.00

1.03 1.03 1.03

1.03 1.03 1.03

1.03 1.03 1.03

1.03 1.03 1.03

1.03 1.03 1.03

1.03 1.03 1.03

1.03 1.03 1.03

1.03 1.03 1.03

1.03 1.03 1.03

1.03 1.03 1.03







SR-30-3 PROP FAN  
8'X6' WIND TUNNEL TESTS  
NASA-LEWIS

P ORDER COMPONENTS  
PEAK STRAIN

RUN. NO.	MACH NO.	BLADE ANGLE DEG	TILT ANGLE DEG	PROP SPEED RPM	BLADE GAGE	1	2	3	4	5
302	0.359	48.	8.13	8995.	B05-2	257.	17.	5.	27.	8.
					B05-3	56.	28.	33.	39.	20.
					B01-1	361.	38.	5.	*****	*****
					B01-3	54.	28.	14.	16.	9.
					B03-1	359.	32.	*****	*****	*****
					B05-1	320.	34.	7.	*****	*****
303	0.357	48.	8.04	8502.	B05-2	246.	41.	13.	11.	12.
					B05-3	31.	18.	14.	8.	12.
					B01-1	332.	44.	*****	*****	*****
					B01-3	15.	*****	22.	10.	9.
					B03-1	320.	51.	*****	*****	*****
					B05-1	291.	47.	*****	*****	*****
304	0.359	40.	8.02	8000.	B05-2	240.	60.	11.	13.	*****
					B05-3	60.	38.	10.	15.	*****
					B05-2	256.	90.	17.	9.	6.
					B05-3	116.	53.	13.	13.	12.
					B01-1	314.	81.	4.	*****	*****
305	0.356	48.	8.04	7501.	B01-3	36.	28.	15.	28.	5.
					B01-1	314.	118.	*****	4.	13.
					B01-3	91.	41.	9.	19.	*****
					B03-1	314.	53.	5.	*****	*****
					B05-1	281.	93.	9.	*****	*****
					---	*****	*****	*****	*****	*****
306	0.357	48.	7.96	6999.	B05-2	225.	97.	8.	*****	12.
					B05-3	158.	46.	*****	19.	*****
					B01-1	271.	89.	5.	*****	*****
					B01-3	123.	29.	19.	*****	*****
					B03-1	277.	62.	*****	*****	*****
307	0.357	48.	8.03	6496.	B05-1	243.	85.	6.	*****	*****
					B05-2	206.	83.	6.	9.	*****
					B05-3	183.	21.	*****	11.	*****
					B01-1	245.	85.	*****	*****	*****
					B01-3	138.	13.	17.	*****	*****
					B03-1	255.	62.	*****	*****	*****
308	0.357	48.	8.02	5998.	B05-1	220.	69.	*****	*****	*****
					B05-2	197.	71.	5.	7.	*****
					B05-3	198.	*****	*****	*****	*****
					B01-1	234.	72.	*****	4.	*****
					B01-3	146.	*****	13.	10.	*****
					B03-1	248.	57.	4.	*****	*****
309	0.359	48.	7.98	5499.	B05-1	209.	55.	*****	*****	*****
					B05-2	164.	41.	6.	*****	*****
					B05-3	159.	14.	*****	*****	*****
					B01-1	193.	44.	6.	*****	*****
					B01-3	118.	12.	*****	*****	*****
					B03-1	207.	36.	*****	*****	*****
310	0.359	48.	8.07	4996.	B05-1	171.	30.	*****	*****	*****
					B05-2	152.	21.	13.	*****	*****
					B05-3	144.	10.	8.	*****	*****
					B01-1	181.	21.	9.	*****	*****
					B01-3	103.	8.	*****	*****	*****
					B03-1	192.	16.	10.	*****	*****
					B05-1	157.	12.	6.	*****	*****

ORIGINAL PAGE IS  
OF POOR QUALITY

SR-3C-3 PROP FAN  
8'X6' WIND TUNNEL TESTS  
NASA-LEWIS

P ORDER COMPONENTS

RNG. NO.	MACH NO.	BLADE ANGLE DEG	TILT ANGLE DEG	PROP SPEED RPM	BLADE GAGE	PEAK STRAIN				
						1	2	3	4	5
311	0.359	48.	7.99	4494.	B65-2	153.	23.	8.	****	5.
					B65-3	126.	20.	8.	****	****
					B61-1	189.	17.	5.	****	****
					B61-3	82.	20.	****	****	****
					B63-1	199.	9.	5.	****	****
312	0.360	48.	7.98	4429.	B65-1	160.	10.	9.	****	****
					B65-2	**** 138	**** 23	****	****	****
					B65-3	**** 110	**** 22	****	****	****
					B61-1	**** 170	**** 17	****	****	****
					B61-3	**** 72	**** 21	****	****	****
					B63-1	**** 180	**** 7	****	****	****
					B65-1	**** 144	**** 10	****	****	****
					B65-2	369.	208.	8.	23.	10.
					B65-3	307.	20.	35.	****	****
					B61-1	460.	239.	****	****	****
315	0.360	48.	14.83	5494.	B61-3	257.	18.	38.	30.	19.
					B63-1	465.	183.	****	****	****
					B65-1	424.	184.	5.	****	****
					B65-2	318.	136.	25.	****	****
					B65-3	287.	29.	****	****	****
					B61-1	390.	149.	17.	****	****
					B61-3	234.	25.	8.	****	****
					B63-1	397.	124.	28.	****	****
					B65-1	357.	119.	18.	****	****
					B65-2	294.	95.	48.	10.	****
316	0.361	48.	14.83	4996.	B65-3	256.	58.	13.	11.	****
					B61-1	360.	96.	22.	6.	****
					B61-3	204.	52.	8.	****	****
					B63-1	369.	82.	41.	****	****
					B65-1	328.	81.	32.	****	****
					B65-2	284.	85.	53.	11.	6.
					B65-3	213.	76.	24.	5.	****
					B61-1	353.	67.	11.	****	****
					B61-3	160.	70.	11.	****	****
					B63-1	363.	68.	41.	6.	****
317	0.361	48.	14.89	4493.	B65-1	319.	67.	38.	5.	****
					B65-2	261.	73.	14.	****	****
					B65-3	173.	77.	****	****	****
					B61-1	333.	64.	9.	****	****
					B61-3	122.	72.	****	****	****
					B63-1	345.	62.	9.	****	****
					B65-1	300.	55.	13.	****	****
					B61-1	665.	104.	8.	6.	****
					B61-3	80.	42.	37.	9.	18.
					B63-1	656.	5.	10.	6.	****
319	0.350	48.	14.88	9006.	B65-1	629.	5.	****	****	****
					B65-2	475.	6.	6.	5.	10.
					B65-3	103.	10.	27.	12.	56.
					B61-1	501.	262.	15.	8.	8.
					B61-3	233.	79.	45.	6.	9.
					B63-1	233.	205.	11.	34.	9.
					B65-1	458.	324.	13.	****	****
					B65-2	**** 249	**** 45	****	****	****
					B65-3	****	****	****	****	****
					B61-1	****	****	****	****	****
350	0.690	50.	5.05	7491.	B61-3	****	****	****	****	****
					B63-1	****	****	****	****	****
					B65-1	****	****	****	****	****
					B65-2	****	****	****	****	****
					B65-3	****	****	****	****	****

